Activity Group 11.

Rail Technology Unit

at

Manchester Metropolitan University

Determination of Tramway Wheel and Rail Profiles to Minimise Derailment

Date: 12th February 2008
RTU Ref: 90/3/A
Client: ORR

Authors: Dr Paul Allen
Senior Research Engineer
Tel: 0161 247 6251
E-mail: p.d.allen@mmu.ac.uk

Dr Adam Bevan
Senior Research Engineer
Tel: 0161 247 6514
E-mail: a.bevan@mmu.ac.uk

OFFICE OF RAIL REGULATION

Project Title	Determination of Tramway Wheel and Rail Profiles to Minimise Derailment (ORR/CT/338/DTR)
Project Manager	Dr. Paul Allen
Client	ORR
Date	12/02/2008
Project Duration	6 Months
Issue	1
Distribution	Dudley Hoddinott (ORR) David Keay (ORR) PDA/AB/SDI/JMS (RTU) Project file
Report No.	90/3/A

Reviewed by: Prof. Simon Iwnicki

Contact: Dr Paul Allen
Senior Research Engineer
Tel: 0161 247 6251
E-mail: p.d.allen@mmu.ac.uk

Summary

As the first phase of a three stage project, the Office of Rail Regulation (ORR) commissioned a wide ranging study to review current tramway systems and their wheel and rail profiles within the UK. Completed by the Health and Safety Executive (HSE) Labs, the work was reported under the Phase 1 ORR study document, entitled 'A survey of UK tram and light railway systems relating to the wheel/rail interface' [1].

Phase 2 of the work, presented within this report, analyses this initial study and extends the work through the application of wheel-rail contact analysis techniques and railway vehicle dynamics modelling to determine optimised wheel and rail profile combinations which minimise derailment risk and wear.

The key findings of the work are summarised below:

- Three profile 'Sets' have been identified; for new light rail and tramway systems; for existing systems with 10mm gauge corner rails and for 'tram-train' schemes. These optimised profile sets offer relatively low contact stresses and values of $T\gamma$ (wheel-rail wear index) when compared to many of the profile combinations in current UK operation.

- The recommended profile sets represent fundamentally compatible wheel and rail profiles, however, the characteristic of any one particular system may dictate detail changes to the suggested profile forms. For example a system with a number of mid-range curve radii may benefit from an increased level of conicity

- New wheel and rail profiles have been recommended which are geometrically compatible in the new condition, this prevents problems with high initial wear rates of wheels and rails and will generally provide profiles which are more stable in terms of shape change

- It has been shown that a conventional wheel profile with a significantly increased flange root radius will not provide sufficient gravitational stiffness force to improve independently rotating wheel (IRW) wheelset guidance

- The concept of adopting profiles which generate single point flange contact, particularly for IRW equipped non-powered axles, has been shown to offer benefits in terms of decreased flange wear rates, these benefits also apply to conventional axles

- The Manchester Metrolink (MML) wheel profile in its new condition was shown to offer a lower level of protection against flange climb relative to the other profiles studied.

However, the MML wheel profile in the new condition is not considered as a derailment risk and relatively low levels of wheel flange wear has been shown to significantly improve the wheel's flange climb protection

- It was demonstrated that flange design methods should include analysis of wheel-rail contact angle and wheel lift as an indicator to flange climb protection

- With the exception of the MML wheel profile, all other wheel profiles studied showed good derailment protection

- Wheelset fit analysis has demonstrated that consideration needs to be given to the groove width, especially in small radius curves, if premature keeper rail wear and subsequent replacement is to be avoided

- Vehicle configuration and highway/pedestrian safety should be a consideration in the selection of groove width, that is, a balance needs to be achieved between sufficient wear allowance and clearance for the wheelset in tight curves and maintaining acceptable levels of surface adhesion/entrapment hazard for other road/surface users

- A light rail and tramway wheel-rail 'Best Practice' guide has been developed which further expands on the practical issues related to the findings of the study and is presented in the best practice guide, titled 'A Good Practice Guide for Managing the Wheel-Rail Interface of Light Rail and Tramway Systems', RTU reference 90/3/B [9].

Acknowledgements

The authors would like to thank Jim Snowdon (Tramtrack Croydon Ltd.), Andy Steel (Hy Brasail Projects) and the project team (David Keay and Dudley Hoddinott, ORR) for their contribution to the working group meetings held during the project. The authors would also like to thanks those who contributed data to the project including; Midland Metro and Manchester Metrolink (Clive Pennington).

Contents

Summary ii

1. Introduction 1
- 1.1 Phase 2 Work Overview 1
- 1.2 Organisation of Report 2

2. Review of Phase 1 Report 4
- 2.1 Derailment Summary 5
- 2.2 Grooved Rail Summary 6
- 2.3 Non-grooved Rail Summary 8
- 2.4 Wheel Profile Summary 11
- 2.5 Vehicle Summary 15
- 2.6 Review of Phase 1 Report – Summary 16

3. Wheel-Rail Profile Analysis 18
- 3.1 Contact Analysis 18
  - 3.1.1 Contact Position 18
  - 3.1.2 Rolling Radius Difference 21
  - 3.1.3 Contact Angle and Wheel Lift 27
- 3.2 Grooved Rail Wheelset Fit 28

4. Profile Selection for Simulation 32
- 4.1 Selected Wheel Profiles 32
- 4.2 Selected Rail Profiles 33
  - 4.2.1 Grooved Rail Profiles 33
  - 4.2.2 Non-Grooved Rail Profiles 34

5. Generic Vehicle Model 35
- 5.1 The VAMPIRE® Package 35
- 5.2 Generic Vehicle Model 35
  - 5.2.1 Generic Vehicle Overview 36
  - 5.2.2 The VAMPIRE® Model 37
  - 5.2.3 Motor Bogie Model 38
  - 5.2.4 Trailer Bogie Model 39

6.	**Dynamic Simulation – Derailment Study**		**40**
	6.1	Derailment Study	41
	6.2	Derailment Study Results	44
		6.2.1 Derailment Study – Results Summary	44
		6.2.2 Derailment Study – Wheel Lift	49
		6.2.3 Derailment Study – Contact Angle	53
		6.2.4 Derailment Study – Angle of Attack	54
		6.2.5 Derailment Study – Y/Q Ratio	55
7.	**Dynamic Simulation – Curving Study**		**58**
	7.1	Curving Study Overview	58
	7.2	Curving Study Results	60
		7.2.1 Curving Study – Tgamma	60
		7.2.2 Curving Study – Contact Stress	64
		7.2.3 Curving Study – Angle of Attack	70
	7.3	Curving Study Summary	71
8.	**Dynamic Simulation – Lateral Stability**		**72**
	8.1	Conventional Axles	72
	8.2	Independently Rotating Wheels (IRWs)	72
		8.2.1 IRW – Simulation Overview	73
		8.2.2 IRW Profiles – Offset Running	74
		8.2.3 IRW Profiles – Flange Wear	76
9.	**Wheel-Rail Profile Recommendations**		**78**
	9.1	Selection Methodology	78
	9.2	Definition of 'Profile Sets'	80
		9.2.1 Profile Set 1 (New System)	80
		9.2.2 Profile Set 2 (Existing System)	81
		9.2.3 Profile Set 3 (Tram-Train)	83
		9.2.4 IRW Wheel Profiles	86
		9.2.5 Wheel-Rail Profile Selection Matrix	86
10.	**Conclusions**		**89**
References			**92**

Appendix A1 Wheel-Rail Analysis Plots

A1.1 Contact Position Plots 93
A1.2 Rolling Radius Difference Plots 95
A1.3 Contact Angle and Wheel Lift Plots 97

Appendix A2 Wheel-Rail Interface Summary Sheets

A2.1 BS 113A Rail Section 102
A2.2 BS 80A Rail Section 105
A2.3 S49 Rail Section 108
A2.4 Ri 59 Grooved Rail Sections 111

Page Intentionally Blank

1. Introduction

Light rail and tramway systems operating in the UK have not adopted standard wheel or rail profile designs. In particular the wheel cross sectional profile has a very significant effect on the running behaviour of the vehicle, the forces generated between the wheel and the rail and the likelihood of derailment. Unlike the mainline railway, which is controlled by Railway Group Standards, there is no clear guidance to engineers responsible for designing and maintaining the critical wheel-rail interface and as a result there is potential for safety critical problems to arise. This is exacerbated by the potential, in the absence of such controlling standards, for wheels, rails, switches and other components originally designed for heavy rail applications to be used inappropriately in light rail applications. A further issue is the tendency for wheel-rail interface issues to be overlooked at the specification and design stage as they tend to fall between the remits of the vehicle builders and infrastructure contractors.

The ORR commissioned a study with the primary aim of optimising wheel and rail profile designs, to reduce the risk of derailments associated with profile incompatibilities. Guidelines will also be developed to ensure good wheel-rail interface practice, for both existing and new system procurement.

The work described in this document reports on Phase 2 of the three-part ORR initiated study, which aims to address the issues described above. Phase 1 of the study carried out by the HSE, was a review of light rail and tramway systems operating in the UK, the range of wheel and rail profiles used and also information on derailments and near misses. An ORR report was produced summarising the Phase 1 findings and this document is reviewed as part of the Phase 2 work described within this document.

Phase 3 which is anticipated to follow the work outlined here, proposes controlled trials of the optimised wheel and rail profiles determined within Phase 2 to verify the findings of the study.

1.1 Phase 2 Work Overview

The following section outlines the original proposed work schedule to complete Phase 2 of this ORR project. The overall aim of the project, in reducing derailment risk and wheel and rail profile wear will be progressed through completion of the following key tasks:

- Review of existing data recorded in ORR report; 'A Survey of UK Tram and Light Railway Systems Relating to the Wheel/rail Interface'. The review will identify the most relevant wheel and rail profile combinations and assist in targeting the

subsequent analysis and simulation work through development of a profile simulation set.

- Using the identified simulation set, assessment will be carried out with respect to derailment risk and wear, using wheel-rail contact and vehicle dynamic simulations, both in-house software and the VAMPIRE® vehicle dynamics software package will be used. Simulations will utilise a representative, generic vehicle model.

- Using the output from the simulation work, two or three wheel and rail profile sets will be developed, these will be optimised for specific system characteristics in order to reduce the risk of derailment and reduce wear.

- It is anticipated that in addition to application to current tramway systems, the profile sets will include profiles which will be selected as 'best practice' profiles and these could possibly be recommended for use by promoters in the tender/procurement stages of new systems.

- Through consultation with the ORR and UK tramway operators, one or more of the profile combinations included within the newly developed profile sets may be selected for trial. It is likely that a selection criteria will be required to optimise the cost benefit of the trial phase and this will be developed through the consultation process, together with agreed output measures to assess the performance of the profiles with respect to the initial project aims.

- The production of a 'Best Practice Guide' for the operation of light rail systems with respect to the wheel-rail interface for both existing and new system procurement

1.2 Organisation of Report

Section 2 presents a review of the Phase 1 report outlining key findings which are of particular relevance to the objectives of the Phase 2 work, including a summary of the rail sections, wheel tyre profiles and vehicle configurations currently used on UK tramway systems.

Section 3 details the preliminary analysis work which was undertaken to analyse each of the wheel and rail profile combinations. This includes analysis of the contact conditions, in terms of contact position, rolling radius difference, contact angle and wheel lift. In addition, for the grooved rail sections, the fit of the wheelset within the gauge is also presented, the objective being to determine the clearances between the wheelset and the grooved rail section in the new condition.

Section 4 describes the profiles which were identified for further analysis work, together with reasons for their selection based on the analysis carried out in the previous sections.

Section 5 provides a description of the VAMPIRE® railway vehicle dynamics simulation software used to assess the performance of the short-listed profiles (see Section 4) with respect to derailment protection and minimisation of wheel and rail profile wear. The 'generic' vehicle model generated to represent the majority of vehicle configurations identified in Section 2 is also described in this section.

Sections 6, 7 and 8 detail the results of the dynamic simulation studies undertaken using the 'generic' vehicle model and the short-listed profiles. Section 6 summaries the results from the derailment study whereas Section 7 describes the results from the curving analysis. Section 8 presents the results with reference to the lateral stability of conventional and IRW axles.

Section 9 describes the methodology and definition of the selected wheel-rail profile sets.

Section 10 presents the conclusions from the work. Appendices A1 and A2 provide a complete set of analysis and simulation results generated during the work.

2. Review of Phase 1 Report

The Phase 1 report entitled 'A survey of UK tram and light railway systems relating to the wheel/rail interface' [1], was authored by Ed Hollis of the Health and Safety Laboratory (HSL). The report details aspects of UK tram and light rail systems which are relevant to the wheel-rail interface. The report contains tables and system data including drawings of wheel and rail profiles which have been used during the Phase 2 study. The following section describes the review of the Phase 1 report, outlining key findings which are of particular relevance to the Phase 2 objectives. Detailed recommendations based on the findings of this review are included in the simulation work, described in Sections 3 and 4 of the report, and in the 'Best Practice Guide' presented in the addendum to this document [9]

.

The National Tramway Museum, Tyne and Wear Metro and Blackpool Tramway system have only been partially included in the analysis as these systems are seen as being too distant from current and likely future direction of light rail to warrant significant application of the project effort. In the case of Tyne and Wear Metro the reason for exclusion being that it is essentially a 'heavy rail' wheel-rail interface system.

2.1 Derailment Summary

		Tramway Network								
		Blackpool & Fleetwood Tramway	Croydon Tramlink	Docklands Light Railway	Manchester Metrolink	Midland Metro	Nottingham Express Transit	Sheffield Supertram	Tyne & Wear Metro	**Totals (% of Total)**
Cause of Derailment	Diamond	2	1							**3 (6)**
	Turnout	6	2	1	9	2	3	4	1	**28 (52)**
	Obstruction (Groove/Trk)	1			1				2	**4 (7)**
	Discrete Track Fault	2								**2 (4)**
	Damaged/Worn Keeper	2			2					**4 (7)**
	Overspeed	1								**1 (2)**
	Flange Climb		1	4	1		2		4	**12 (22)**
										54 (100)

Table 2.1 – Derailment Summary

With reference to Table 2.1 above, it can be seen that just over 50% of all derailments, reported within the Phase 1 work, can be attributed to incidents at turnouts. Detailed information on these derailments was not available in all cases, however, it was evident that the majority of the turnout derailments were due to detection and closure failures rather than wheel-rail interface issue. Cases where the wheel-rail interface was at fault were generally caused by flange climbing or striking of the switch tip.

At 22% of cited derailments, flange climb was the next highest cause of casualties. These include only incidents outside turnouts and may be related to a combination of poor wheel-rail interface conditions and contributory factors such as track twist, poor bogie setup, high friction condition or poor wheel finish following turning, again, not all details were available.

Damaged or worn keeper rails attributed to 7% of derailments, as systems become older this figure is likely to increase, unless suitable maintenance measures are put into place, such as keeper renewal, change of rail section or better control of gauge.

Obstructed groove and un-specified issues at diamond crossing make up the majority of the remainder, with discrete track faults and over-speed being listed at 4% and 2% respectively.

In summary, closure issues must be addressed and this would likely benefit from improved or more suitable switch blade actuation and detection coupled with, where appropriate, better protection against wheel flange climbing or running behind a partially closed switch blade.

Flange climb derailments (not within turnouts) should in the most case be preventable through fully compatible wheel and rail profiles which are designed to operate on the curvatures present on the system, coupled with good friction management, turning methods and correct bogie setup (no excessive static wheel load offsets etc).

Keeper wear and ultimate failure is a relatively new problem as systems reach a critical stage of wear. System operators are beginning to understand how to maintain and prevent problems related to excessive keeper rail contact and resultant wear. Reliance on keeper rail contact for curving can and has resulted in derailments. Measures to correctly specify new grooved rail sections and also to safely maintain worn keeper section is a key part of the Phase 2 output. It is also important to provide understanding to operators as to how keeper rail running can lead to derailment. There has sometimes been a misconception that keeper rails are check rails and therefore contact with the Flangeback is a feature of the design.

2.2 Grooved Rail Summary

The Phase 1 report identified that there are many different types of grooved rail profiles currently used within the UK light rail and tramway systems. Table 2.2 below shows a review of the grooved rail profiles, as identified in the Phase 1 report, used by each of the UK light rail and tramway systems.

		Tramway Network							
		Blackpool & Fleetwood Tramway	Croydon Tramlink	Manchester Metrolink	Midland Metro	National Tramway Museum	Nottingham Express Transit	Sheffield Supertram	**Totals**
Grooved Rail Profile	BS 7					•			1
	BS 8					•			1
	Ri 59-R10			•					1
	Ri 59-R13 (Ri 59N)		•						1
	Ri 60-R10	•							1
	Ri 60-R13 (Ri 60N)		•						1
	SEI 35G			• (1:40)	•	•		•	4
	SEI 35GP							•	1
	SEI 41GP						•		1

Table 2.2 – Grooved rail summary (installed vertical unless otherwise stated)

To understand the differences in the rail sections identified in Table 2.2, the cross section of each of the profiles (excluding BS 7 and BS 8 profiles) have been aligned and superimposed, as illustrated in Figure 2.1.

It can be seen that the railhead profile for each of the rail sections, except for the Ri 59-R13 (Ri 59N) and Ri 60-R13 (Ri 60N) profiles, are identical with the only differences apparent in the geometry of the groove and keeper section of the rail. The Ri 59-R13 and Ri 60-R13 profiles differ from the other profiles due to the rail head being inclined at 1:40 and an increased gauge corner radius of 13mm.

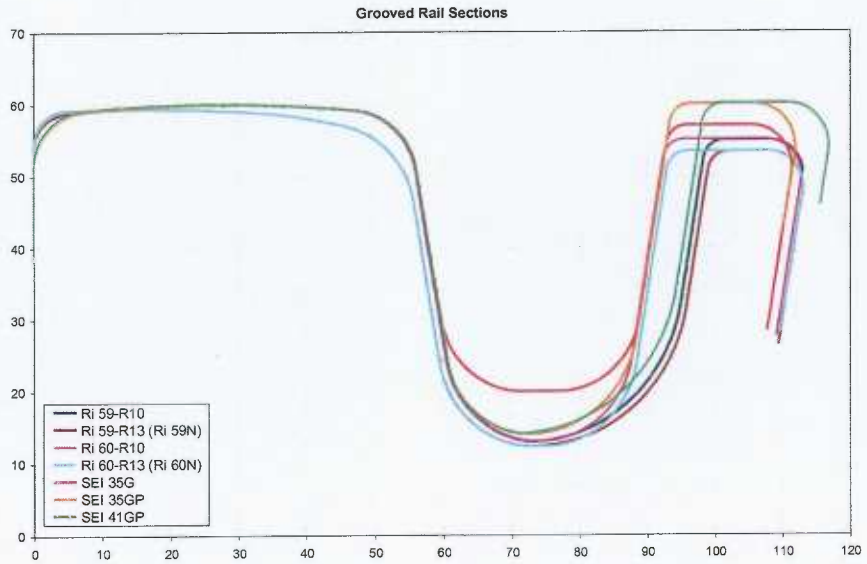

Figure 2.1 – Comparison of the cross section of grooved rail profiles

To summarise the differences in the rail sections the characteristics of the profiles (groove width, gauge corner radius etc.) have been listed in Table 2.3 below.

Rail Profile	Groove width* (mm)	Groove depth (mm)	Gauge corner radius (mm)	Rail head inclination	Keeper height rel. to rail head (mm)	Rail section height (mm)
BS 7	28.58	31.75	7.94	1:40	-4.76	177.80
BS 8	28.58	36.51	7.94	1:40	-4.76	177.80
Ri 59-R10	42.00	47.00	10.00	Vertical	-5.00	180.00
Ri 59-R13 (Ri 59N)	42.00	47.00	13.00	1:40	-6.00	180.00
Ri 60-R10	36.00	47.00	10.00	Vertical	-5.00	180.00
Ri 60-R13 (Ri 60N)	36.00	47.00	13.00	1:40	-6.00	180.00
SEI 35G	36.00	40.00	10.00	Vertical	-3.00	152.50
SEI 35GP	36.00	45.90	10.00	Vertical	Level	152.50
SEI 41GP	41.00	45.90	10.00	Vertical	Level	152.50

Table 2.3 – Characteristics of grooved rail sections

(*Groove width is measured at a distance of 9mm from the top of the rail)

Excluding the BS 7 and BS 8 profiles used only by the National Tramway Museum, the groove width typically varies from 36mm to 42mm. The use of wider grooved profiles, such as Ri 59 and SEI 41GP profiles, allow for increased sidewear to the running rail before contact with the keeper can occur but can potentially increase the safety hazard to pedestrians, motorists and cyclists that travel over them.

Generally grooved rails profiles were designed with the intention of being installed vertically. This is the case for the majority of UK tramway system with the exception of Manchester Metrolink, which has sections of SEI 35G rail installed with an inclination of 1:40, and the Ri 59-R13 (Ri 59N) / Ri 60-R13 (Ri60N) profiles which have been designed to include a 1:40 inclination in the rail head when the rail is installed vertically.

Typically grooved rail sections include either a 10mm or 13mm gauge corner radius. The majority of UK tramway systems use profiles with a gauge corner radius of 10mm with the exception Croydon Tramlink which uses Ri 59-R13 / Ri 60-R13 rail sections employing a radius of 13mm. The work described later in the report will look at the compatibility of profiles with different wheel flange root and rail gauge corner radii.

As identified in Table 2.3 and illustrated in Figure 2.1, the grooved rail sections include different levels of keeper height. In some instances, such as the SEI GP profiles, the keeper rail is level with the running surface of the rail whereas in others it is slightly lower. Depending on the level of wear on the railhead the keeper may eventually become higher than the railhead resulting in a potential safety hazard. The Ri 59-R13 / Ri 60-R13 profiles offer the greatest clearance between the top of the keeper and the railhead (~-6mm) due to the rail head inclination.

The grooved rail sections identified above, along with a number of additional rail sections not currently used in UK light rail and tramway systems, are defined in BS EN 14811-1 [2].

2.3 Non-Grooved Rail Summary

Table 2.4 includes a summary of the non-grooved rail sections currently used within the UK light rail and tramway systems, as identified from the Phase 1 report.

It can be seen that a large variation in profiles exist, with Manchester Metrolink using five different types of non-grooved rail sections, although some of these are installed over short sections of track or may have been completely removed during recent rail renewal programs.

The most frequently used non-grooved rail sections include BS 80A, with both a 1:20 and 1:40 rail inclination, and BR 113A sections. BR 113A rail section appears frequently due to light rail and tramway systems using (or sharing) old British Rail lines.

		Tramway Network								
		Blackpool & Fleetwood Tramway	Croydon Tramlink	Docklands Light Railway	Manchester Metrolink	Midland Metro	Nottingham Express Transit	Sheffield Supertram	Tyne & Wear Metro	**Totals**
Non-Grooved Rail Profile	BS 95RBH	•			•					**2**
	BR 109lb				•					**1**
	BS 80A			•	•	• (1:40)	• (1:40)	• (1:40)		**5**
	BS 110A (BS 113A)		•	•	•					**3**
	BR 113A	•	•	•	•	•			•	**6**
	S49		•							**1**

Table 2.4 – Non-grooved rail summary (installed at 1:20 unless otherwise stated)

To summarise the differences in each of the non-grooved rail sections the cross section of each of the profiles have been aligned and superimposed (excluding the BS 95RBH profile), as illustrated in Figure 2.2, and the defining characteristics have been tabulated in Table 2.5 below.

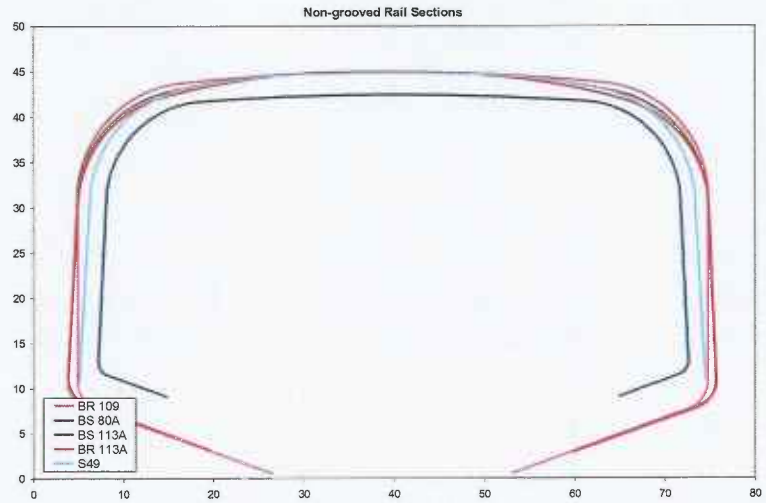

Figure 2.2 – Comparison of the cross section of non-grooved rail profiles (vertical)

Rail Profile	Crown radius (mm)	Gauge corner radius (mm)	Rail section height (mm)
BS 95RBH	304.80	12.70	145.26
BR 109lb	228.60	12.70	158.75
BS 80A	304.80	11.11	133.35
BS 110A* (BS 113A)	304.80	12.70	158.75
BR 113A*	304.80	12.70	158.75
S49	300.00	13.00	143.00

Table 2.5 – Characteristics of non-grooved rail sections
(*Note different designation for 113A rail sections)

It can be seen that the majority of the non-grooved rail sections include a similar gauge corner radius, 12.7mm – 13mm, with the exception of the BS 80A rail section which has a gauge corner radius of 11.11mm. The compatibility of the gauge corner radius with the wheel flange root radius has been investigated during the stage 2 work and is described later in the report.

The rail crown radius of each of the non-grooved profiles varies from 228.60mm for the older 109lb rail to 304.80mm for the newer 80A and 113A rail sections. Ideally this should be consistent with that of the grooved rail section in order to prevent transition problems such as

undesirable wear patterns in the rails, increased noise levels and general variation in wheel rail contact conditions.

The effect of different rail inclination, as seen with BS 80A rail, has been considered during this work to investigate the potential benefits for a given wheel profile.

The different designations of 113A rail section specified in Tables 2.4 and 2.5 have been used to differentiate between the differences apparent in the old and new 113A rail sections. The BR 113A profile is based on the original British Rail design whilst the BS 113A profile is as specified in British Standard (BS 11). The only difference between the two profiles is the crown head width which is 12mm on the BR version and 19.05mm on the BS version.

The non-grooved rail sections identified above, along with a number of additional rail sections not currently used in UK light rail and tramway systems, are defined in part 1 and 4 of BS EN 13674 [3,4].

2.4 Wheel Tyre Profile Summary

Using the information included the Phase 1 report, and the digital representations of the wheel tyre profiles generated during the project, a comparison of characteristics of each of the UK light rail and tramway system wheel profiles has been conducted. Table 2.6 below summaries the characteristics of the different profiles; including flange depth, flange thickness, flange root radius and wheelset back-to-back dimension.

		Croydon Tramlink	Croydon Tramlink (prototype)	Docklands Light Railway	Manchester Metrolink	Midland Metro	Nottingham Express Transit	Sheffield Supertram	Tyne & Wear Metro
Reference name		CR4000	CT3	DRL5	MML-2	T69 (Rev-A)	P-3-102639	Mod. DIN25	P8
Flange thickness Sd (mm)		23.2 (23.2)	22.4 (22.4)	27.5 (27)	22.3* (22)*	23 (23.02)	22.81 (22.81)	23 (23.02)	29 (28.5)
Flange height Sh (mm)		25.5 (25.5)	27 (27.0)	30 (29.5)	26.3 (25.9)	24 (24.05)	24 (24.0)	24 (24.05)	30 (29.3)
Flange gradient qR (mm)		4.9 (4.9)	6.43 (6.43)	11 (10.5)	8.5 (8.3)	3.0 (3.02)	3.4 (3.4)	3.0 (3.02)	12.5 (12.1)
Flange angle (deg)		70	70	69.5	68	76	76	76	68
Flange root radius (mm)		15	15	22	13	13	14	13	13
Cone angle (grad)		1:20	1:26 to 1:10	1:19.08	1:20	1:40	1:40 to 1:20	1:40	n/a
Flangeback dim. (mm)		1380	1380	1362	1362	1379	1380	1379	1362
Wheel diameter (mm)	**New**	630	630	740	740	680	660	670	740
	Worn	550	550	660	680	620	580	588	675
Taperline, L2 (mm)		60	60	68	70	58	60	58	70

Table 2.6 – Wheel profile summary (*true flange thickness)

The flange height and thickness measurements included in Table 2.6 have been calculated with reference to the recommended taperline for each profile as presented in the table. For comparison of the different profiles flange height and thickness measurements have also been calculated at a nominal taperline of 60mm, these results are presented in parentheses in Table 2.6.

The current tyre profiles operated by Croydon Tramlink, Midland Metro, Nottingham Express Transit and Sheffield Supertram can generally be classified as modified DIN-type wheel profiles, with the tyre profiles used by Midland Metro and Sheffield Supertram being very

similar. Nottingham Express Transit profile differs slightly from the others as it includes a second angle of 1:20 on the outer edge of the tyre. Large flange angles in the range 70° – 76° can be seen on the modified DIN-type profiles. The flange root radius of these profiles varies from 13mm to 15mm. All of these profiles are equipped with flat flange tips for flange running.

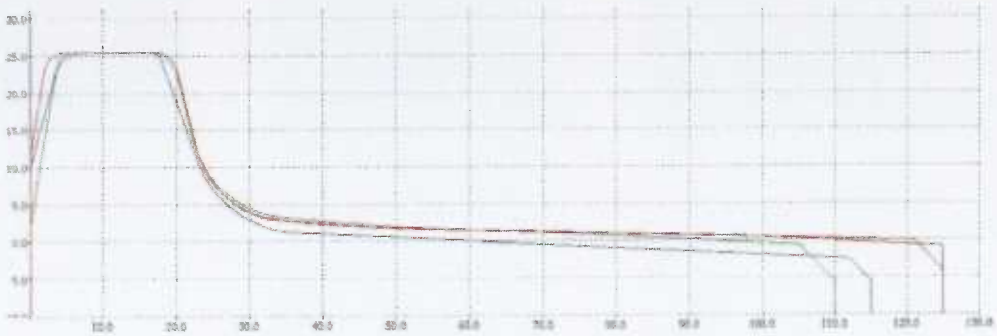

Figure 2.3 – DIN-type wheel tyre profiles, Croydon CR4000 (blue), Nottingham P-310239 (green), Midland T69 Rev.A and Sheffield Mod-DIN25 (red)

The profile operated by Manchester Metrolink differs from those operated by other conventional tramway systems as it includes a full flange geometry and a cut-out in the flangeback of the profile. This cut-out was introduced to accommodate the difference in flangeback spacing required for both light and heavy rail track works. This methodology has been used in other European railways to allow light rail vehicles to operate on other parts of the railway network (dual-mode light rail vehicles) and therefore has potential for UK tram-train applications.

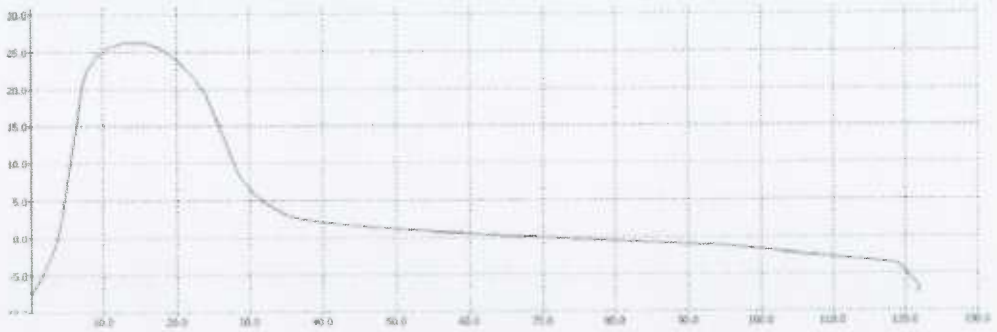

Figure 2.4 – Manchester MML2 wheel tyre profiles

The Tyne and Wear Metro and Docklands Light Railway use mainline type tyre profiles with the Tyne and Wear Metro using a typical British Rail 'P8'-tyre profile. Docklands DLR5 profile is a modified 'heavy rail' profile which includes a large flange root radius to generate a

significant rolling radius difference, increasing steering performance around tight curves. The Tyne and Wear BR-P8 and Docklands DLR5 tyre profiles are illustrated in Figure 2.5 below.

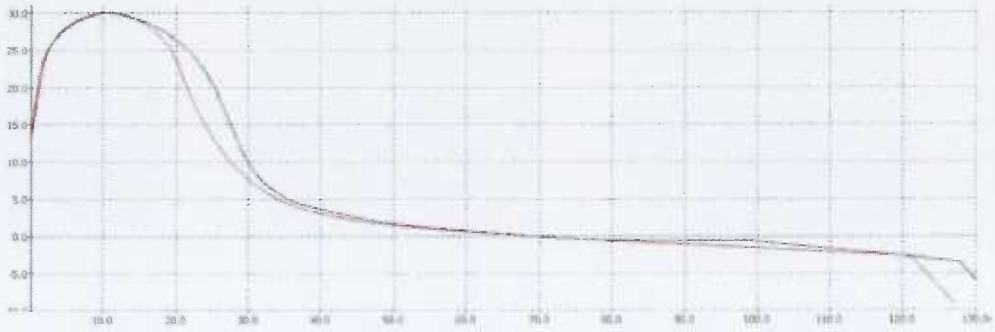

Figure 2.5 – Tyne and Wear BR-P8 (blue) and Docklands DLR5 (red) wheel tyre profiles

The Croydon CT3 tyre profile is a prototype profile designed to produce better wheel-rail interface performance on the Croydon Tramlink network. The profile geometry is similar to that used by KVB in Cologne on their fleet of K-4000 vehicles, from which the CR-4000 vehicles operated by Croydon Tramlink are based, but includes a rounder flange tip and a gauge corner radius of 15mm instead of 13mm on the KVB profile. Generally, the CT3 tyre profile has a 'worn' profiles shape when compared to the current CR4000 profile, with a number of blended radii. A comparison of the current Croydon CR4000 and prototype CT3 tyre profiles can be seen in Figure 2.6.

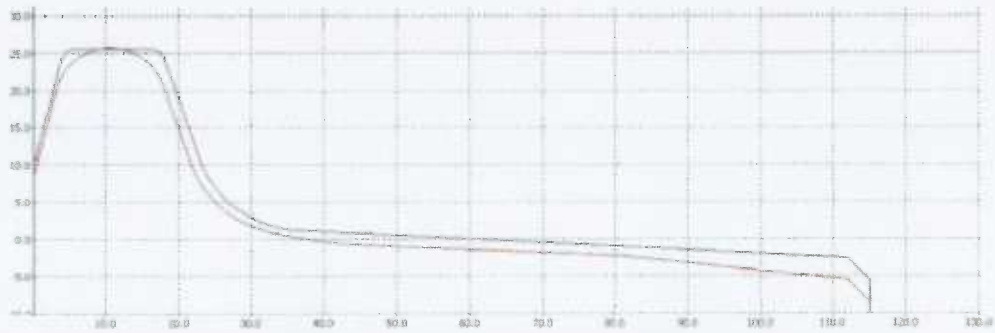

Figure 2.6 – Croydon CR4000 (blue) and 'prototype' CT3 (red) wheel tyre profiles

A variation in wheel diameter is also observed in the Phase 1 report with values ranging from 630mm to 740mm when new, as shown in Table 2.6.

2.5 Vehicle Summary

Table 2.7 below illustrates the variety of vehicle configurations currently operating in the UK. In this case, the National Tramway Museum has been neglected as the vehicles are non-conventional in the modern sense.

		Tramway Network								
		Blackpool & Fleetwood Tramway	Croydon Tramlink	Docklands Light Railway	Manchester Metrolink	Midland Metro	Nottingham Express Transit	Sheffield Supertram	Tyne & Wear Metro	**Totals**
Configuration	IRW on trailer only		•			•				2
	Powered IRW						•			1
	All Conventional	•		•	•			•	•	5
	Slewing ring		•	•	•	•		•		5

Table 2.7 – Vehicle Configurations

Presently, the most common vehicle configuration is a conventional axle setup on all bogies. Generally a slewing ring is used to allow almost friction free rotation of the bogie. In the case of the Croydon Bombardier CR4000 tram, the arrangement is not strictly a slewing ring and has the addition of friction sidebearers to increase bogie rotational resistance.

It is relatively common practice to combine conventional powered axled bogies with independently rotating wheel (IRW) equipped trailer 'truck' sections at articulations. This configuration allows for a low floor section with ramps or steps to allow access to the body sections above the axles, which provides accessibility advantages but can result in trailer-truck wheel wear issues and increased derailment hazard due to the nature of operation of IRW's.

The only vehicle operating powered IRW axles is the NET tram. The behaviour of powered IRW's in terms of curving/wear and derailment is complex as they are neither pure IRW's nor purely conventional but usually a mechatronic combination of both systems. The effect of this on the behaviour of the vehicles was briefly investigated during this work, in collaboration with the vehicle manufacturers.

From initial consultations with the vehicle manufacturers it appears that the current consensus for future tram development is a move back towards conventional axles, using ramped floor sections to provide the required accessibility. This seems a sensible option as it reduces the potential problems which are associated with the lack of guidance of trailer IRW's and the un-certainty of the 'real-world' performance of powered IRW's. A possible alternative direction is the adoption of steered IRW bogies, but this is beyond the scope of the work.

2.6 Review of Phase 1 Report – Summary

The review of the Phase 1 report has resulted in a number of observations relevant to the objectives of the Phase 2 work. Essentially the report forms a data library of nine UK tram and light rail systems, with the addition of summary tables and derailment histories.

2.6.1 Derailments

- 50% of all derailments, reported within the Phase 1 work, can be attributed to incidents at turnouts, the majority of these derailments were due to detection and closure failures rather than wheel-rail interface issue.
- 22% of cited derailments were caused by flange climb, these may be related to a combination of poor wheel rail interface conditions and contributory factors such as track twist, poor bogie setup, high friction condition or poor wheel finish following turning.
- 7% of derailments were attributed to keeper wear. 4% and 2% respectively were caused by obstructed groove and un-specified causes at diamond crossings.

2.6.2 Grooved Rails

- All grooved rail, head profiles are identical with the exception of the Ri 59-R13 and Ri 60-R13 profiles; the rail head being inclined at 1:40 with an increased gauge corner radius of 13mm.
- Groove width typically varies from 36mm to 42mm. Although wider grooved profiles do exist, such as 67-R1 (Ph37a), as defined in BS EN 14811-1 [2].
- Ri 59-R13 / Ri 60-R13 profiles offer the greatest clearance between the top of the keeper and the railhead (~-6mm).

2.6.3 Non-grooved Rails

- The most frequently used non-grooved rail sections include BS 80A, with both a 1:20 and 1:40 rail inclination, and BR 113A sections.
- Non-grooved rail sections have a similar gauge corner radius, 12.7mm – 13mm, with the exception of BS 80A rail which uses a radius of 11.11mm.

2.6.4 Wheel Tyre Profiles

- Wheel profiles operated by Croydon Tramlink, Midland Metro, Nottingham Express Transit and Sheffield Supertram can generally be classified as modified DIN-type wheel profiles. Characteristics of these profiles include;
  - Large flange angles in the range 70° – 76° can be seen on the modified DIN-type profiles
  - The flange root radius of these profiles varies from 13mm to 15mm
  - All of these profiles are equipped with flat flange tips for flange running
  - The tyre profiles of Midland Metro and Sheffield Supertram are very similar
- The profile operated by Manchester Metrolink includes a full flange geometry and a cut-out in the flange-back of the profile to accommodate the difference in flangeback spacing required for both light and heavy rail track works.
- Docklands DLR5 profile includes a large flange root radius to generate significant rolling radius difference, increasing steering performance in tight curves.

2.6.5 Vehicle Configuration

- Presently, the most common vehicle configuration is a conventional axle setup on all bogies.
- It is relatively common practice to combine conventional powered axled bogies with independently rotating wheel (IRW), but this can result in trailer-truck wheel wear and increased derailment hazard.
- The only vehicle operating powered IRW axles is the NET tram.

3. Wheel-Rail Profile Analysis

Using the data generated from the review and analysis of the Phase 1 report, wheel and rail profile combinations were selected for further analysis. In general all profile combinations were considered, with the exception of; repeated combinations, combinations where there is insignificant adoption of a particular profile or the profile combination has been deemed to be unlikely to contribute significantly to the later work.

The following section details the preliminary analysis work which was carried out on the wheel and rail profile combinations. In overview this included analysis of the contact conditions, in terms of contact position, rolling radius difference, contact angle and wheel lift. In addition, for the grooved rail sections, the fit of the wheelset within the gauge was analysed, the objective being to determine the clearances between the wheelset and the grooved rail section in the new condition.

3.1 Contact Analysis

The contact analysis work formed the first step in analysing the contact conditions between new wheel and rail profiles for each of the tramway systems. Using a combination of the VAMPIRE® software contact pre-processor and in-house developed MATLAB® software routines, contact position, rolling radius difference, contact angle and wheel lift were analysed. These parameters were chosen as together they describe the commonality of the profiles (likely initial wear), their ability to steer the vehicle and also resist derailment.

Due to the number of profile combinations, wheel-rail contact analysis has been conducted for each of the combinations identified in Table 2.2 and 2.4 with the aim of reducing the number of simulations required during the dynamic analysis, as described in Section 6, 7 and 8.

The results presented in this section have been selected to demonstrate the more extreme variations in the possible profile combinations; a full set of contact analysis data is included in Appendix A1.

3.1.1 Contact Position

Using the output from the VAMPIRE® contact pre-processor an in-house developed MATLAB® software routine was used to indicate where contact was occurring between the wheel and rail for a ± 10 mm lateral shift. With reference to the contact position plots shown in Figures 3.1 to 3.4, the blue lines, drawn between the wheel and rail profiles, indicate the points that are in contact on the wheel and rail for a given lateral displacement of the wheelset

with respect to the track. The red line indicates the position of the contact patch when the wheelset is in its nominal mid-position.

Figure 3.1 below shows the contact positions for Croydon Tramlink CR4000 wheel tyre profiles when combined with Ri 59-R13 and BS 113A rail sections. This combination results in non-conformal 2-point contact, with no contact present between the gauge corner and rail head. The nominal running position (zero lateral displacement) is situated on the crown of the rail.

Non-conformal initial contact conditions in the new condition can cause high contact stresses, resulting in high initial wheel and rail profile wear, ideally the new wheel and rail profile should have a more even distribution of contacts across the wheel and rail.

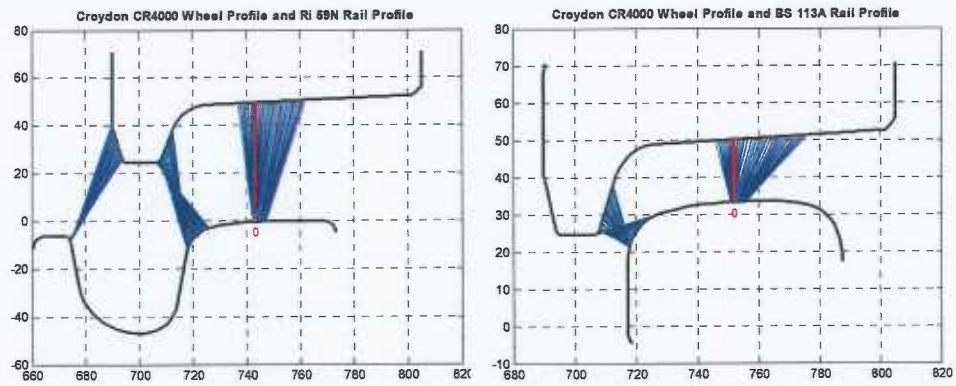

Figure 3.1 – Wheel-rail contact position, Croydon Tramlink CR4000 wheel and Ri 59-R13 (left) and BS 113A (right) rail

The prototype CT3 tyre profile generates similar contacts to the CR4000 profile on BS 113A rail section but more conformal single-point contact on Ri 59-R13, as shown in Figure 3.2.

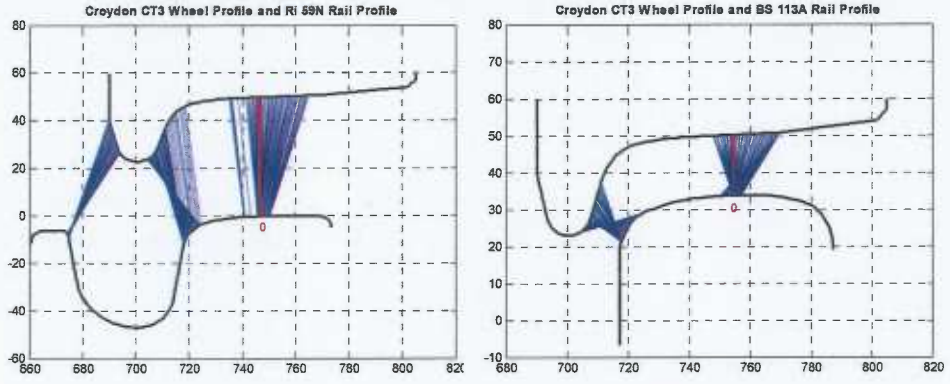

Figure 3.2 – Wheel-rail contact position, Croydon Tramlink CT3 wheel and Ri 59-R13 (left) and BS 113A (right) rail

In contrast, greater conformality can be seen in the contact position on the Nottingham Express Transit, particularly in flange root of the wheel and gauge corner of the rail, as shown in Figure 3.3. It is also worth noting that the nominal running position of the wheel is shifted towards the gauge corner of the rail.

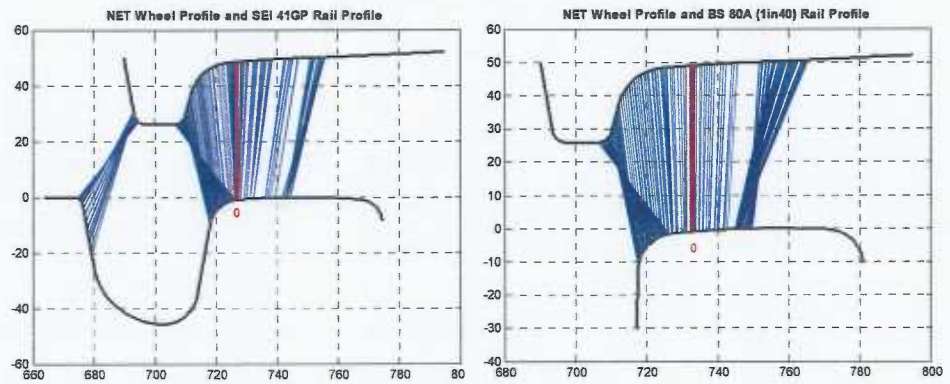

Figure 3.3 – Wheel-rail contact position, Nottingham Express Transit P-3102639 wheel and SEI 41GP (left) and BS 80A (right) rail

The Manchester Metrolink MML2 tyre profile produces conformal contact on the grooved rail section with less contact with keeper due to the cut-out on the flange-back of the wheel. When combined with the BS 80A rail section a large jump in the contact position can be seen, as shown in Figure 3.4, this can result in high contact stresses and instantaneous peaks in wheelset forces, these effects have been attributed to rolling contact fatigue (RCF) in heavy rail systems. Generally, RCF does not occur in light rail systems as normal and tangential stresses are too low.

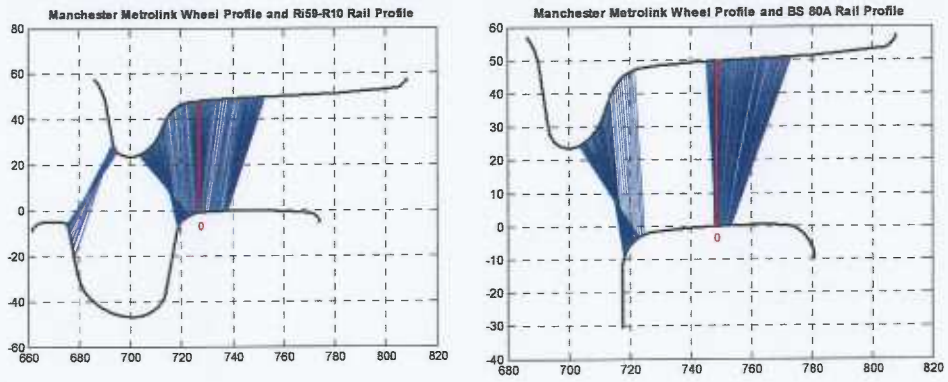

Figure 3.4 – Wheel-rail contact position, Manchester Metrolink MML2 wheel and Ri 59-R10 (left) and BS 80A (right) rail

As part of the Phase 2 simulation work, contact position plots as presented above, have been used to analyse the proposed new wheel and rail profile combinations to assess conformality and position of the contact on the rail head and the point at which flange contact occurs.

3.1.2 Rolling Radius Difference

When a wheelset is running with symmetrical wheels on identical rails and the wheelset is centred within the track gauge, then the rolling radius of the left and right wheels is equal. Due to the conical form of a typical wheel profile, as the wheelset moves from the central position a rolling radius difference (RRD) is generated, the rolling radius of one wheel increases whilst the other decreases. An example plot of rolling radius difference for a 6mm shift to both the left and right (positive to the right) is shown in Figure 3.5 below.

The RRD between the left and right wheels for a given lateral shift of the wheelset can be used as an indicator of conicity. In general terms, the greater the slope of the curve, the greater the effective conicity. Increased conicity enables the wheelset to negotiate smaller radius curves without flange contact. The design conflict in terms of conicity is that high conicity can lead to lateral instability of the wheelset, known as 'hunting'. Usually this is not a common problem in light rail systems, as maximum linespeeds tend to be relatively low (≈50mph maximum)

The RRD has been calculated for each wheel-rail combination identified in Tables 2.2 and 2.4 in Section 2. Profile combinations which demonstrate the greatest variation in characteristics are presented below. The complete set of curves is included in Appendix A1.

Figure 3.5 below shows the RRD graph for the Croydon Tramlink CR4000 wheel profile and the rail sections on which it runs. It can be seen that a similar RRD is obtained with all rail

sections. The consistency in the contact conditions is a beneficial feature of the profile design, as it simplifies the monitoring and maintenance of the tramway system. However it is also noted that the level of conicity generated is relatively low, suggesting that depending on the curve radius distribution of the system, there could be margin to improve steering, with benefits in terms of flange wear and rail side and keeper wear. An Instantaneous contact angle change can be seen by the rapid increase in RRD as the wheel goes into flange contact, this is a result of the low level of conformality between wheel flange and gauge corner radius, this can lead to high initial wear rates and possible degeneration of lateral ride as there is little transition between tread and flange contact.

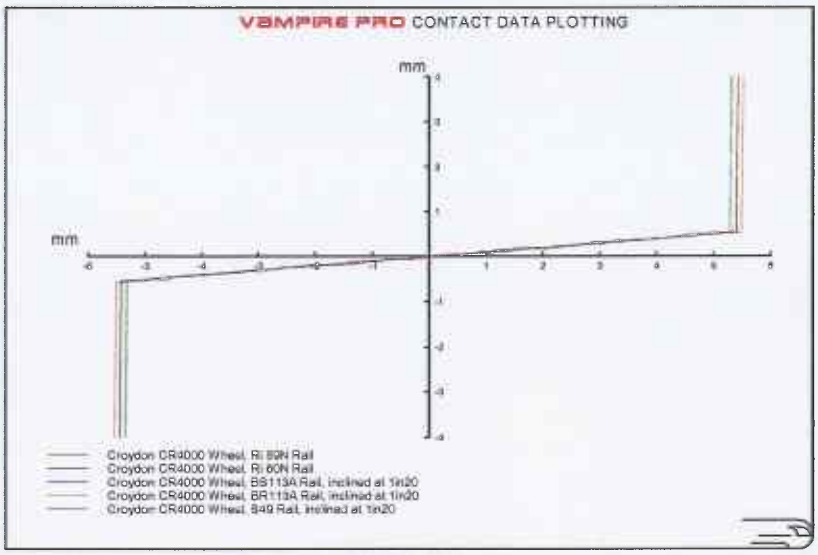

VAMPIRE Plot

Figure 3.5 – Rolling radius difference, Croydon Tramlink CR4000

Figure 3.6 below shows a comparison of the RRD generate using the current Croydon CR4000 tyre profile with the prototype CT3 profile on Ri 59-R13 (Ri 59N) and S49 (inclined at 1:20) rail sections. A slight reduction in the RRD can be seen when using the CT3 profile with an increase in allowable lateral displacement before contact with the flange.

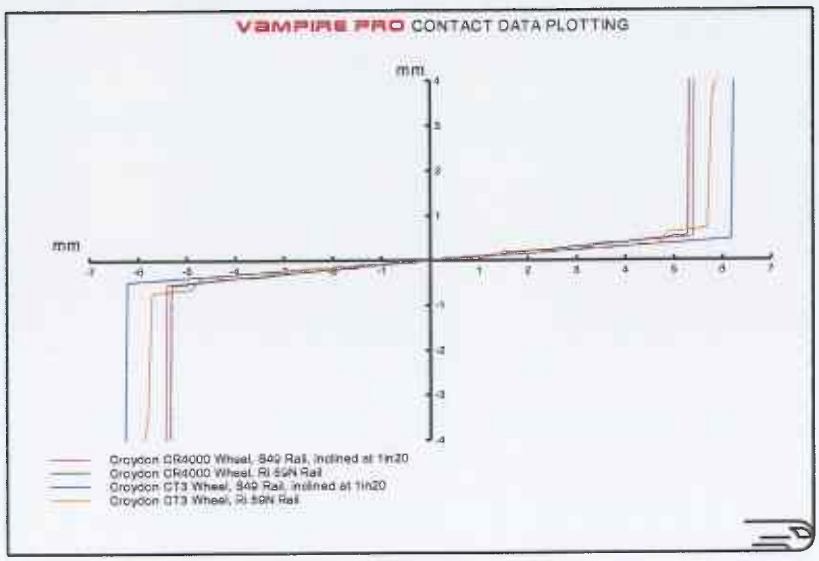

VAMPIRE Plot

Figure 3.6 – Rolling radius difference, Croydon Tramlink current CR4000 and prototype CT3 tyre profiles

In comparison the wheel-rail combination adopted by Nottingham Express Transit generates good conicity with grooved and non-grooved rails, inclined at 1:40, as shown in Figure 3.7. The profile does not show the same consistency across the rail sections used as the Croydon profile but provides a smooth transition between tread and flange contact, which can be beneficial in terms of ride quality and wear.

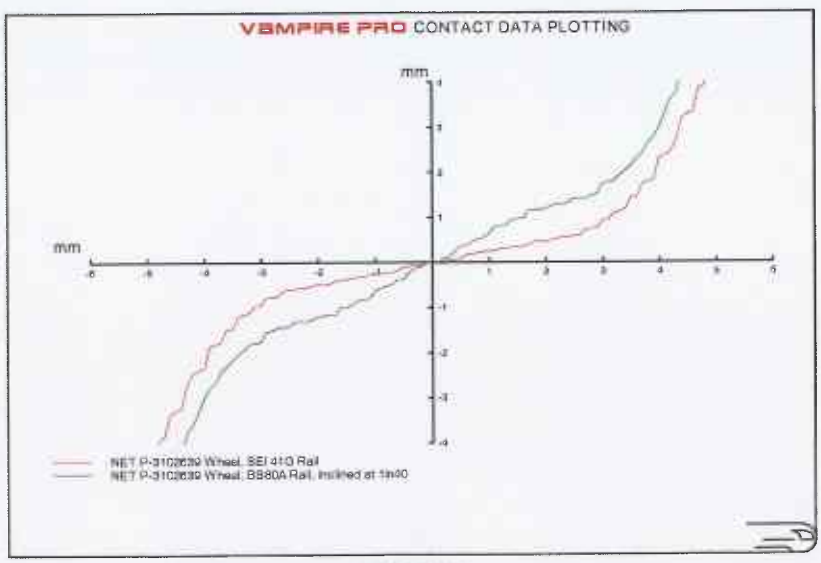

VAMPIRE Plot

Figure 3.7 – Rolling radius difference, Nottingham Express Transit

Figure 3.8 below shows the range of RRD graphs for the Manchester Metrolink tramway system. A very large variation in conicity is found, with low conicity generated on BS 113A and BS 80A rail profiles, and medium to high conicity levels on Ri 59-R10 and SEI 35G embedded sections. In the case of SEI 35G, the high conicity is due to the reduced 1:40 rail inclination. Such a variation in conicity can lead to difficulties in managing the wheel-rail interface, as maintenance requirements can vary widely. As the conicity increases to high levels, issues with vehicle lateral instability may arise. The Metrolink wheel, when combined with Ri 59-R10 and SEI 35G rail profiles provides a smooth transition between tread and flange contact, which is in contrast to the transition obtained with the other adopted rail sections. This highlights the difference in conformality between flange root and gauge corner.

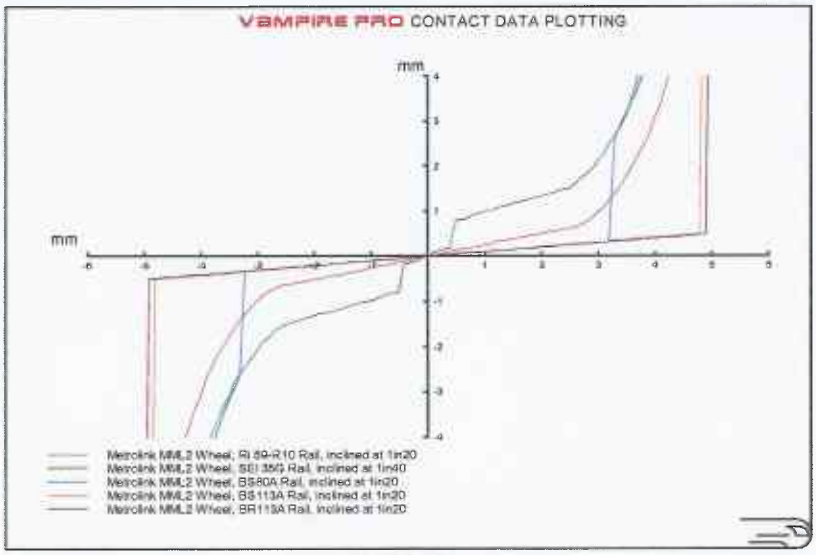

Figure 3.8 – Rolling radius difference, Manchester Metrolink

As described previously in the report, the wheel tyre profiles used by Midland Metro and Sheffield Supertram include very similar tread and flange geometry resulting in similar contact conditions when combined with their respective rail profiles, as shown in Figure 3.9. Both produce low conicity on BS 80A rail, even when inclined at 1:40, and a higher conicity on grooved SEI 35G rail section.

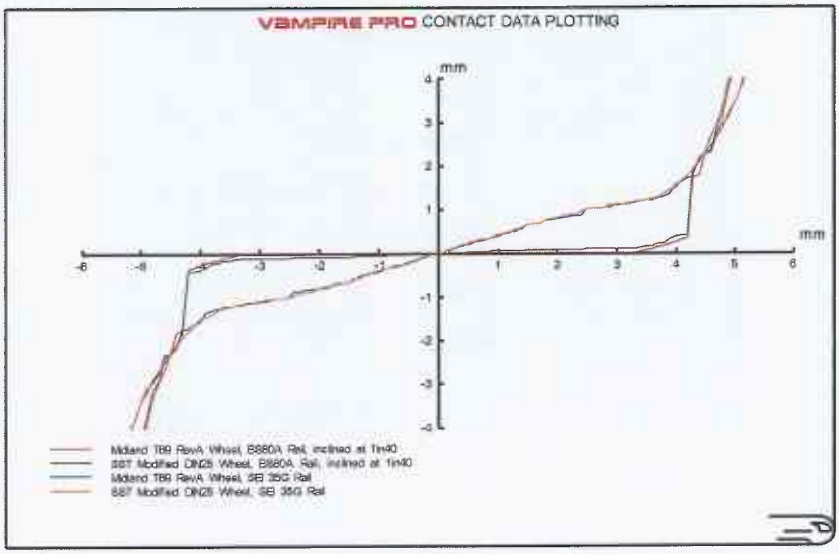

VAMPIRE Plot

Figure 3.9 – Rolling radius difference, Midland Metro and Sheffield Supertram

Based on the plots of rolling radius difference the equivalent conicity of each wheel-rail combination has been calculated using the method generally adopted in the UK. The equivalent conicity is calculated by assuming that the wheelset lateral shifts will vary according to a normal distribution about the zero shift position. A weighted best-fit line is then calculated to the slope of the rolling radius difference graph. The equivalent conicity is given by half the slope of this line.

Figures 3.10 and 3.11 below show the comparison of the equivalent conicity values obtained for grooved and non-grooved rails respectively.

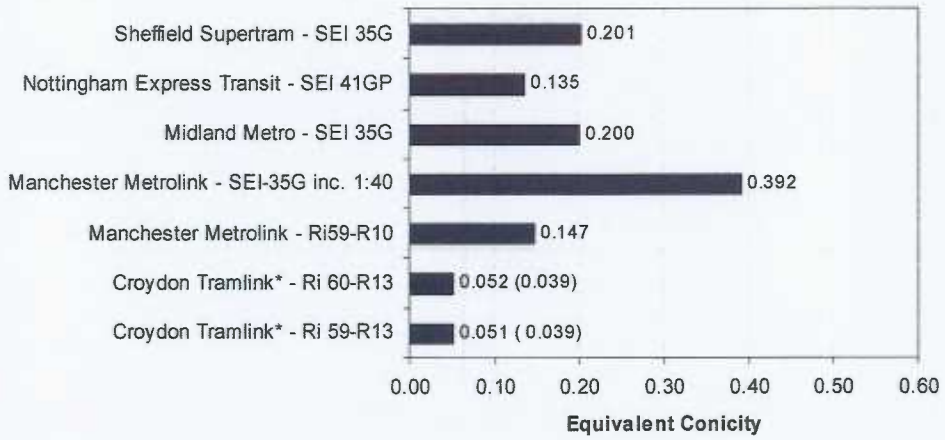

Figure 3.10 – Equivalent conicity, grooved rail sections, installed vertically unless otherwise stated (*Croydon CT3 values are in parentheses)

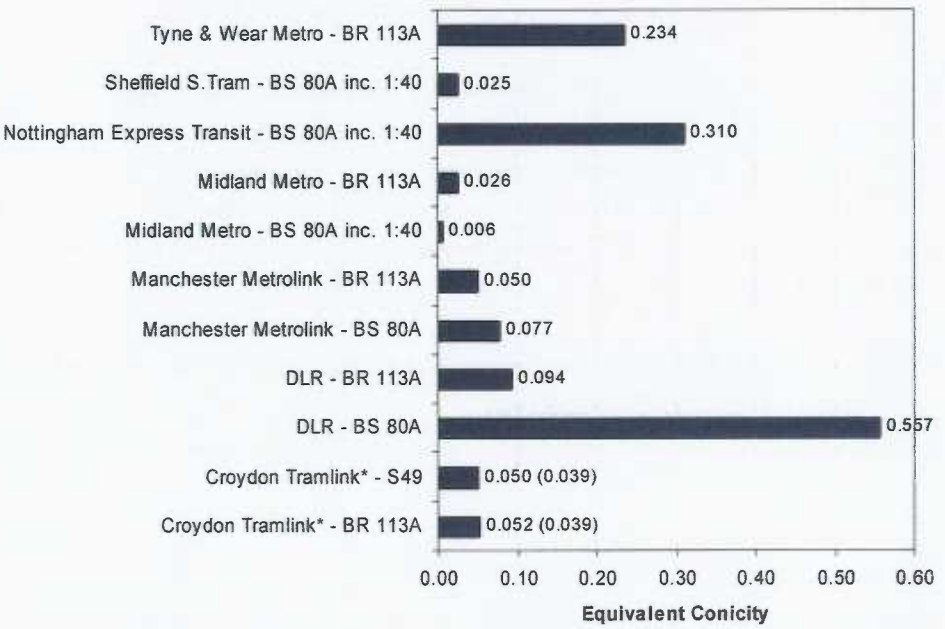

Figure 3.11 – Equivalent conicity, non-grooved rail sections, inclined at 1:20 unless otherwise stated (*Croydon CT3 values are in parentheses)

It can be seen from Figures 3.10 and 3.11 that a large variation in conicity occurs, with values ranging from 0.06 to 0.557. Generally the lower conicity values are seen on non-grooved rail sections with BS 80A producing the lowest values.

In terms of the Phase 2 objectives this variation is very positive as it demonstrates that by combining aspects of different profile combinations there is an opportunity to create wheel and rail sets which can meet the wheel-rail interface requirements of systems with widely differing characteristics. It also demonstrates that at present there doesn't appear to be a 'design for conicity' philosophy, with an apparently random distribution of conicity values evident. The ability to optimise conicity for a given system can lead to gains in terms of reduced wheel and rail wear and lowered derailment propensity.

3.1.3 Contact Angle and Wheel Lift

A useful indicator of proximity to derailment is the vertical lift or flange climb of the wheel relative to the rail, referred to as wheel lift in mm. Vertical wheel lift indicates the amount of flange climb seen by the wheel. Flange climb can be tolerated without necessarily causing derailment, so long as it is not so great as to reach the zone of rapidly reducing contact angle. When this zone is reached the probability of derailment is far greater, as the contact angle can become small. Therefore the relationship between contact angle and wheel lift can be used as guide to the protection against derailment offered by a given profile combination.

As an example, Figure 3.12 below shows a comparison of wheel lift and contact angle, plotted against lateral shift of the wheelset. The plot includes a DIN-type wheel profile (Sheffield mod. DIN25) and the more non-conventional Docklands DLR5, which includes a large flange root radius designed to allow curving down to a small radius without excessive flange contact. Both wheels are running on BS 80A rail section.

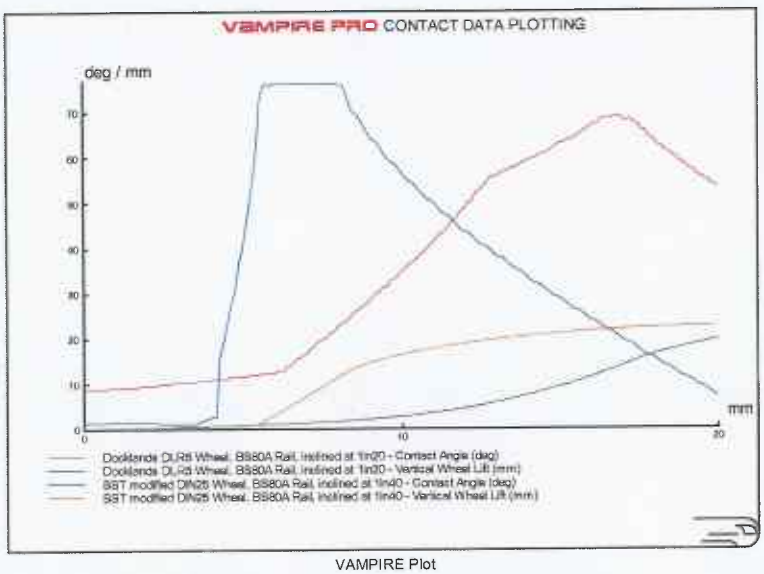

VAMPIRE Plot

Figure 3.12 – Contact angle v wheel lift

Considering Figure 3.12, which uses a combined y-axis of wheel lift in mm and contact angle in degrees, it can be seen that there is a significant difference in the contact angle and wheel lift relationship for the two profiles. The flange root of the DIN-type profile results in a very rapid rise in contact angle, once flange contact occurs. The flange angle remains high up to 8mm of lateral shift. However, significant wheel lift is occurring at this point, of approximately 10mm. Any movement beyond 8mm of lateral shift results in a rapid decrease in contact angle, whilst wheel lift continues to increase. At 15mm lateral shift the contact angle has dropped from 75 to only 30 degrees for 17mm of wheel lift. At this point derailment would be very likely.

In contrast, at 8mm lateral shift, the DLR profile shows almost no wheel lift, the increase in contact angle is far more progressive. At 15mm of lateral shift the contact angle remains in its initial rising stage, showing 60 degrees with only 8mm of wheel lift. It can be seen that for the same lateral shift, the DLR profile can generate a large rolling radius difference, together with a high level of derailment protection, provided by a high contact angle

The contact angle and wheel lift relationship of the DLR profile is a function of its intended design philosophy of steering the wheelset using the flange root. It is an extreme case but demonstrates the usefulness of this type of analysis.

Tram profiles generally exhibit the contact angle and wheel lift relationship shown by the DIN-type profile above, the full set of plots can be found in Appendix A1.

3.2 Grooved Rail Wheelset Fit

As all the UK tramway systems use grooved rail sections it is essential to understand the fit of the wheelset within the grooved rail section. The initial fit in the new 'design' condition will dictate the life-cycle performance of the wheelset in terms of available flangeway clearance and hence ability to generate rolling radius difference (ability to steer and reduce angle of attack) but also in terms of the degree to which sidewear can be tolerated before the keeper rail makes contact with the flangeback of the wheel. Additionally once keeper rail contact does occur the thickness of the keeper section is likely to dictate the remaining life of the rail section, or where significant maintenance intervention will be required.

The clearances identified in the following section should be viewed in the context of maximising the time in terms of rail sidewear before keeper rail wear occurs. It is considered that keeper wear will ultimately lead to the life expiry of the rail section as it will no longer be able to withstand the loads being imparted on it by the flangeback of the wheel and will therefore begin to present a derailment hazard.

Figure 3.13 below shows the wheelset fit for two tramway systems with very different clearances. The wheelset is shown in its central position within the track gauge in the upper plot. The centre plot shows the wheelset at the point of flange contact, the final lower plot shows the wheelset in heavier flange contact with a small amount of wheel lift. The figures adjacent to the centreline show the wheelset lateral shift from the central position.

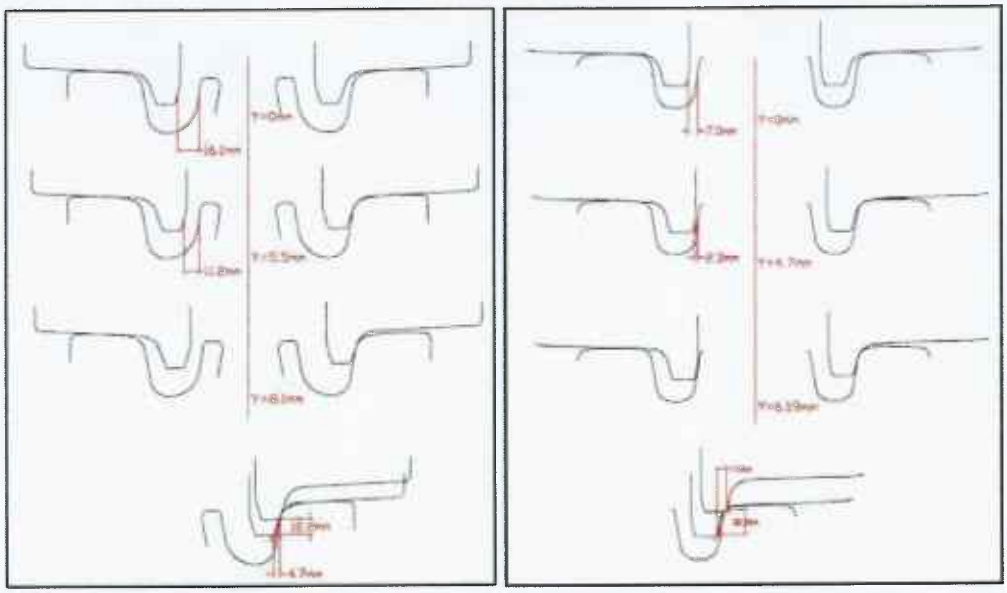

Croydon Tramlink Ri 59N Sheffield Supertram SEI 35G

Figure 3.13 – Wheelset fit

With reference to the above figures, the difference in design clearances is evident between the two systems. With the wheelset in the central position Croydon tramway shows a clearance of 16.1mm to the keeper rail, this compares to 7mm in the case of Sheffield Supertram.

When in flange contact Croydon tramway shows a good level of clearance of 11.2mm, whilst at Sheffield Supertram the clearance drops to 2.3mm. With a little further lateral shift and a small amount of wheel climb (which has been witnesses at Sheffield Supertram), the clearance to the keeper rail is eliminated completely.

It is clear from the above simple geometry manipulation that with a small amount of sidewear the wheelset at Sheffield Supertram will be wearing the keeper rail and reducing the life of the rail section, whilst in contrast, the Croydon system will have a greatly extended section life before keeper wear begins to cause problems.

In addition to the keeper clearance, Figure 3.13 also shows the approximate wheel safety height and width as described in Guidelines [5].

Table 3.1 below summarises Figure 3.13 with the addition of results from the same analysis applied to the other tramway systems.

	Tramway Network (Grooved Rail Profile)						
	Croydon Tramlink* (Ri 59-R13)	Croydon Tramlink* (Ri 60-R13)	Manchester Metrolink (Ri 59-R10)	Manchester Metrolink (SEI-35G)	Midland Metro (SEI 35G)	Nottingham Express Transit (SEI 41GP)	Sheffield Supertram (SEI 35G)
Flangeback Dim./mm	1380	1380	1362	1362	1379	1380	1379
Track Gauge/mm	1435	1435	1435	1435	1435	1435	1435
Tie Bars	No	No	No	No	No	No	No
Flangeway Clearance/mm	5.5 (6.7)	5.5 (6.7)	3.6	3.6	5.1	5.0	4.7
Keeper Clearance/mm (Centered)	16.1 (15.5)	10.0 (9.4)	**15.7**	9.3	**7.0**	14.1	**7.0**
Keeper Clearance/mm (Flanging)	11.2 (10.4)	4.7 (3.9)	**12.0**	5.5	**2.1**	9.3	**2.3**
***Safety Height/mm**	12.2 (16.9)	12.2 (16.9)	13.1	13.1	17.8	16.4	18.2
***Safety Width/mm**	4.7 (7.6)	4.7 (7.6)	6.8	6.8	7.0	6.5	7.4

Table 3.1 – Grooved Rail Wheelset Fit
(*Croydon CT3 values are in parentheses)

Considering Table 3.1, the differences in grooved rail based systems is apparent. SEI 35G offers low keeper clearance due to its relatively small groove width (see Figure 2.1), resulting in low clearances at both Midland Metro and Sheffield Supertram, whilst the wider Ri 59-R13 profiles' wider groove width allows for greater clearances. It should be noted that the small keeper clearance does not pose a great problem at Midland Metro as the system is relatively straight, this point demonstrates the requirement to design for application.

The majority of the tramway systems have flangeback dimensions nominally of 1380mm, with the exception of Manchester Metrolink, which operates at 1362mm. This difference is accommodated in the relief of the back of the flange, effectively creating increased clearance to the keeper.

None of the systems studied use tie bars, this is significant when considering that one of the major causes of premature keeper rail is gauge spread due to curving forces. The adoption of tie bars would significantly increase the life of the rail section in curved track.

Flangeway clearances, the nominal clearance between the wheel flange and the rail gauge corner, is generally in the order of 5mm, with the exception of Manchester Metrolink which operates at only 3.6mm, despite a smaller flangeback dimension. This lower value can be attributed to the lack of conformality between flange and gauge corner radius, resulting in early contact. A lack of conformality can lead to high initial rail sidewear rates, this will be discussed in more detail in Section 7 of the report.

4. Profile Selection for Simulation Cases

Due to the large number of possible combinations of wheel and rail profiles, it was essential for the later simulation work that the number of scenarios was reduced. The following section describes the profiles which were identified for further analysis work, together with reasons for their selection. The selection criterion is primarily based on the analysis carried out in the previous sections.

4.1 Selected Wheel Profiles

Table 4.1 below shows the five wheel profiles currently proposed for the simulation work. These profiles were approved at the working group meeting held on 13th July 2007.

Case	Profile	Reason(s) for Selection
A1	NET P-3102639	Medium-high conicity on grooved / non-grooved rail
		Conformal contact conditions
		Dual cone angle of tread, benefits conicity and conformality
A2	SST Mod DIN25	Replaces Midland Metro as almost identical
		Different flange root radius and cone angle to NET DIN-type
		Good conicity on SEI 35G
B	Metrolink MML2	Use of flangeback cut-out for potential tram-train application
		Round tip flange design
C	Croydon CR4000	Consistent contact conditions across a range of rail profiles
		15mm flange root radius
D	CT3	Tramway optimised profile
		Good contact and conicity conditions, 15mm flange root radius

Table 4.1 – Proposed Wheel Profiles

The proposed wheel profiles offer a range of characteristics which should, when combined with a suitable rail section, cover the likely demands of many types of tramway system design layouts. The philosophy of the Phase 2 work is that this will be demonstrated through vehicle dynamic simulation as described in Sections 6, 7 and 8 of the report.

Table 4.2 below summarises the profiles rejected and the reason for rejection.

Profile	Reason(s) for Non-Selection
Midland Metro	Similar profile geometry and contact conditions to SST
Tyne & Wear	Conventional mainline railway profile

Table 4.2 – Rejected Wheel Profiles

4.2 Selected Rail Profiles

Rail profiles were selected primarily on the basis of current frequency of use, availability and also whether they could be represented by another profile, i.e. some profiles could be eliminated as they are identical to other profiles other than for example groove width and depth.

The following section outlines the rail profiles, both grooved and non-grooved, which were selected for further analysis work. The suggested combinations were agreed at the working group meeting held on the 13th July 2007.

4.2.1 Grooved Rail Profiles

Through analysis of the Phase 1 report, Figure 4.1 (also Figure 2.1) was created which allows the comparison of head and groove profile for effectively all the grooved rail sections commonly used and available to tramways.

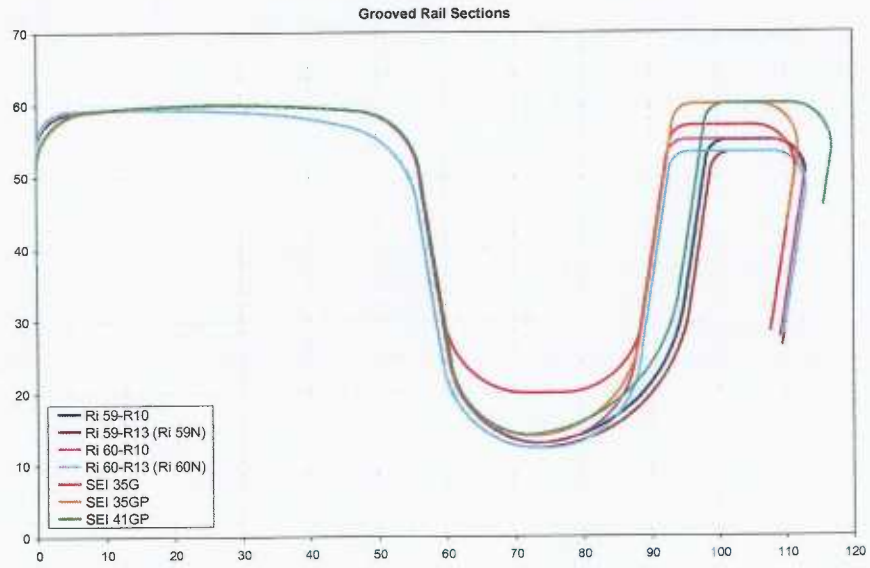

Figure 4.1 – Grooved Rail Profiles

With reference to the above figure it can be seen that essentially there are only two types of rail head profile, the Ri 59/60-R10 (10mm gauge corner radius) and the Ri 59/60-R13, which has a 13mm gauge corner radius and is inclined at 1:40, as opposed to vertically for the other profiles. Otherwise the differences between the profiles are due only to the groove depth and keeper rail clearance, thickness and height.

Table 4.3 below shows the grooved rail sections selected for the simulation stage of the Phase 2 work and reasons for selection.

Case	Profile	Reason(s) for Selection
A	Ri 59-R10	Identical rail head profile to other grooved rail sections
		10mm gauge corner radius
B	Ri 59-R13 (Ri 59N)	Inclined rail head profile, 1:40
		13mm gauge corner radius

Table 4.3 – Selected Grooved Rail Sections

As can be seen from the above table, just two grooved rail profiles cover the required rail head shape. The wide variation of groove width will be accommodated within the VAMPIRE® simulations through variation of the track design parameter file. Parameters such as groove depth and keeper thickness will be presented in the 'Best Practice' guide [9].

4.2.2 Non-Grooved Rail Profiles

The selection of non-grooved rail section was more complex than that of the grooved rails as there is a lack of similarity in the head profiles. However, the profiles selected and the reason for selection are summarised in Table 4.4 below.

Case	Profile	Reason(s) for Selection
A	BS 80A (1:20 and 1:40)	Frequently used on UK tramway and light rail systems
		Generally results in low conicity unless inclined at 1:40
B	BR 113A (1:20)	Frequently used on UK tramway and light rail systems
		Benefits for future 'Tram-Train' links
C	S49 / UIC 54 (1:20)	Frequently used on European tramway systems

Table 4.4 – Selected Non-Grooved Rail Sections

5. Vehicle Dynamic Simulation Overview

A key objective of this profile optimisation study is to assess the performance of the short-listed profiles (see Section 4 for details on the profile selection) with respect to derailment protection and minimisation of wheel and rail profile wear. This analysis was performed using the VAMPIRE® railway vehicle dynamics simulation software.

5.1 The VAMPIRE® Package

VAMPIRE® has been developed and validated over a number of years, formerly by BR research and latterly by AEA Technology Rail (now DeltaRail Ltd). VAMPIRE® uses a multi-body modelling method, where a dynamic system, such as a rail vehicle, can be considered as a collection of rigid bodies, with masses acting at their geometric centres. These bodies are then interconnected by massless spring and damper elements to build up a complete system representing the vehicle. Equations of motion are generated automatically, along with contact tables to represent wheel and rail geometry. As VAMPIRE® is specifically written for the simulation of rail vehicles, small angle approximations are used, to increase solver speed, resulting in low simulation times, without sacrificing accuracy over the small angles involved.

VAMPIRE®'s post-processing capabilities include statistical, time and frequency domain analysis, peak counting, stability and wheel-rail wear algorithms, along with the ability to model suspensions with coulomb friction and dynamic normal forces.

5.2 Generic Vehicle Model

The adopted philosophy in terms of vehicle dynamic modelling is to use a 'generic' vehicle model which is capable of representing the majority of vehicle configurations identified in Section 2.5. Neglecting Blackpool tramway and the National Tramway Museum, six out of the remaining seven vehicles use conventional axles, with two of these being equipped with independently rotating wheel (IRW) equipped trailer-trucks. NET tramway is the only operator to use all independent wheels but these are powered. At the time of writing the degree to which powered IRW's behave as conventional wheelsets was un-confirmed.

Given the above, the chosen approach was to use a vehicle model which combined a powered bogie with conventional axles, but also incorporated an IRW equipped trailer-truck section. This would cover the general performance of six of the seven UK tram vehicles.

It could be suggested that this approach does not accommodate other aspects which may effect the steering, derailment resistance and likely wheel-rail wear of a tramway vehicle, however, limits must be imposed to be able to practically analyse a large combination of wheel and rail profiles.

The fundamental basis of the generic approach is to provide a relative indication of the performance advantages of a particular wheel and rail profile combination. This can be achieved using a single generic vehicle model as the improvements will in the most case carry over to vehicles with differing articulation lengths, wheel bases etc, of course the magnitude of potential gains my differ but the general improvement trend will remain.

5.2.1 Generic Vehicle Overview

The vehicle selected as a generic vehicle model is a bi-directional tram, with driving cabs at both ends, consisting of two car bodies connected by an intermediate articulated section.

The two main body sections are coupled to the centre section by spherical joints and therefore the centre bogie supports the end mass of these two sections, together with the centre section.

The two outer bogies are powered using a mono-motor setup i.e all four wheels driven together, the primary suspension arrangement uses a twin rubber conical spring arrangement acting on an outboard axlebox, a level of damping is provided by the spring's rubber construction (hysteresis). Secondary suspension is provided via a bolster, to the car body, using airsprings, and is equipped with lateral and vertical hydraulic dampers. The primary arrangement is shown in Figure 5.1 below.

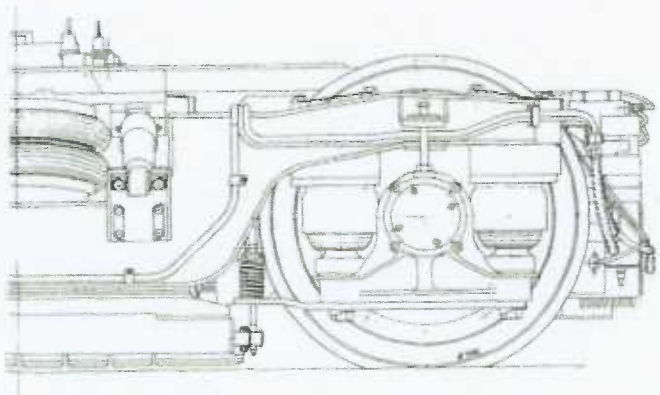

Figure 5.1 – Motor Bogie Primary Suspension Arrangement

A slewing ring provides bogie rotation relative to the body, this is a low friction interface and does not provide significant rotational damping or stiffness to the bogie.

The central trailer bogie is quite different to the two motor bogies, operating with independently rotating wheels, this permits a low floor between the two outer bogies. Primary suspension on the trailer bogie is a less conventional bell-crank type arrangement, a radial arm extends behind the wheel, as shown in Figure 5.2, and supports the wheel within the bogie frame, via a large radial bearing. The stiffness is provided by a metalastic type chevron spring shown directly above the radial bearing. This also provides a level of damping through its rubber elements.

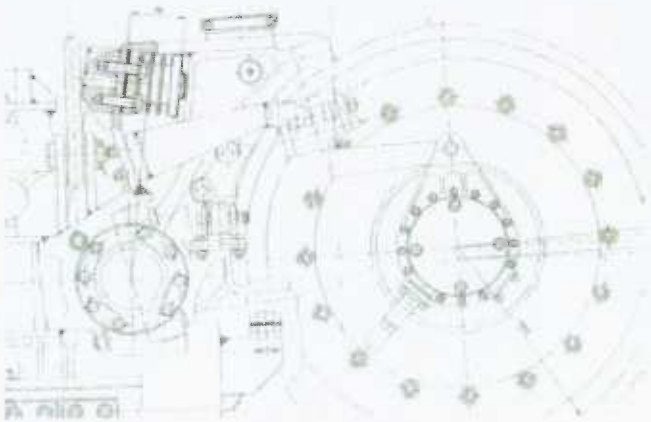

Figure 5.2 – Trailer (centre vehicle) Primary Suspension

Secondary suspension is provided by airsprings mounted directly between bogie and body. Longitudinal (traction and braking) restraint between the body and bogie is provided by traction stops, rather than the rods used in the motor bogies, lateral bumpstops also act between body and bogie. Secondary damping is provided both laterally and vertically by hydraulic dampers.

5.2.2 The VAMPIRE® Model

The generic vehicle model was setup and validated using the calculated inter-body static loads and frequency response data from the manufacturers report. The vehicle model is shown in Figure 5.3 and consists of the following elements:

- 16 Masses
- 6 Linear springs
- 16 Shear springs
- 7 Viscous dampers
- 4 Bumpstops (non-linear springs)
- 11 Pin links

- 20 Bush elements

The model consists of 102 Degrees of Freedom (DoF).

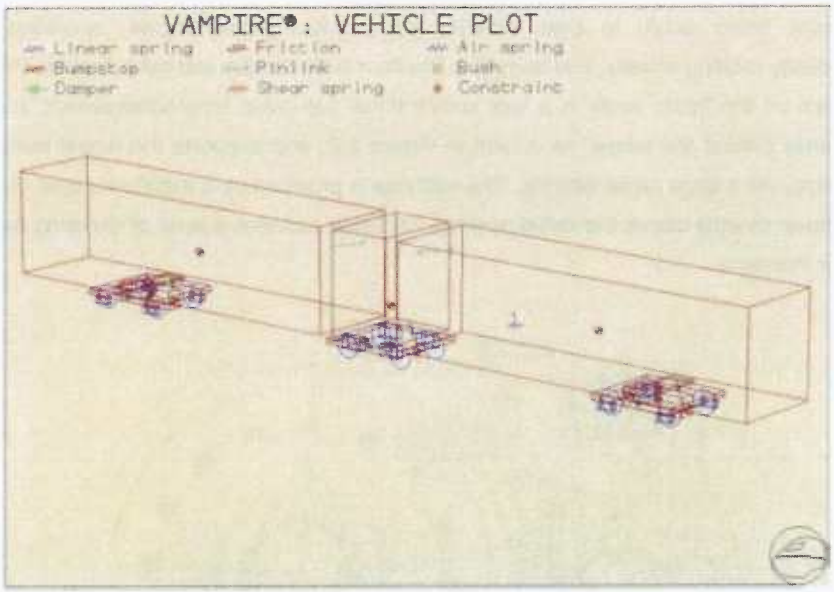

Figure 5.3 – VAMPIRE® Generic Vehicle Model

5.2.3 Motor Bogie Model

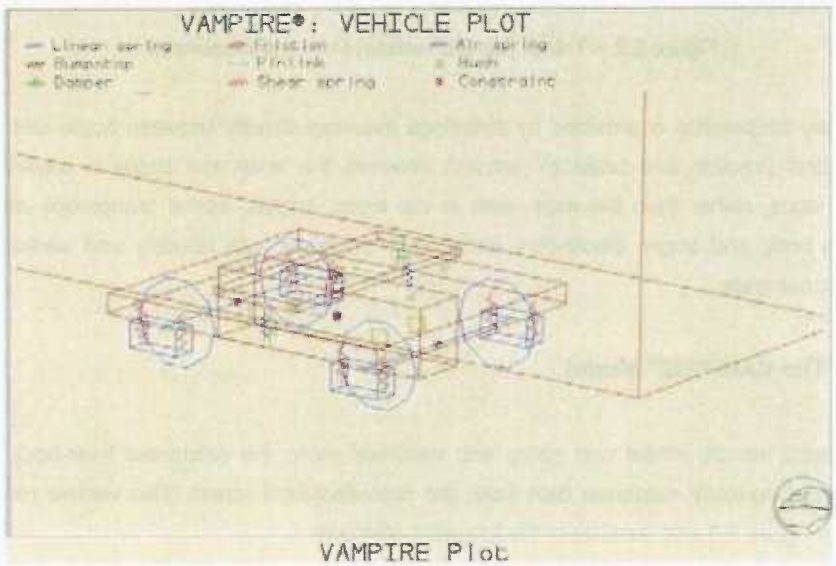

Figure 5.4 – VAMPIRE® Motor Bogie Model

With reference to Figure 5.4 above, the primary suspension was set up using two shear springs per axlebox, providing longitudinal, lateral and vertical restraint to the wheelset. The

bolster and slewing ring were incorporated as a separate mass, connected to the body via a bush element and to the bogie via the secondary suspension. Pin link elements allowed accurate representation of the inclined secondary lateral hydraulic dampers and traction rods. Vertical secondary damping uses a standard damper element. Airspring elements were used to represent the installed airsprings.

5.2.4 Trailer Bogie Model

With reference to Figure 5.5, the trailer bogie model was developed around the bell-crank suspension arrangement, these can be seen as rectangular boxes around the wheels, with a pivot bush used at their lower inner corner to represent the radial bearing.

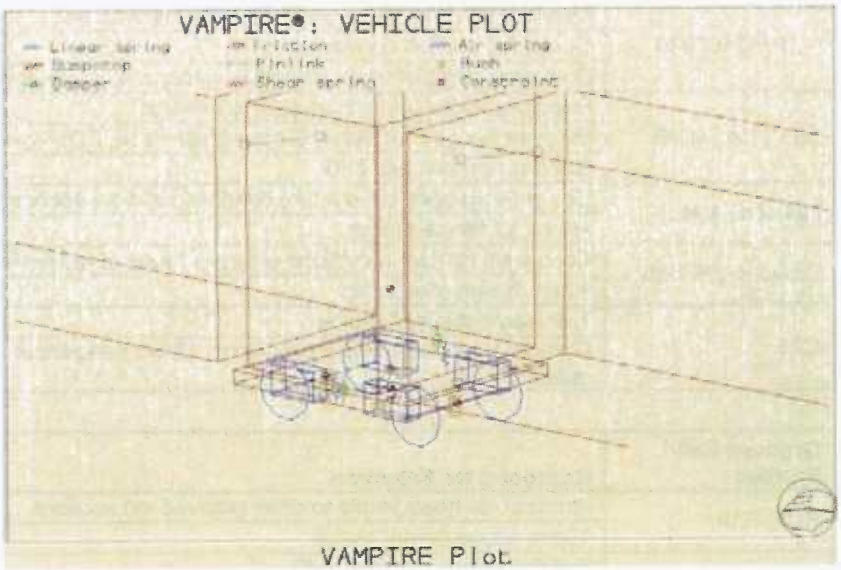

Figure 5.5 – VAMPIRE® Trailer Bogie Model

The primary springs were attached to the bell-crank arrangement. This essentially gives the wheelset only a vertical degree of freedom (actually a rotation about the bell-crank), as the radial bearing provides a relatively high stiffness in the other directions. There was no separate bolster mass in the trailer bogie model, the airsprings are connected directly to the body and no slewing ring is required, the centre bogie acting as a 'truck' and assuming a tangential position in curves.

The secondary suspension incorporates a single lateral damper, represented by an inclined pinlink. The two vertical dampers are modelled using standard linear elements. Airspring elements are used to represent the airsprings. Traction stops and lateral bumpstops are included between the bogie and body.

6. Dynamic Simulation – Derailment Study

The following sections (6, 7 and 8) detail the results of the simulation studies. In total, five wheel and six rail profile combinations (30 sets) were analysed. Later in the work additional simulations were performed with modified wheel and rail profile configurations, these will be documented later in the report.

Table 6.1 below describes the five wheel and six rail profile combinations selected as a result of the initial contact study described in Section 4.

Case	Wheel Profiles	Reason(s) for Selection
A1	NET P-3102639	Medium-high conicity on grooved / non-grooved rail
		Conformal contact conditions
		Dual cone angle of tread, benefits conicity and conformality
A2	SST Mod DIN25	Replaces Midland Metro as almost identical
		Different flange-root radius & cone angle to NET DIN-type
		Good conicity on SEI 35G
B	Metrolink MML2	Use of flangeback cut-out for potential tram-train application
		Round tip flange design
C	Croydon CR4000	Consistent contact conditions across a range of rail profiles
		15mm flange root radius
D	CT3	Tramway optimised profile
		Good contact and conicity conditions, 15mm flange root radius

Case	Grooved Rail Profiles	Reason(s) for Selection
A	Ri 59-R10	Identical rail head profile to other grooved rail sections
		10mm gauge corner radius
B	Ri 59-R13 (Ri 59N)	Inclined railhead profile, 1:40
		13mm gauge corner radius

Case	Non-grooved Rail Profiles	Reason(s) for Selection
A	BS 80A (1:20 and 1:40)	Frequently used on UK tramway and light rail systems
		Generally results in low conicity unless inclined at 1:40
B	BR 113A (1:20)	Frequently used on UK tramway and light rail systems
		Benefits for future tram-train links
C	S49 / UIC 54 (1:20)	Frequently used on European tramway systems

Table 6.1 – Wheel and rail profiles selected for simulation

In order to assess the performance of the selected wheel and rail profile combinations, two dynamic simulation case studies were developed. The first study was used to assess the derailment protection offered by each of the profile combinations, by subjecting the vehicle to

severe track twist and curvature, the second study employs a curvature assault course and was used to assess steering ability, predicted wear levels and contact stress. An additional stability study was carried out to investigate application of higher conicity profiles to independent wheel equipped bogies, this is detailed in Section 8.

All profiles were simulated in their new condition, with 1435mm track gauge and a flangeback spacing relevant to the system from where the wheel profile originated. The generic vehicle model in a tare loading condition was used for all simulations. The tare condition was selected based on it being the worst case in terms of derailment propensity. A friction coefficient of 0.30 for wheel and rail was used in the curving study and 0.4 for the derailment study.

Following analysis of the simulation work, the combinations of profiles listed above will be reduced in number, to form profile sets. The profile sets will contain wheel and rail profiles which have through the simulation work, been demonstrated to be compatible with each other, in terms of maximising derailment protection and minimising wheel and rail wear. The final selection of profiles sets will be explained in Section 9.

As there are a large number of simulation cases, the entire set of simulation results will not be presented in the body of the report, only those which are most relevant to the final profile selection. A complete set of simulation results is provided in the Appendix.

6.1 Derailment Study Overview

As described above, a method was required to assess the derailment protection offered by each of the selected wheel and rail profile combinations. The proximity of a wheel and rail profile to derailment is usually assessed through analysis of the Y/Q ratio, this is a ratio of the lateral force (Y) to the vertical force (Q), acting on a wheel attacking the gauge corner of the rail. The simplified forces acting on the wheel and rail can be seen in Figure 6.1 below.

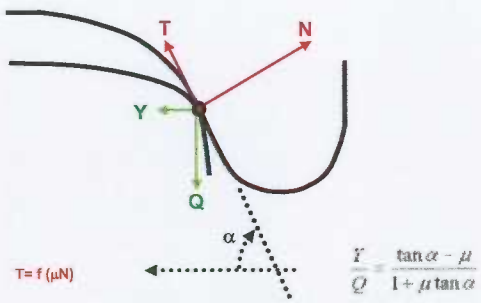

Figure 6.1 Y/Q relationship

If the component of T (a function of μ and N) exceeds the combined component of Y and Q then flange climb will initiate. The Nadal formula dictates that a Y/Q ratio of 1.2 is the limiting value for a flange angle of 68 degrees with a typical friction coefficient.

The Y/Q ratio is an approximation of the proximity of the wheelset to derailment, therefore supplementary data is extracted from the simulation, this includes the amount of wheel lift or flange climb and also the change in vertical load on a wheel, in relation to the static load, denoted as the ΔQ/Q ratio. Typically in a dynamic situation a limit value of 0.8 (80% unloading) of the wheel is permitted.

In general it is not straightforward to derail a railway wheelset, often curvature alone is not sufficient as cant deficiency tends to load the wheel attacking the flange, thereby increasing the 'Q' value and maintaining resistance to derailment. Typically, to cause derailment it is necessary to have an increased lateral force 'Y', combined with a reduction in vertical load 'Q'. In practice this usually occurs due to either one or a combination of track twist and cant excess (unloads flanging wheel), cant excess often occurring due to low speed running, possibly through speed restrictions etc. In order to fully understand the derailment protection offered by the selected wheel-rail combinations, the derailment simulation scenario must promote flange climb derailment, this will reveal the extent of derailment protection at the extremes of operating conditions. Figure 6.2 shows the VAMPIRE® track file developed to promote flange climb derailment within the simulations.

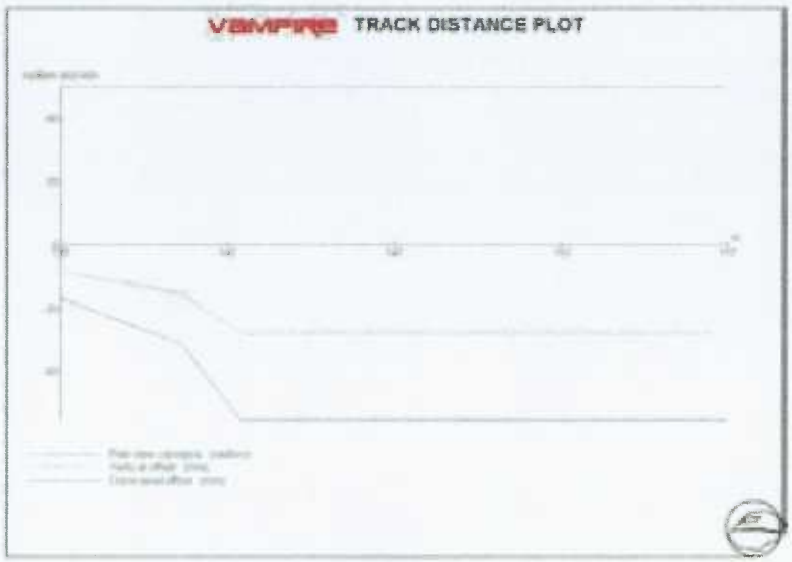

Figure 6.2 – Derailment study track file

With reference to the Figure 6.2, the y-axis is a combined axis representing curvature in rad/km, vertical track position and crosslevel (cant) both in mm.

A constant 20m curve radius (50km^{-1} curvature) is combined with a two-part twist profile of 1:200 across the bogie centres and 1:75 across the bogie wheelbase. The track twist is achieved through application of the vertical and crosslevel profiles shown in the above figure and pictorially in Figure 6.3. The vehicle traverses the track section at approximately 10kph, resulting in a 50mm cant deficiency in the steady-state section of the profile. This is deemed to be a typical value based on light rail system speed/cant/curvature profiles.

To further promote flange climb, the friction coefficient between wheel and rail was increased from a typical value of 0.32 up to 0.4.

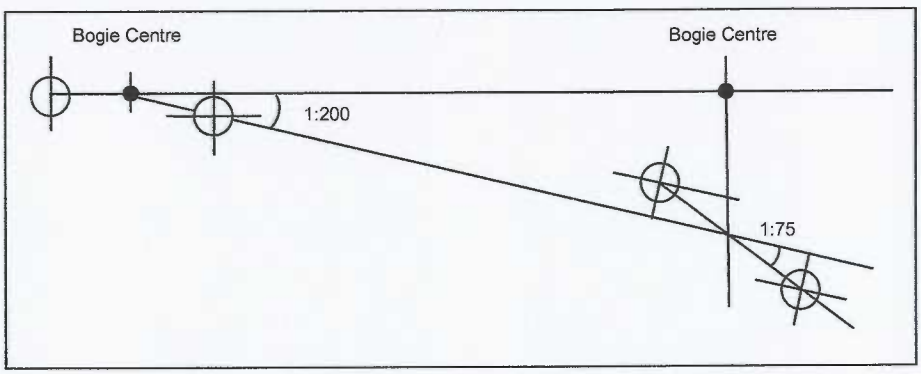

Figure 6.3 - Track twist profile applied in derailment study

Figure 6.3 above illustrates the track twist profile applied in the derailment case study, this is in addition to a constant curvature of 20m radius.

The application of a small radius curve promotes derailment through generation of a high angle of attack between the wheel and rail, this in turn moves the contact patch forward of the axle centre line and reduces the effective flangeway clearance, all these factors increasing the risk of derailment. The lateral force is also increased (an increase in 'Y') through cant deficiency and attack angle.

The application of a twist profile unloads the leading wheel which is attacking the high rail, this reduces 'Q'.

An increase in the flange friction coefficient increases the climb-out force, 'T', which is opposed by the 'Q' force, therefore this is effectively a reduction in 'Q' (see Figure 6.1).

6.2 Derailment Study Results

The derailment study involved subjecting the vehicle and wheel-rail combinations to the VAMPIRE® track file and simulation scenario described above.

Results and commentary are presented for Y/Q ratio, wheel lift, contact angle and angle of attack, for typical cases. Before presenting the detailed results, a summary of the results is described.

6.2.1 Derailment Study – Results Summary

The first point to note from the derailment simulations is that the Manchester Metrolink (MML) profile in the new condition derailed when combined with any of the six rail sections. In contrast there were no simulated derailments for any of the other wheel profiles.

The cause of the problem with the MML profile is believed to be associated with the flange shape, as shown in Figure 6.4 below.

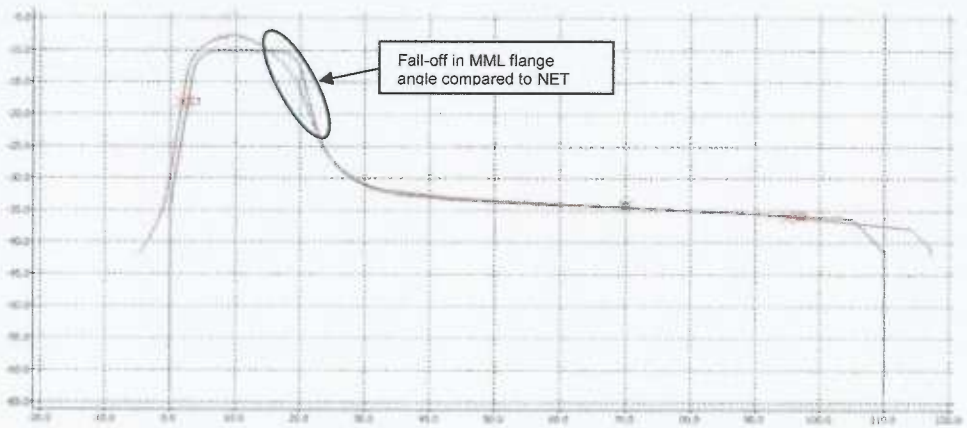

Figure 6.4 – MML (red) and NET (blue) wheel flange shapes

With reference to the above figure which shows the MML and the Nottingham Express Transit (NET) wheel profiles, it can be seen that MML profile has a significantly greater flange height, which would perhaps suggest greater derailment protection. However, the flange angle can be seen to drop off rapidly at the blend of the flange root radius and flange face (-25 on y-axis), when compared to the NET profile.

It will be seen from Figure 6.5 and 6.6 below that this flange shape encourages wheel lift and it is this lift which further encourages derailment.

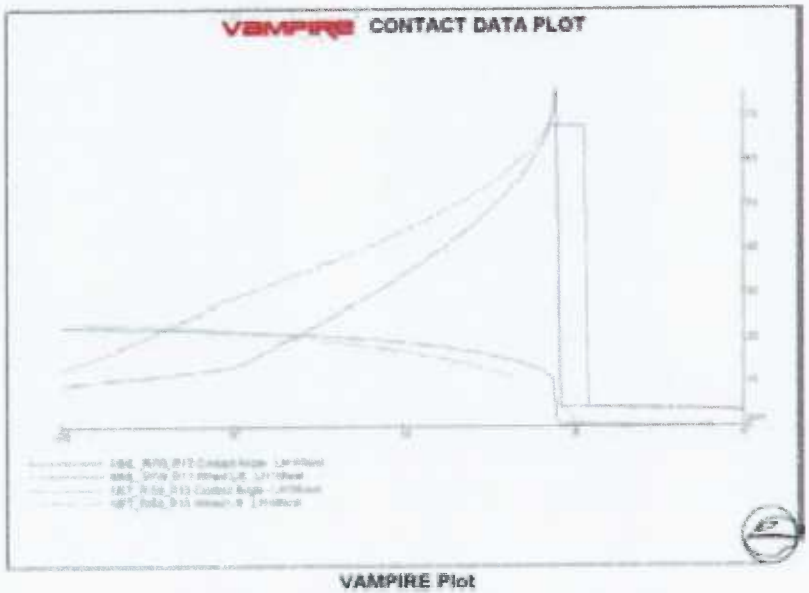

Figure 6.5 – MML and NET contact angle v wheel lift

Figure 6.5 shows the relationship between contact angle, the angle of the plane of the contact patch to the horizontal, and the vertical lift (flange climb) of the wheel plotted against lateral shift of the left wheel when moving towards the rail gauge corner.

The contact angle between wheel and rail is critical to protecting against derailment, a certain amount of wheel lift can be tolerated, providing that the contact angle remains high enough so as to cause the wheel to drop back down into the gauge. The above plot would suggest that the MML wheel profiles is superior in this sense to the NET profile as the contact angle does not fall off as rapidly and also has a distinct sustained contact angle of 68°, just under 5mm on the x-axis. Also the wheel lift is less for a given lateral shift. So in summary for any lateral shift the MML, wheel lift is lower and the contact angle is higher, suggesting higher derailment protection than the NET profile. It is only when looking closer at the wheel lift to lateral shift relation that the reason for the MML wheels inferior derailment performance becomes apparent.

Figure 6.6 below shows the relationship between wheel lift, as presented above but without the contact angle, plotted against the lateral shift of the wheelset, but for all five wheel profiles studied, on Ri 59-R13 embedded rail.

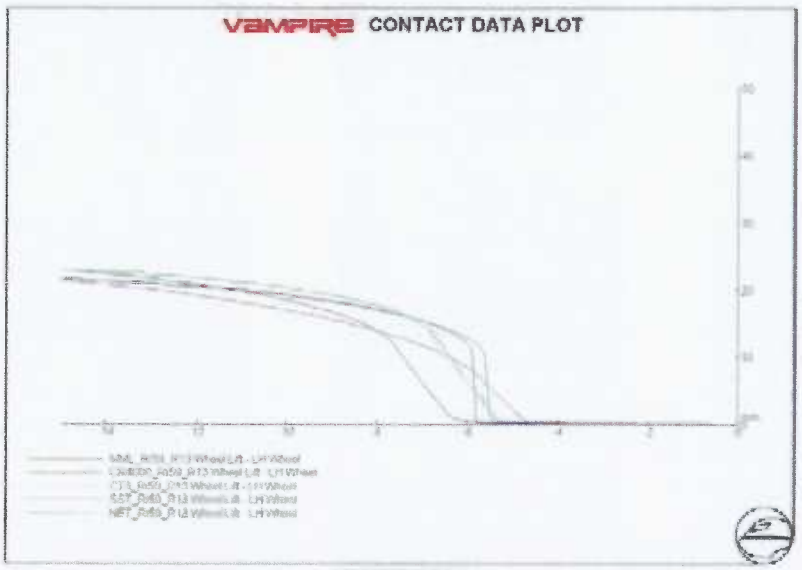

Figure 6.6 – Wheel lift characteristic – all wheel profiles

With reference to the above figure, there is a clear difference between the wheel lift characteristic of the MML profile when compared to the other wheels studied. Wheel lift begins early at around 4.8mm lateral shift and has an initially lower gradient, particularly when compared to the DIN-type tramway profiles such as NET and SST. At the point where the flange root radius meets the flange face, around 5.6mm lateral shift the rounding off of the flange face (see Figure 6.4), causes a significant further reduction in the slope of the wheel lift relation.

Despite a higher contact angle, the slope of the wheel lift relation seems to govern the likely climb-out behaviour of the wheel, the characteristic relates well to the simulated derailment performance and the observed shape of the profile seen in Figure 6.4. All profiles with steeper wheel lift gradients resisted derailment, even with higher absolute lift values and lower contact angles.

Therefore it can be concluded that the relation between wheel lift and contact angle, particularly the gradient of the lift characteristic has a significant effect on derailment propensity.

Due to the simulated derailments using the new condition MML wheel profiles, additional simulations were performed combining new wheels with worn rails and worn wheels with new and worn rails.

It was found that the new wheel also failed the derailment assault course when running on a worn rail profile, however when a worn wheel profile was simulated, this resisted derailment when running on both new and worn rail profiles.

It should be noted that the derailment assault course used in this study is an extreme derailment assessment and the track geometry used would fall outside any system twist limits, therefore the fact that the MML profile exhibits a tendency to derail when subject to this track geometry does not indicate, in absolute terms, that the wheel profile is unsafe, only that it has a lower protection against flange climb derailment relative to the other profiles studied.

With regard to the general derailment performance of the selected wheel profiles, the study shows that the SST and NET profiles, both DIN-type profiles, offer the greatest resistance to flange climb. This is evidenced through a generally lower Y/Q level across the six rail profiles simulated and a consistently high contact angle. The high contact angle is a function of the relatively steep flange angle (70-75°) and also the flange tip geometry, where the flange angle is sustained up to the point where the flange face meets the tip radius.

The Croydon Tramlink CR4000 and CT3 profiles show greater levels of wheel lift across all rails sections, this is a function of their greater flange root radius, which promotes tread lift through the flange root running up the gauge corner. This does not necessarily result in greater derailment risk as a high contact angle is maintained throughout the wheel lift stage.

The SST profile shows generally low levels of wheel lift, with the exception of when combined with S49 rail at 1:20 inclination and BS 113A at 1:20, where wheel lift become significantly greater, typically 7-8mm. This is caused by the interaction of the flange root and gauge corner radii at 1:20 inclination. Effectively, the gradient of the wheel lift versus lateral shift characteristic becomes greater for these tow profiles, resulting in higher lift values. A high contact angle sustains good derailment protection.

The NET profile shows a similar trend to the SST wheel but shows increased lift when combined with BS 80A rail inclined at 1:40. Similarly, the amount of wheel lift is a function of the combination of flange root and gauge corner radius at a given rail inclination. As is the case with all profiles other than MML, resistance to derailment is maintained through a consistently high contact angle and high gradient of the wheel lift, lateral shift relation.

As would be expected, the response of the vehicle to the severe twist and curvature profile of this study results in high Y/Q values, typically lying in the range of 1 to 1.2 for all profiles, with the exception of the MML profile which exceeds these levels at derailment. It is interesting to note that despite these high Y/Q values derailment is not predicted for any profile other than MML, highlighting the conservatism of the Nadal Y/Q quotient.

The angle of attack indicates how far a wheelset has moved from a radial steering position. If a wheelset is steering perfectly then there will be a zero angle of attack. In very low radius curves, steering is completely broken down and the angle of attack becomes high. The higher the angle of attack, the greater the risk of derailment (See Figure 6.7).

Due to the fact that at very low radius steering has broken down for all the wheel profiles, the angle of attack essentially becomes the same for all profiles. This is because at these radii, the angle of attack becomes a simplified function of the bogie wheelbase, curve radius and flangeway clearance, see Figure 6.8.

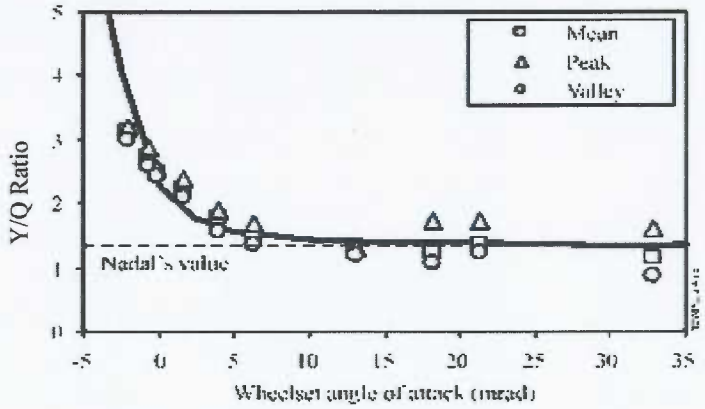

Figure 6.7 – Influence of angle of attack on Y/Q ratio

Figure 6.7 above demonstrates that increasing angle of attack rapidly reduces the limit value of the ratio of Y/Q. Above angles of approximately 15mrad angle of attack, the reduction reaches a steady state value. It can be seen that the Nadal limit value of 1.2 represents a conservative, worst case value, accommodating large angles of attack.

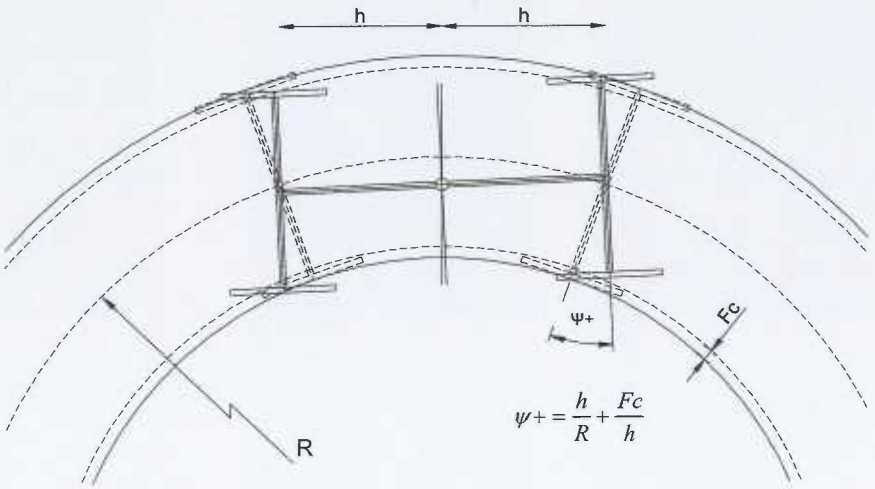

Figure 6.8 – Approximation of angle of attack – (ineffective steering)

With reference to Figure 6.8, when steering breaks down within a small radius curve, the angle of attack Ψ+, effectively becomes equal to a function of the above parameters. For this reason all the profiles show a very similar angle of attack in the derailment assessment which uses a very small curve radius of 20m.

The following section presents a number of plots illustrating the results described above in the summary of the derailment study.

6.2.2 Derailment Study – Wheel Lift

Figure 6.9 below shows the wheel lift characteristic for all the studied wheel profiles when combined with S49 rail inclined at 1:20.

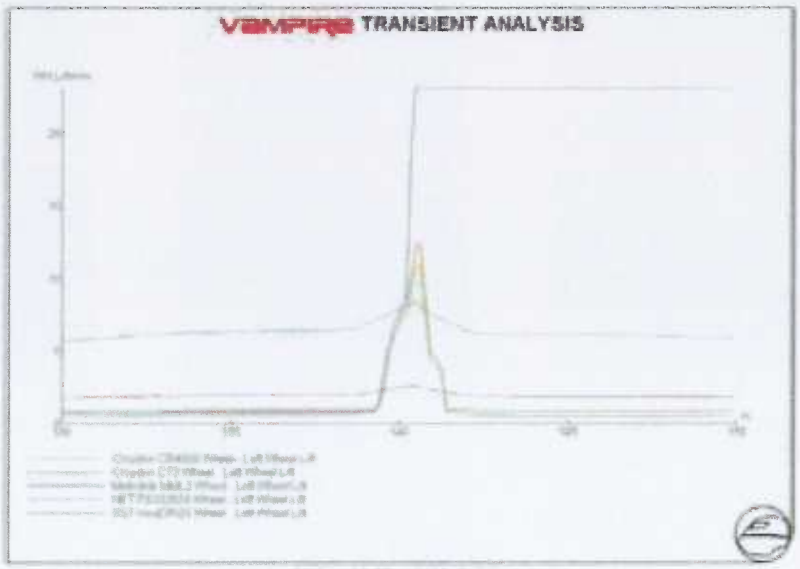

Figure 6.9 – Wheel lift for all profiles on S49 1:20 Rail

It can be seen that the lift characteristics vary considerably across the wheel profiles. The typically higher lift values of the CT3 and CR4000 profiles with a larger 15mm flange root radii, is evident. In this case the SST profile is showing significant lift compared with the similar NET DIN-type profile, the difference between the two being attributed to small differences in flange root radius. As in all rail cases studied, the MML profile derails and this is reflected in the large wheel lift.

Figure 6.10 below shows the wheel lift relation for the selected wheels when running on S49 rail inclined at 1:40, an inclination which matches that of the Ri 59-R13 (Ri 59N) embedded rail section.

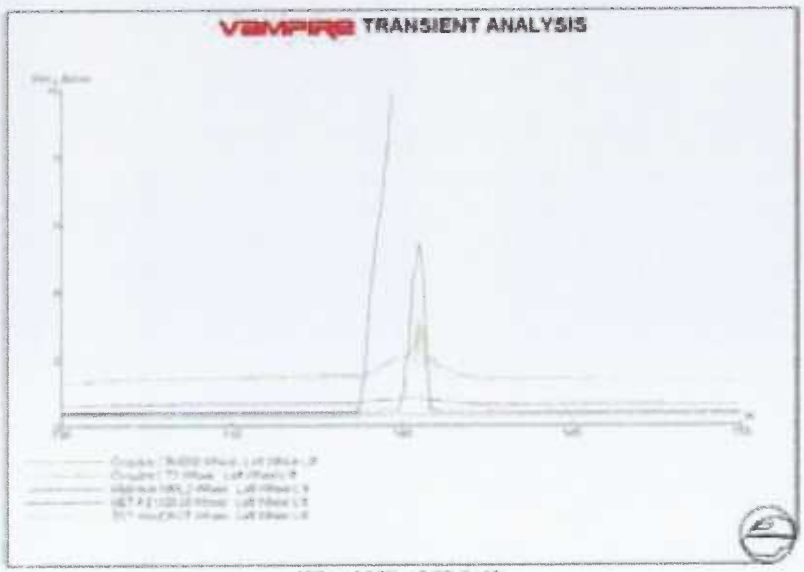

Figure 6.10 – Wheel lift for all profiles on S49 1:40 Rail

With reference to the above plot, the MML profile extends to over 20mm lift due to derailment, therefore the y-axis has been re-scaled to allow a clear view of the profiles which do not derail.

It can be seen that the DIN-type profiles show almost zero lift, with the CT3 profile also showing a low level of wheel lift with a value of approximately 3mm. This compares to 5mm for the CR4000 profile. When compared to Figure 6.9, the above plot illustrates the influence of rail inclination on the flange climb (wheel lift), behaviour. As identified previously, a high contact angle prevents wheel lift continuing and promoting derailment.

When installed inclined at 1:40, it is likely that the S49 profile would be combined with Ri 59-R13 (effective 1:40 rail head inclination), street running grooved rail. Figure 6.11 below illustrates the wheel lift experienced by the wheel profiles when running on this rail section.

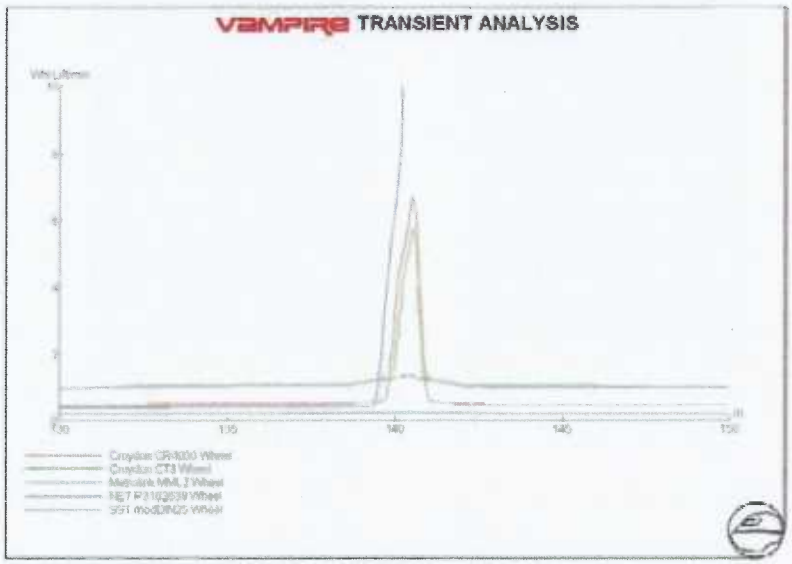

Figure 6.11 – Wheel lift for all profiles on Ri 59-R13 Grooved Rail

A similar trend as seen with S49 rail exists when running Ri 59-R13, in that the DIN type profiles of SST and NET, show low lift values, whilst the 13mm flange root radius profiles of the CT3 and CR 4000 show higher values. Again the MML profile results in a simulated derailment.

The wheel lift plots presented in this section are typical of the results across the six rail profiles selected. Generally, other than where highlighted, the DIN-type profiles show lower wheel lift values. The CT3 and CR4000 profiles show generally higher lift, with the CT3 being lower than the CR4000. In all cases high contact angles were maintained, with Y/Q ratios of between 1 and 1.2.

6.2.3 Derailment Study – Contact Angle

The following section presents the contact angles for the cases of S49 rail inclined at 1:40 and Ri 59-R13 grooved rail. These correspond to the wheel lift plots presented in Section 6.2.2 above.

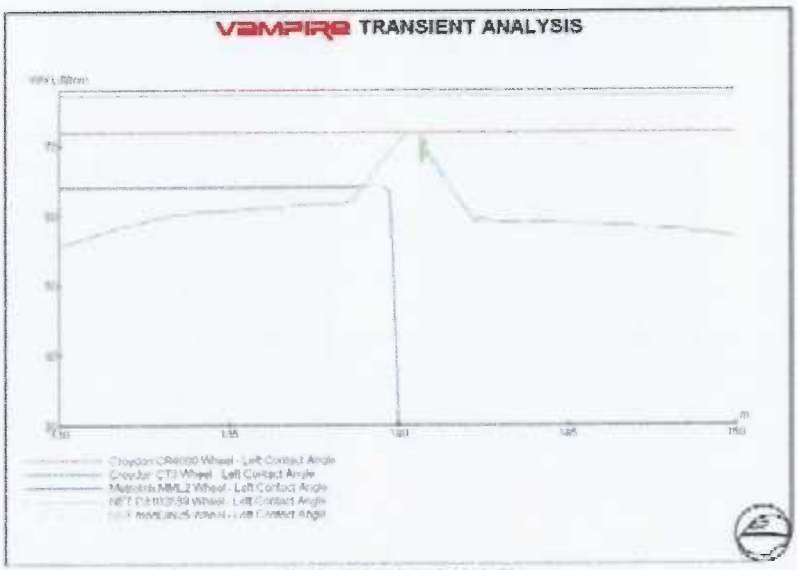

Figure 6.12 – Contact angle for all profiles on S49 Rail at 1:40

Figure 6.12 above shows a typical contact angle plot, NET and SST show a consistently high contact angle, with the small wheel lift assisting in maintaining this constant relation. The high contact angle is provided by the use of a 76° flange face angle.

The CT3 profiles can be seen to have a more non-linear contact angle relationship than the similar CR4000 wheel, the CT3 profile showing an increase in contact angle as the wheel begins to lift. It is this effect which maintains derailment protection.

Similarly the contact angle is plotted in Figure 6.13 below for all wheels when running on Ri 59-R13 grooved rail section.

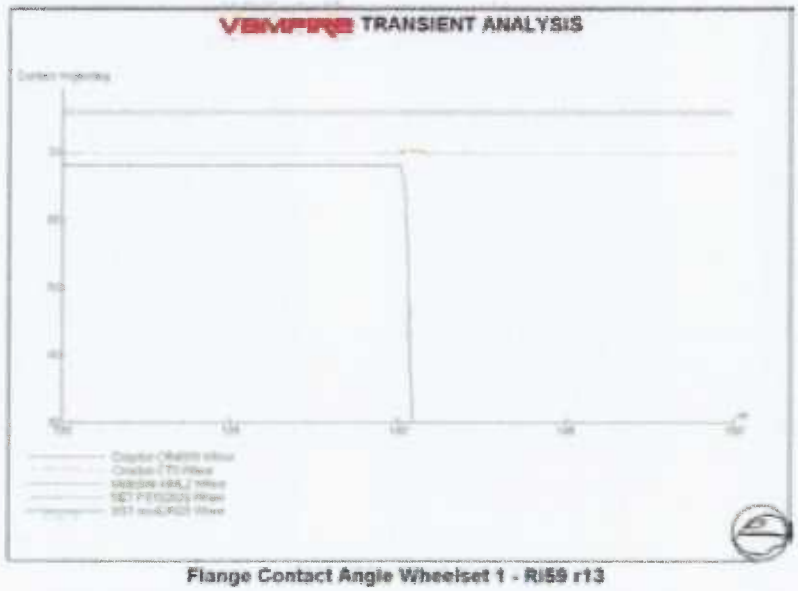

Figure 6.13 – Contact angle for all profiles on Ri 59-R13 grooved rail

The above figure demonstrated the consistent contact angle seen for all profiles other than MML, when running on Ri 59-R13 grooved rail. Again, the higher flange face angle of the DIN-type profiles of SST and NET is evident.

The contact angle plots presented in this section are typical of those found across the selected rail profiles, where a high contact angle offers good derailment protection even at higher values of wheel lift.

6.2.4 Derailment Study – Angle of Attack

As discussed in Section 6.2.1, at the very low curve radius used in the derailment study (~20m), the angle of attack generated between the wheel and rail, effectively becomes a function of the vehicle configuration and track geometry, this can be seen in the example angle of attack plot of Figure 6.14 below, for the selected wheels running on Ri 59-R13 grooved rail.

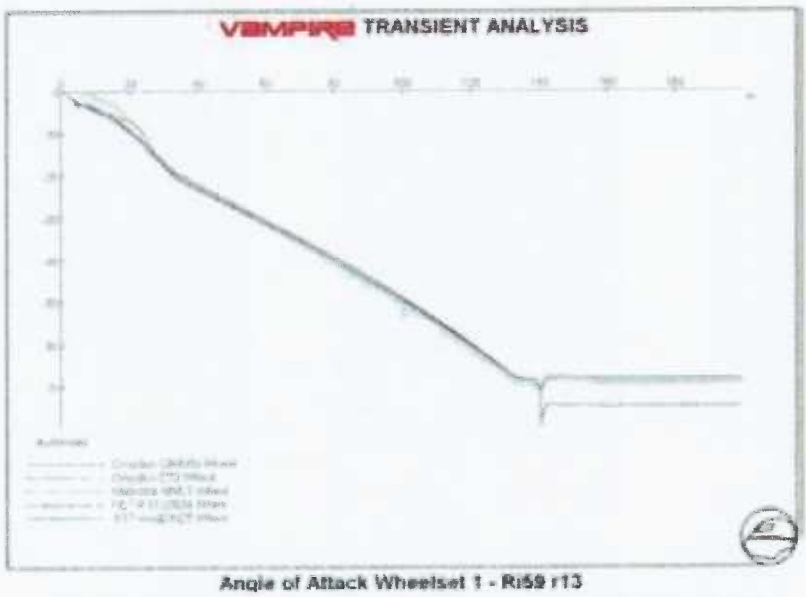

Figure 6.14 – Angle of attack for all profiles on Ri 59-R13 grooved rail

It can be seen from the above figure that the angle of attack (AoA) is almost identical across the selected wheel profiles, at 65mrads. Considering this result, no further plots will be presented for AoA.

6.2.5 Derailment Study – Y/Q Ratio

As described in Section 6.2.1, the ratio of lateral to vertical force (Y/Q), provides an estimate of the proximity of a wheel and rail profile pair to derailment. The derailment case created is designed to promote high Y/Q values but whilst Y/Q is a good indicator of derailment risk the quotient does not take direct account of the true contact angle generated between a wheel and rail. It is believed that wheel lift values and contact angle provide a clearer view of the proximity to derailment. This opinion is evidenced by the fact that the MML profile can be seen to derail at a significantly lower Y/Q value than some of the other profiles studied, even when taking account of its lower flange face angle of 68°.

Figure 6.15 shows a typical Y/Q relationship for the selected profiles running on Ri 59-R13 grooved rail.

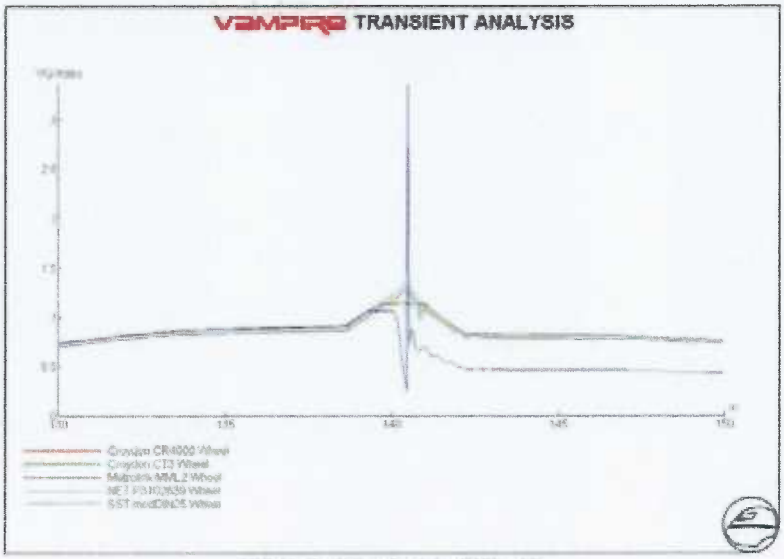

Figure 6.15 – Angle of attack for all profiles on Ri 59-R13 grooved rail

The Y/Q ratio is based on the sum of the vertical and lateral loads on the wheel and will therefore be effected by factors including the effective conicity of the wheel, contact angle and flangeway clearance. The ability of a wheel to resist high Y/Q levels depends largely on flange geometry e.g. the flange face angle but also the resultant contact angles and wheel lift characteristic. In the case presented above 1.1 to 1.3 is a typical Y/Q value but it can be seen that the MML profile derails when operating at a Y/Q value of 0.95.

With the above Y/Q plot being typical of the wheel profile behaviour, no further plots will be presented based on the Y/Q ratio.

It can be concluded that with the exception of the MML profiles, the flange geometries of the other four profiles were effective in resisting derailment for Y/Q values of in excess of 1.3.

The derailment study has demonstrated that, with the exception of the MML profile, the remaining four profiles of SST, NET, CR4000 and CT3 profiles all provide good resistance to flange climb derailment, with any of these profiles being suitable for selection beyond the scope of derailment performance.

The SST and NET DIN-type profiles offered the most consistent performance but not of significant margin to warrant selecting these profiles on the basis of derailment protection alone.

The final selection of wheel and rail combinations will be based on the results presented for both derailment protection and those described in the following section derived from the curving study.

7. Dynamic Simulation – Curving Study

Using a similar philosophy to the derailment study, a VAMPIRE® track file was developed in order to assess the likely level of wheel and rail profile wear, together with other key wheel-rail performance indicators.

7.1 Curving Study Overview

The primary factors analysed included Tgamma ($T\gamma$), a wheel-rail wear index (see Section 7.2.1), contact stress and angle of attack.

Figure 7.1 below shows the VAMPIRE® track file which was developed for the purpose of the curving study.

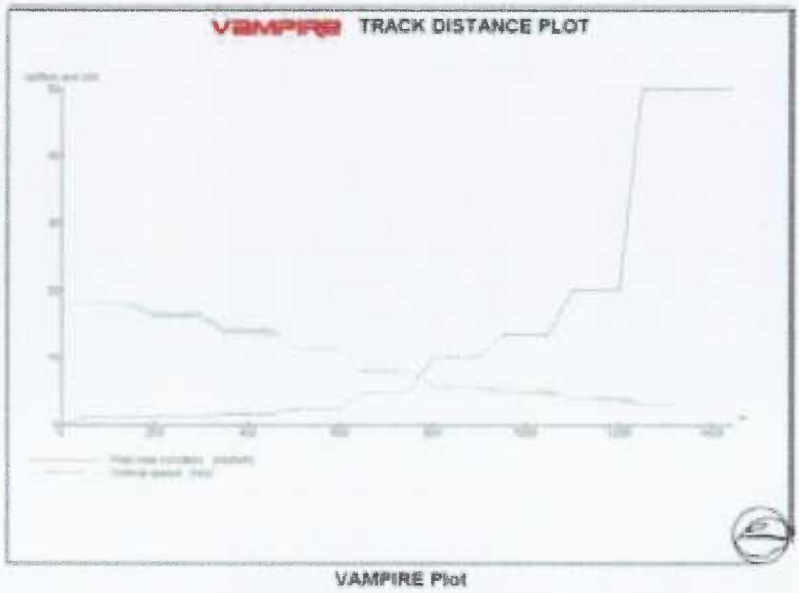

Figure 7.1 – Curving study track file

As in the derailment study, the y-axis of the above figure is combined to indicate vehicle speed in m/s and track curvature in km^{-1}. The x-axis represents the track distance, in m, and is arranged starting with the largest radius of 1000m, reducing to the smallest of 20m at a track distance of 1250m. There is no applied cant in the curves (typical of embedded street rail), therefore the vehicle speed is varied to maintain a constant 50mm cant deficiency. A summary of the above plot is tabulated in Table 7.1 below to aid interpretation of the results.

Track Distance /m	Curve Radius /m	Vehicle Speed /ms^{-1} (kph)
50-150	1000	18.1 (65)
200-300	800	16.2 (58)
350-450	600	14.0 (50)
500-600	400	11.4 (41)
650-750	200	8.1 (29)
800-900	100	5.7 (21)
950-1050	75	4.9 (18)
1100-1200	50	4.0 (15)
1250-1450	20	2.7 (10)

Table 7.1 – Curving Study Tabulated Track Data

As described above the curving study aims to assess the likely wear between wheel and rail combinations in their new condition. Profile combinations will of course wear from their new state to an 'average' of the wheel and rail profiles. The purpose of the study is to select a number of profile combinations that in the new condition will be stable in terms of wear rate and also offer good derailment protection.

It is difficult to predict the worn profile shape but by ensuring compatibility in the new condition, prevents problems with high initial wear rates of wheels and rails and will generally provide more stable profiles in terms of shape change. This is often especially true in the case of light rail systems where wheel turning is carried out on a regular basis. Generally, wheel and rail profiles wear to become more conformal resulting in a larger contact area for a given force and therefore reducing $T\gamma$ and contact stress.

The curving simulations include output measures which will provide the information to select compatible profile pairs, the use of a curvature assault course allows for a consistent platform to do this, isolating features such as track irregularities and varying cant deficiency which can complicate the analysis.

Simulation output is calculated in the steady-state sections for each curvature, the average value of this 100m section is recorded and used in the analysis.

A full description of the output measures and their relevance to profile selection is included in the simulation results section.

7.2 Curving Study Results

The curving study involved subjecting the vehicle and wheel-rail combinations to the VAMPIRE® track file and simulation scenario described above. Results and commentary are presented for Tgamma ($T\gamma$), contact stress and angle of attack, for typical cases.

7.2.1 Curving Study – Tgamma

The wear of a wheel and rail can be expressed as a function of the energy dissipated (or work done) in the contact patch, therefore a wheel which is in contact with the rail at a high level of lateral force (work) and at high levels of creepage (rate of work) will experience high levels of wear. Experiments have been carried out, originally by British Rail (BR) Research [6] and later by Lewis et al [7], which have shown that the rate of wear between two bodies moving relative to each other is related to the energy dissipation in the contact patch. The energy dissipation is expressed as the product of the creep force and creepage Tgamma ($T\gamma$) and has units of J/m (or N), energy per unit distance rolled. $T\gamma$ can be expressed mathematically as the vector sum of the product of the creepage and creep force in the lateral and longitudinal directions, see Equation 7.1.

$$T\gamma = \left| T_y\gamma_y + T_x\gamma_x \right| \tag{7.1}$$

The wear rate of rails can be described as a loss in cross-sectional area due to the passage of a known number of vehicle axles. Laboratory tests undertaken by BR Research resulted in an empirical relationship between wear rate (mm^2/1000 axles) and $T\gamma$, as shown in Figure 7.1. This empirical relationship does not take in to account the effects of containments (lubrication, environmental) that might be present on the rail but represents a 'worst wear' situation.

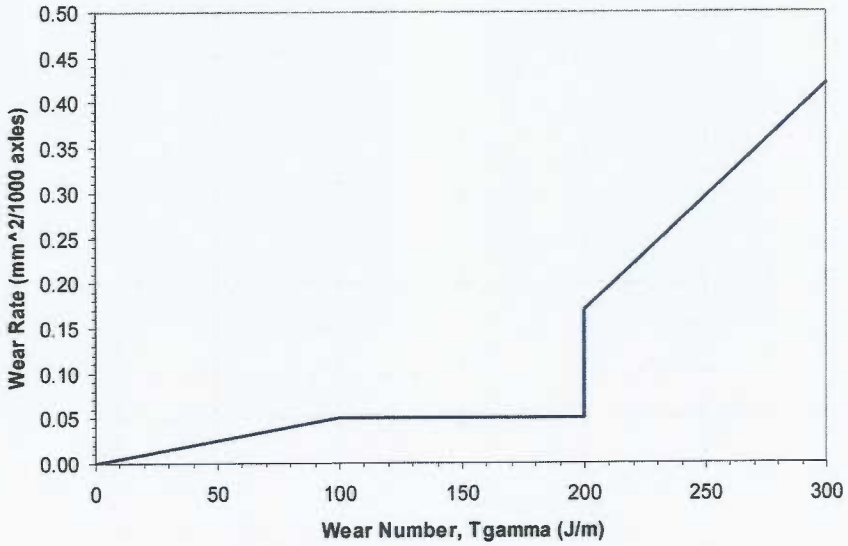

Figure 7.2 – $T\gamma$ and wear relationship

As can be seen from Figure 7.2 above, that the relationship between the rate of metal removal (wear) and the energy dissipated in the contact patch is non-linear. It has been found that the relationship is a two stage process, at low values of $T\gamma$ the rate of wear increase up to a $T\gamma$ value of 100 J/m, in 'mild' wear regime. After a region of constant 'mild' wear, the 'severe' wear regime initiates at a $T\gamma$ value of 200 J/m and continues as a linear relationship. Based on this relationship it would clearly be an advantage to control the curving forces and remain in the mild wear region of the curve. Using this relationship it is possible to assess the likely wear occurring at the wheel-rail interface.

Included below is a summary of the $T\gamma$ results for grooved and non-grooved rail sections. The plots of $T\gamma$ included in this section illustrate the total $T\gamma$ (total work done) by both the tread and flange contacts.

All tyre profiles generate moderate $T\gamma$ values on the tread (<100J/m) when combined with BS 80A rail section inclined at 1:40. The NET tyre profile produces significantly higher values of $T\gamma$ (approximately +30%) at 20m radius curve than the other tyre profiles. Inclining the BS 80A rail section at 1:20 generally produces lower $T\gamma$ values across all wheels compared to BS 80A inclined at 1:40, with the exception of the DIN-type profiles at curve radii below 200m. The DIN-type profiles move directly into flange contact at a curve radius of 1000m with a $T\gamma$ value of 70J/m with the SST tyre profile consistently higher (approximately +20%)

across the entire curvature range. MML and CT3 generate the lowest $T\gamma$ on BS 80A inclined at 1:20.

When combined with BS 113A, inclined at both 1:20 and 1:40, all tyre profiles generate significantly higher $T\gamma$ values at high- to mid-radius curves (1000m to 200m). The highest values of $T\gamma$ were simulated using the DIN-type profiles (SST and NET), whereas the CT3 tyre profile generated the lowest values of $T\gamma$ across the whole curvature range.

Figure 7.3 below shows a comparison of the average $T\gamma$ results for CT3 and SST tyre profiles on BS 80A and BS 113A rail section inclined at 1:20. It can be clearly seen from Figure 7.3 that the CT3 tyre profile remains in the 'mild' wear regime until a curve radius of approximately 100m where the $T\gamma$ value steadily increase to a maximum of approximately 1760J/m at 20m radius curve for both rail sections. The SST DIN-type profile on the other hand remains in the 'severe' wear regime for the entire curvature range when combined with the BS 113A rail section.

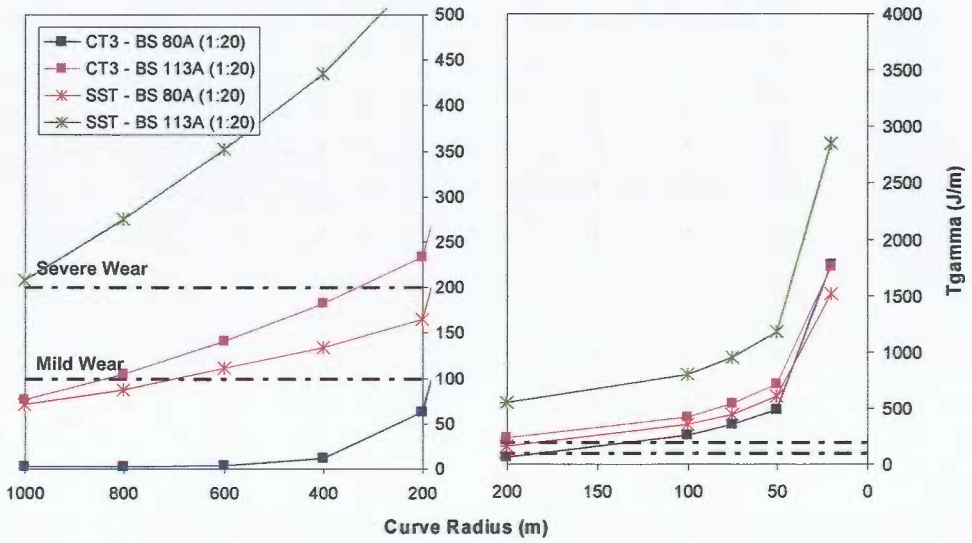

Figure 7.3 – Comparison of $T\gamma$ generated using CT3 and SST (DIN-type) tyre profile on BS 80A and BS 113A rail sections (inclined at 1:20)

When using S49 rail section, inclined at 1:20 and 1:40, similar values of $T\gamma$ to those simulated for the BS 113A rail section are generated for all tyre profiles. Generally these values are higher than the values simulated when using BS 80A rail section with the exception of the CT3 tyre profile which produces the lowest $T\gamma$ values on S49. Generally

lower values of $T\gamma$ were obtained on S49 rail section with a 1:40 rail inclination rather than 1:20.

Figure 7.4 below shows a comparison of the average $T\gamma$ results for CT3 and SST tyre profiles on BS 80A and S49 rail section inclined at 1:40. These two profiles show the extremes of the results obtained, with CT3 producing the lowest and SST the highest $T\gamma$ values. Again, as in the previous figure, the CT3 profile remains in the 'mild' wear regime down to a curve radius of 100m. As the curve radius reduces from 100m the CT3 profile moves in to flange contact and the $T\gamma$ values steadily increase to a maximum of 1500J/m on S49 and 1712J/m on BS 80A rail. The SST profile produces significantly higher $T\gamma$ on S49 rail section through the entire curvature range with a maximum of approximately 3500J/m at a curve radius of 20m. These results are consistent with the philosophy that higher conicity profiles generate higher values of $T\gamma$.

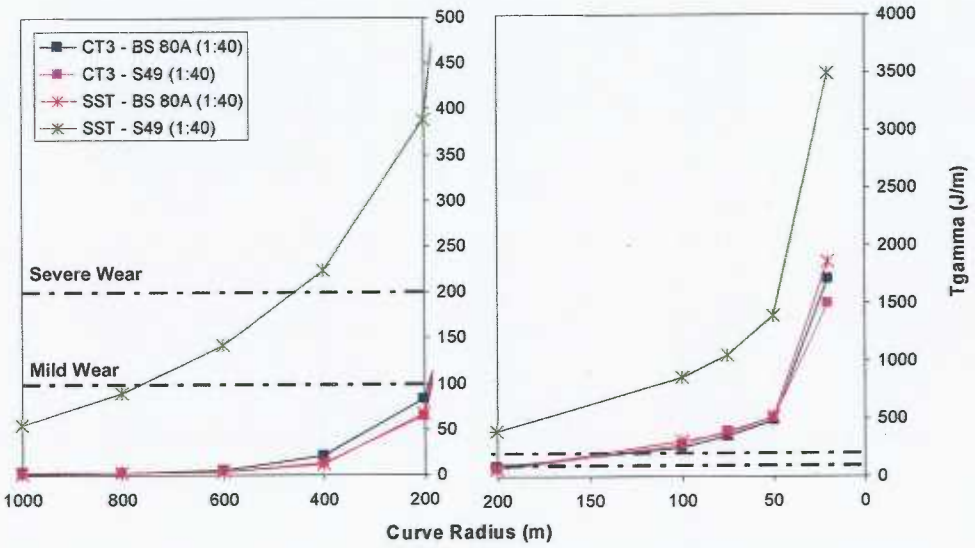

Figure 7.4 – Comparison of $T\gamma$ generated using CT3 and SST (DIN-type) tyre profile on BS 80A and S49 rail sections (inclined at 1:40)

Generally on Ri 59-R10 all profiles show low (<100J/m) to moderate $T\gamma$ values (<500J/m) down to a curve radius of 50m. As the curve radii tightens $T\gamma$ increase further into the 'severe' wear regime, with the DIN-type profiles producing 20% higher $T\gamma$ values due to being in two-point flange contact.

In comparison, on Ri 59-R13 all tyre profiles generate higher values of $T\gamma$ on high- to mid-radius curves than Ri 59-R10, with the exception of CT3 which is generally the same. At smaller radius curves the DIN-type profiles generate 25% higher $T\gamma$ values than the other tyre profiles. Although the $T\gamma$ values generated using Ri 59-R13 are high compared to Ri 59-R10 the R13 grooved rail section produces lower contact stresses as described in Section 7.2.2.

Figure 7.5 below shows a comparison of the average $T\gamma$ results for CT3 and SST tyre profiles on Ri 59-R10 and Ri 59-R13 grooved rail sections. It can be seen that the DIN-type profile (SST) produces significantly higher $T\gamma$ values on Ri 59-R13, moving into the 'severe' wear regime at a curve radius of 400m, compared to a radius of approximately 100m on Ri 59-R10. This demonstrates the incompatibility of the SST flange root radius (13mm) with the 13mm gauge corner radius of the Ri 59-R13 rail section. It can also be seen that the CT3 profile generates similar levels of $T\gamma$ for both grooved rail sections down to a curve radii of 20m.

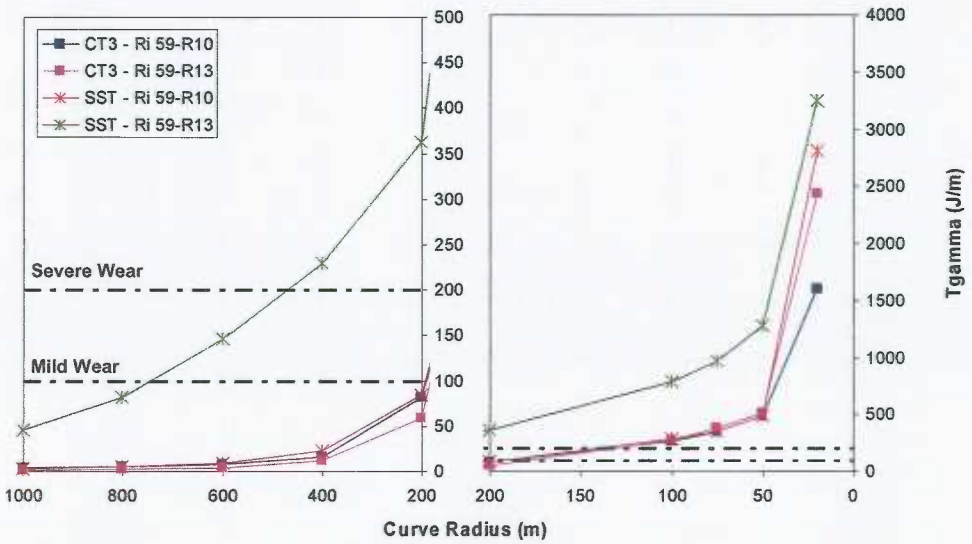

Figure 7.5 – Comparison of $T\gamma$ generated using CT3 and SST (DIN-type) tyre profile on Ri 59-R10 and Ri 59-R13 rail sections

7.2.2 Curving Study – Contact Stress

The contact stress is calculated from the normal load (N) and the area of the contact patch, derived from the elliptical dimensions of the wheel-rail geometry (a, b), as shown in Equation 7.2. The size of the contact patch and therefore the intensity of the stress in the

wheel and rail depend on a number of factors including wheel diameter, wheel load and the transverse profile of the wheel and rail.

$$\sigma_{max} = 1.5\frac{N}{\pi ab} \tag{7.2}$$

Contact stress is an important factor when considering the likely occurrence of rolling contact fatigue (RCF) and other forms of wheel-rail surface damage. Historically, in the railway industry the concept of material shakedown [8] has been used to describe the conditions likely to result in the development of surface damage and RCF.

For a given material, a shakedown diagram can be plotted which defines the relationship between the wheel-rail contact stress and the traction coefficient (or shear force coefficient). Tests on typical rail steels has resulted in the development of a shakedown limit which defines the combinations of contact stress and shear force coefficient which are likely to accumulate plastic strain and ultimately rail surface damage. Figure 7.6 shows a typical shakedown diagram previously used for rail steels. At low shear force coefficients and low contact stresses (<~1000MN/m^2) the rail steel material behaves elastically, as the contact stress increases, up to approximately ~2100MN/m^2, the elastic shakedown limit is reached. Below which plastic flow can take place during the first few cycles, but plastic deformation, residual stresses and strain hardening may enable the structure to reach a cyclic-elastic response, known as 'elastic shakedown'. Above this limit, plastic deformation takes place with each loading cycle. As the shear force coefficient increases the threshold limits decrease as shown in Figure 7.6.

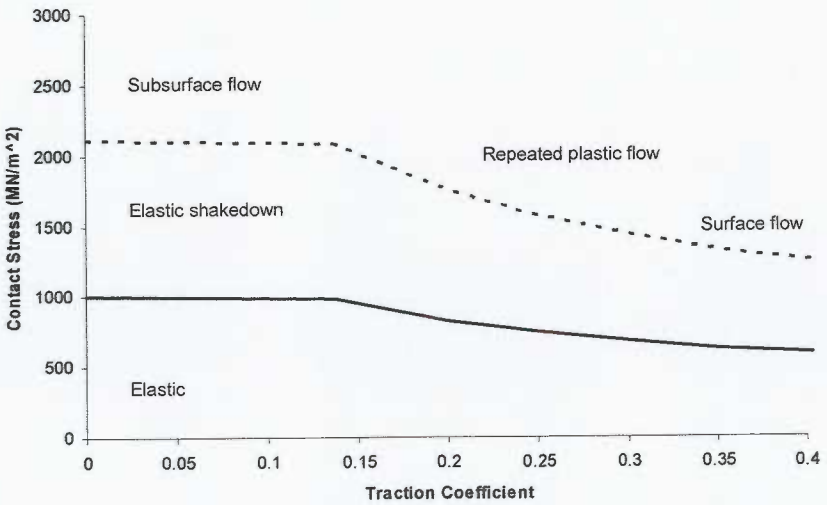

Figure 7.6 –Theoretical shakedown diagram for typical rail steels

Typically, as the wheelset moves laterally into flange contact the contact stress will increase as contact occurs on parts of the transverse wheel and rail profiles which have smaller radii and therefore smaller contact areas. Additionally flange contact results in higher contact angles, significantly increasing the normal load (N) and hence contact stress. If two point contact occurs then the peak contact stress tends to be lower than single point contact due to the tread reacting a proportion of the vertical load, but this depends on the conformality between the flange root and gauge corner radii. However $T\gamma$ values tend to be greater when in two-point contact.

Due to the differences at tread and flange contacts described above, the plots presented in the following sections will separate the tread and flange contact stress results.

On BS 113A rail section all tyre profiles move into flange contact at 1000m radius curve. This generates two-point contact resulting in both tread and flange contact stresses, with the flange showing higher values. The highest flange contact stress values were observed with the rail inclined at 1:20 when combined with the DIN-type profiles, as shown in Figure 7.7. CT3 generated the lowest contact stress on both the tread and the flange with values remaining below 1500MN/m^2 (elastic region of shakedown diagram, see Figure 7.6) for the entire curvature range.

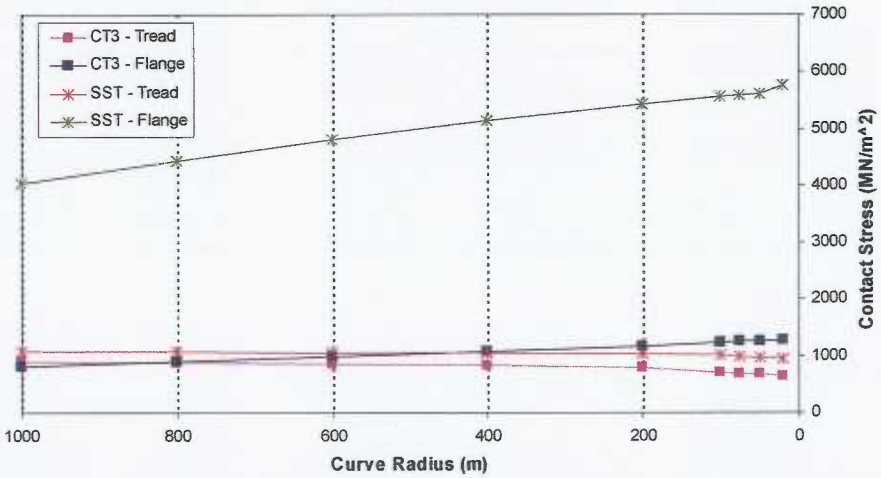

Figure 7.7 – Comparison of average tread contact stress for CT3 and SST tyre profiles on BS 113A rail section inclined at 1:20

When running on S49 rail section the CT3 tyre profile generates the lowest contact stress in flange contact with the rail inclined at both 1:20 and 1:40, whereas the NET tyre profile generates the lowest tread contact stresses with the rail inclined at 1:20. On BS 80A rail section the CT3 profile generates the highest contact stresses on the tread with the DIN-type profiles producing significantly lower stress values. With a rail inclination of 1:40

two-point contact does not occur until a curve radius of approximately 100m for SST and CR4000 and 20m for the other selected profiles.

Figure 7.8 below shows a comparison of the tread contract stresses generated when combining the CT3 and SST tyre profiles with the BS 80A and S49 rail section, inclined at 1:40. It can be seen that the contact stress predicted when using both the CT3 and SST tyre profiles on S49 rail section remain below 1500MN/m^2 on the tread for the entire curvature range, within the elastic region of the shakedown diagram at low traction coefficients (see Figure 7.6). On BS 80A rail the CT3 profile generates significantly higher stress values (~max. 3200MN/m^2) whereas the DIN-type SST profile remains below 1500MN/m^2, similar to that predicted for the S49 rail section.

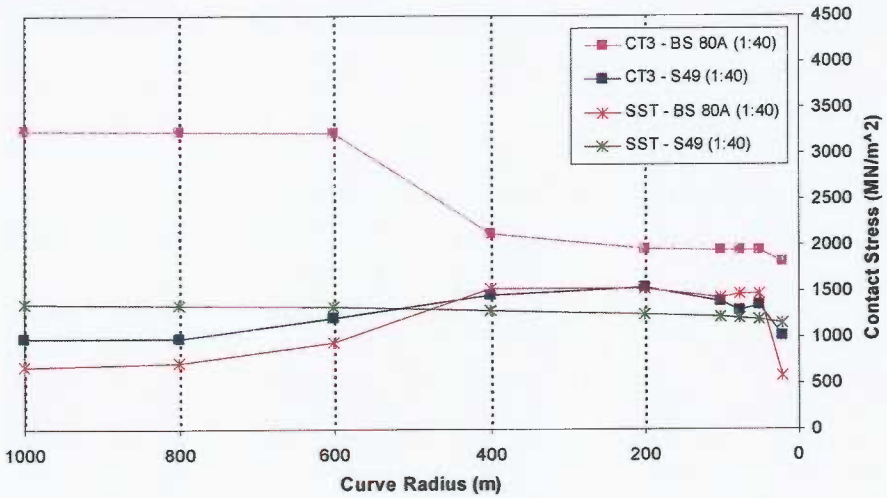

Figure 7.8 – Comparison of average tread contact stress for CT3 and SST tyre profiles on BS 80A and S49 rail section inclined at 1:40

Figure 7.9 below shows a comparison of the flange contact stresses generated when combining the CT3 and SST tyre profiles with the BS 80A and S49 rail section, inclined at 1:40. It can be seen that the CT3 tyre profile is not in two-point until a curve radius of approximately 75m on both BS 80A and S49 rail, therefore generating zero contact stress in the flange contact. When two-point contact does occurs (at a curve radius of 75m) the value of the contact stress reaches a maximum of 2000 MN/m^2. In comparison, the SST profile moves into two-point contact immediately, at a curve radius of 1000m, resulting in a gradual increase in flange contact stress, as the curve radii reduces, up to a maximum of 2400MN/m^2.

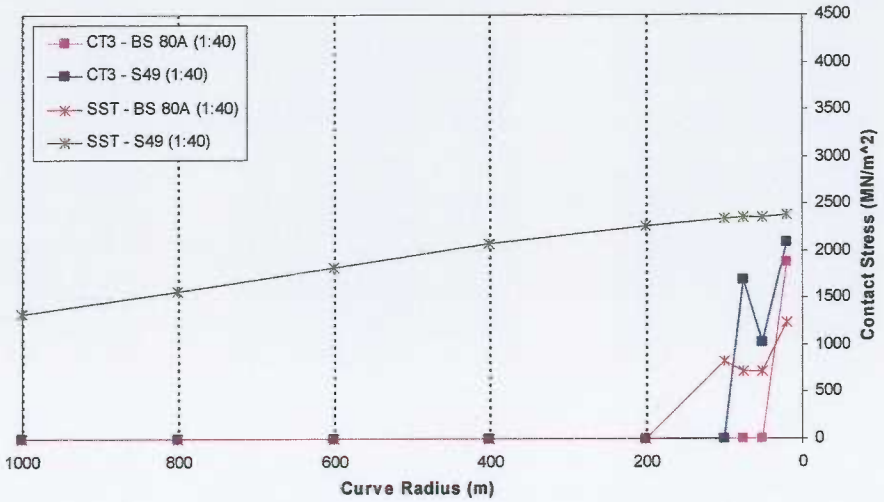

Figure 7.9 – Comparison of average flange contact stress for CT3 and SST tyre profiles on BS 80A and S49 rail section inclined at 1:40

Figure 7.10 below shows a comparison of the average contact stress for the CT3 and NET tyre profiles on Ri 59-R10 grooved rail. This is typical of the results obtained for the Ri 59-R10 rail section, with all profiles (with the exception of CT3) generating a contact stress in the region of 1700-2100MN/m^2. The CT3 profile generates significantly higher stresses at high- to mid-radius curves due to the differences in the contact area generated when matching the 15mm flange root radius of the CT3 profile with the 10mm gauge corner radius of the Ri 59-R10 rail section. It can be seen that both NET and CT3 tyre profiles only contact the flange at a curve radius of 20m, resulting in two-point contact.

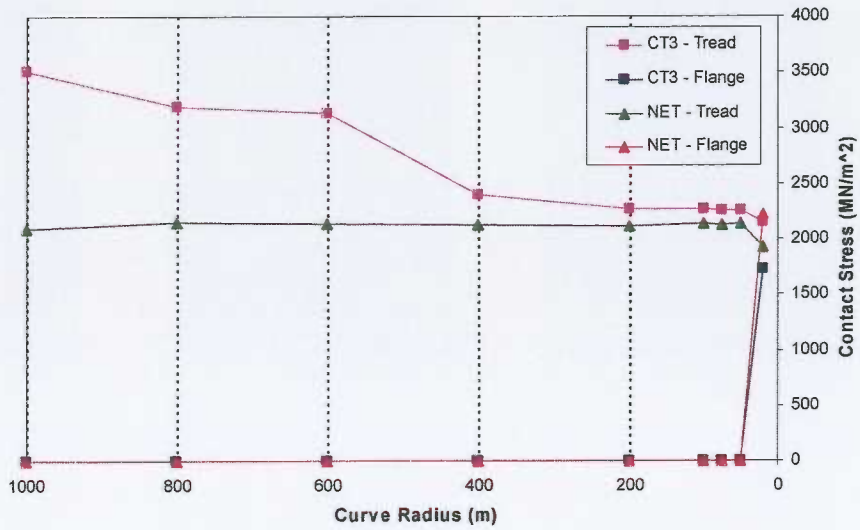

Figure 7.10 – Comparison of contact stress generated using CT3 and NET tyre profiles on Ri 59-R10 grooved rail section

Figure 7.11 below shows a comparison of the average contact stress for the CT3 and NET tyre profiles on Ri 59-R13 grooved rail. On Ri- 59-R13 all the DIN-type profiles move into flange contact at 1000m radius curve, significantly earlier than on Ri 59-R10 rail. This generates two-point contact resulting in lower contact stresses on the tread but higher stresses on the flange. The CT3 profile remains in one-point contact until 20m radius curve where it can be seen that the stresses on the tread reduce and increase on the flange as the load is transferred from the tread to the flange as two-point occurs. The CT3 profile produces significantly lower contact stresses on Ri 59-R13 than Ri 59-R10 with the stress remaining below 1500MN/m^2 until two-point contact occurs at a curve radius of approximately 20m.

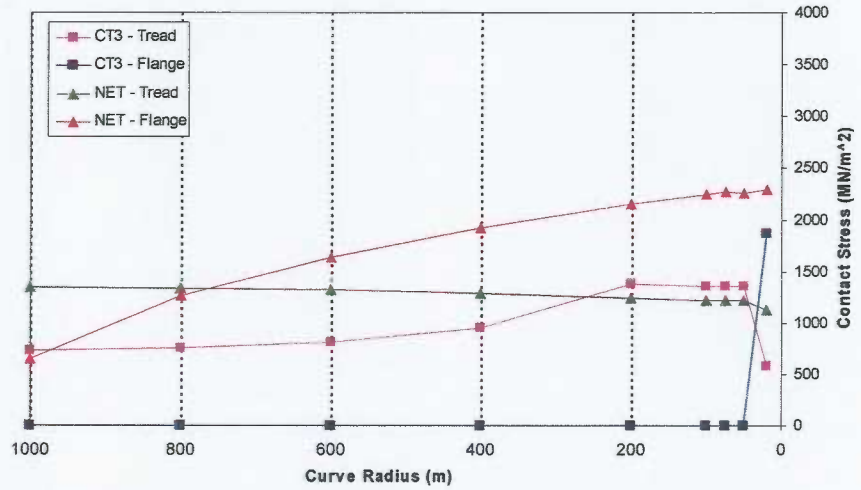

Figure 7.11 – Comparison of contact stress generated using CT3 and NET tyre profiles on Ri 59-R13 grooved rail section

7.2.3 Curving Study – Angle of Attack

Using the curvature assault course the angle of attack of the wheelset was also output and plotted against curve radius. As described in Section 6.2.1, at low radius curves the angle of attack essentially becomes the same for all tyre profiles due to the fact that at very low radii steering breaks down. This effect has also been seen in the results of the curving study, where all profiles generate the same angle of attack on curves with a radius of less than 200m. Therefore the results presented in this section will only consider curves with radii of greater than 200m.

When combined with BS 113A, BS 80A (1:40), S49 (1:20) and Ri 59-R10 all tyre profiles show no significant difference in the simulated angle of attack. On BS 80A (1:20), S49 (1:40) and Ri 59-R13 rail sections the CT3 profile generates an angle of attack close to zero, indicating nearly radial steering, on curves with a radius greater than 600m. On curves with radius in the range of 600m-200m the angle of attack for the CT3 profile remains approximately 2mrad below that produced by the other profiles.

These differences in angle of attack can be accounted for by the difference in the tread and flange-root radius of the profiles, with the CT3 being better matched to the rail sections shown in Figure 7.12. This results in the CT3 profile generating a greater rolling radius difference, and conicity, for a given wheelset lateral displacement improving the steering performance in high- to mid-radius curves.

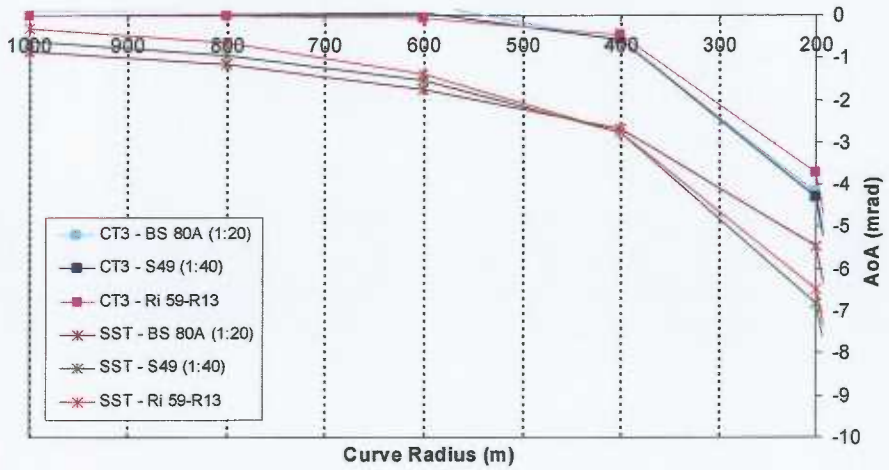

Figure 7.12 – Comparison of average angle of attack for CT3 and SST tyre profile on various rail sections

7.3 Curving Study – Summary

In summary, some high $T\gamma$ values have been observed, but these are generally combined with low contact stresses resulting in the unlikely generation of RCF. Non-grooved rail sections show higher $T\gamma$ values due to the head radius, producing higher conicity. Differences in flange $T\gamma$ values are attributed to the conformality of the flange root and gauge corner and tread $T\gamma$ to head radii and inclination/cone angle of the wheel-rail combinations.

Overall, the CT3 tyre profile generated the lowest $T\gamma$ values on the majority of the rail sections, especially S49 (inclined at 1:40) non-grooved and Ri 59-R13 grooved rail sections. Lower values of $T\gamma$ were also observed when using SST DIN-type profile on Ri 59-R10 and BS 80A rail sections.

The CT3 profile generated lower contact stresses on S49 and Ri 59-R13 rail sections with the DIN-type profiles producing lower contact stresses on the BS 80A and Ri 59-R10 rail sections.

Lower values of angle of attack were observed when using the CT3 tyre profile on BS 80A (1:20), S49 (1:40) and Ri 59-R13 down to a curve radius of 200m, due to the increase in rolling radius difference that is generated with these combinations.

8. Dynamic Simulation – Lateral Stability

The equivalent conicity can defined from rolling radius difference generated by a wheel and rail profile pair. High levels of conicity enable a vehicle with conventional axles to steer around smaller radius curves without flange contact but can lead to vehicle instability caused by the wheelset kinematic hunting motion becoming unstable.

The point at which a vehicle becomes unstable is very much dependant on the vehicle parameters, such as plan view suspension stiffness, damping levels and body/bogie inertias. As the modelling work uses a generic vehicle model, the likely stability behaviour of the profiles would only apply to the vehicle being modelled and therefore dynamic simulation results covering vehicle lateral stability will not be presented in this report, a descriptive summary of the simulation results is provided below.

8.1 Conventional Axles

All the wheel and rail profiles studied were subjected to simulations to investigate lateral stability (hunting) behaviour when running under the conventional axles of the generic vehicle model. All combinations provided stable running at up to 50mph and this is deemed to be acceptable. As discussed above, due to the influence of a particular vehicle configuration, the relative stability performance of a particular profile/vehicle combination should be inferred from the equivalent conicity values presented in Section 3.1.2. Vehicles with relatively low plan view suspension stiffness or systems with higher linespeeds should pay particular attention to these values and consider the use of lower conicity wheel and rail combinations if it is likely that lateral stability may become an issue.

8.2 Independently Rotating Wheels (IRWs)

The generic vehicle model used in the simulation work includes IRWs on the centre trailer-truck section. Through the removal of the rotational coupling (the axle) between the two wheels, the restoring forces generated by wheel-rail conicity are no longer present, therefore IRWs exhibit different running behaviour to conventional axles. In curved track the wheelset will tend to move rapidly towards flange contact, on straight track there tends to be a general lack of guidance, leading to either the wheelset 'wandering' from flange to flange or running in an offset position. A benefit however, of IRWs, is that the removal of the axle eliminates the problem of kinematic hunting, associated with high conicity and conventional axles.

The lack of guidance in the running behaviour of IRWs can cause wheel wear issues, particularly increased flange wear and can also make the wheel more susceptible to

impacting (and derailing) at partly closed switch blades, as the wheelset is more likely to be running offset from the track centre, close to the stock rail, than a conventional axle.

It is usual practice to apply the same wheel tyre profile shape to all wheels of a vehicle but possible gains may be achieved by using an increased conicity profile on IRW trailer-truck wheels. Significantly increased conicity through the incorporation of a large flange root radius can begin to produce a self-centring force on the wheelset induced by the gravitational forces acting (known as gravitational stiffness).

Simulations have been performed to assess any potential advantages that could be gained by introducing higher conicity wheels on IRW axles.

8.2.1 IRW – Simulation Overview

The potential benefit of using higher conicity wheel profiles on IRW axles has been demonstrated through assessment of the running behaviour of the vehicle on straight track. Assessment through curves has not been performed as the small gravitational self-centring effect of increased conicity is not sufficient to improve the steering behaviour of an IRW but can improve offset running and general poor guidance on straight track.

The simulation uses a stability assessment method whereby the vehicle is subjected to 100m of vertical and lateral track irregularity, after this distance the irregularities are held constant. The lateral displacement of the wheelset is output, to assess the level of offset running and likely levels of resulting flange wear.

In order to promote and offset running attitude (as reported by Midland Metro) a 1mrad of wheelset yaw misalignment is introduced to the vehicle model.

Two wheel profiles have been selected for comparison against the standard DIN-type profile currently used at Sheffield Supertram and Midland Metro. The first is the current Docklands Light Railway (DLR), DLR5 profile, which incorporates a 22mm flange root radius, the second test profile being the Croydon Tramlink CT3 prototype profile, which uses a smaller 15mm flange root. The DIN-type wheel profiles are typical in having two-point contact in the flange contact zone, whilst the CT3 and particularly the DLR5 are single point contact profiles.

The simulations combine the above wheel profiles with S49 rail section inclined at 1:40, the S49 generates similar contact conditions to the Ri 59-R13 grooved rail section and for the purpose of this study the results can be considered to apply to this rail section also.

The simulations have been used to assess any improvement in guidance of the wheelset which would be likely to lead to a reduction in flange contact and wear. This is assessed through the wheelset lateral position and the resultant Ty values.

8.2.2 IRW Profiles - Offset Running

Figure 8.1 below shows the lateral displacement of the independent third axle, using the DLR5, CT3 and the SST tyre profiles when running on S49 rail section, inclined at 1:40.

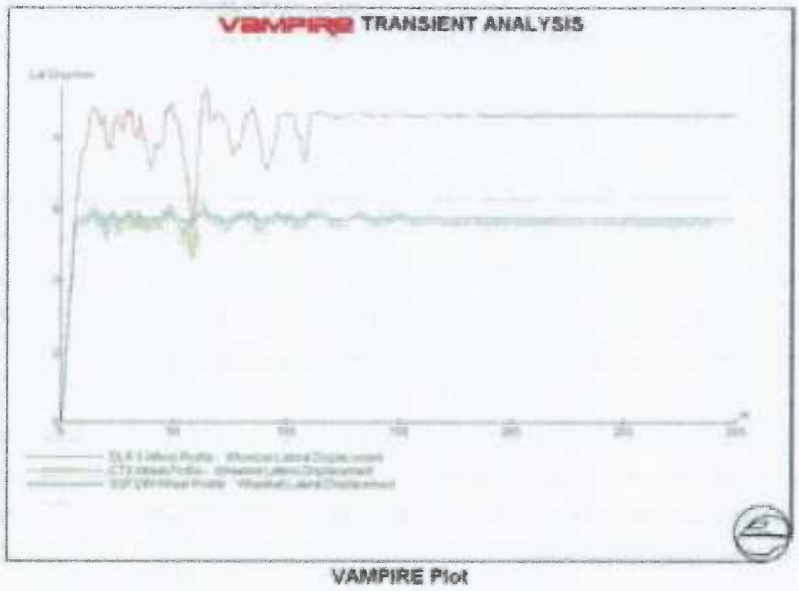

Figure 8.1 – IRW wheelset lateral displacement – IRW axle

With reference to the above figure, it can be seen that the smaller flange root profiles of the SST (root radius = 13mm) and CT3 (root radius = 15mm), move into flange contact as a result of the lateral creep force generated by the 1mrad (approximately 1mm longitudinal offset at the axlebox) wheel misalignment. The DLR5 profile is a purely single point contact wheel profile and moves approximately 8mm laterally, moving up the large flange root radius.

None of the wheel profiles demonstrate a significant self centring effect but it must be noted that the tread profiles are conventional and therefore the gravitational stiffness effect only acts in the flange region, where a significant contact angle difference is created. This can be explained in Figure 8.2 below.

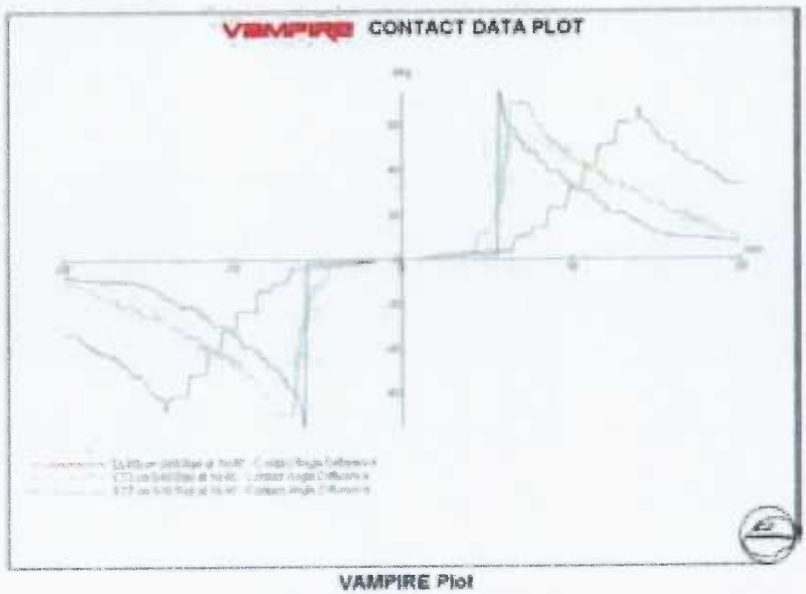

Figure 8.2 – Contact angle difference

Figure 8.2 above shows the contact angle difference, for the three profiles considered for evaluation for use on IRW's, plotted against lateral shift of the wheelset. By generating a contact angle difference between the left and right wheels, a net self-centring force is generated from the normal forces acting at the wheels.

It can be seen by comparing Figure 8.2 with that of Figure 8.1, that for the smaller flange root profiles, the contact angle difference is generated at around 6mm lateral shift, the large root radius of the DLR5 profile does not have a distinct flange contact point but in the simulation case presented, an equilibrium point is found at 8mm lateral shift (approximately 20° contact angle difference).

The above simulations demonstrate the problem that even with larger flange root radii, an IRW trailer trucks bogie will run off-centre in response to very low lateral forces. This can result in offset running and resultant flange wear.

8.2.3 IRW Profiles – Flange Wear

The results presented in the previous section highlight the problem of potential offset running with IRW trailer trucks. Without adopting radical profile shapes for the IRW axles, which may cause problematic worn rail profile shapes, offset running is difficult to avoid.

The following plot shows the $T\gamma$ wear parameter (as described in detail in Section 7), for the three profiles analysed in the previous offset running study. Higher values of Tgamma indicate greater wear, with an accelerated severe wear regime for $T\gamma$ values above 200J/m.

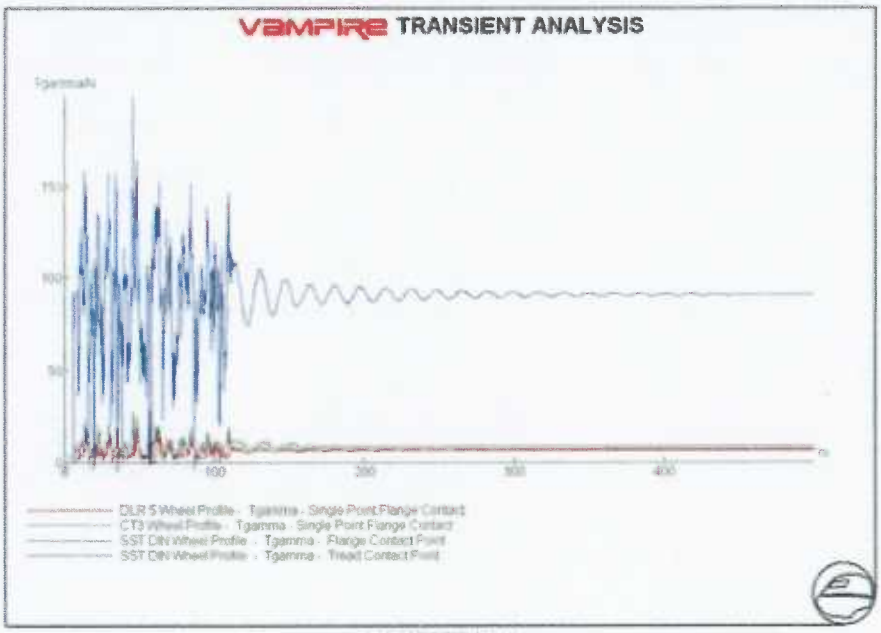

Figure 8.3 – Tgamma values, IRW axle

When considering Figure 8.3 above, it is important to note a fundamental difference in the wheel-rail contact between the SST DIN-type profile and that of the CT3 and DLR5 profile, that is, the SST profile promotes two-point contact.

From the results of the offset running study, the significantly larger flange root radius of the DLR5 profile resulted in a larger lateral shift of the wheelset. This allows the wheel to oppose lateral force without contacting the flange at high contact angles. Larger contact angles result in greater spin creepage and higher wear. In comparison the CT3 profile showed a lower lateral shift but remained in single point contact, albeit at a slightly higher contact angle than

the DLR5, although not very clear from the scale of Figure 8.3, this results in slightly higher $T\gamma$ for the CT3 profile over the DLR5.

Figure 8.3 shows that a standard DIN-type profile such as SST, promotes two-point contact and this causes much higher Tgamma values than seen in the cases of CT3 and DLR5.

This result demonstrates that for IRW wheelsets a wheel profile which remains in single point contact is beneficial in terms of reducing flange wear. It is also clear that the profile does not necessarily require a large flange root radius to achieve this (CT3 flange root = 15mm) and therefore a wheel profile could be designed to operate effectively on both the conventional and IRW axles, eliminating the concern of problematic worn rail profiles shapes caused by using mixed wheel profiles.

It is possible that further improvements could be made to the running behaviour of IRW wheels through the design of a non-conventional wheel profile but this would be unlikely to be compatible with a conventional axle and would therefore require two profile types for a typical tramway vehicle. Further design work for a non-conventional IRW optimised profile is beyond the scope of this work.

9. Wheel-Rail Profile Recommendations

The fundamental objective of the study presented in this report is to determine wheel and rail profiles which are compatible in manner which reduces the risk of derailment and wheel and rail wear. The following section brings together the detailed technical analysis work of the subsequent sections and formulates a wheel-rail compatibility matrix based on the analysis findings.

In evaluating the profile selection options presented, it is important to consider the practicalities of the project task, in that, it is not possible to suggest a wheel profile which is compatible with the complete set of rail profiles and inclinations currently used in the UK. It is also not possible to have a single wheel profile which will work for every system type. However, by adopting a matrix of possible wheel and rail profile combinations, then a wheel and rail profile set can be selected which will operate safely on many systems with an acceptable level of wear.

It was considered that three final profile sets should be created; Set 1, an optimal profile set for new systems, Set 2 for systems constrained 10mm gauge corner rails and Set 3, a tram tram-train compatible profile set. These sets will be fully explained in Section 9.2.

9.1 Selection Methodology

A methodology was required to further reduce the wheel profile combinations from the five wheels and six rails studied in the simulation work to form an optimal set of profiles which will offer compatibility in terms of derailment protection and resistance to high wear rates. The philosophy was to select a small number of combinations of the new wheel and rail profiles which through being inherently compatible in the new condition would not suffer from high initial wear rates.

With the derailment analysis indicating that all profiles, with the exception of the MML profile in the new condition, should offer good derailment protection, the results from the curving analysis became the focus of the methodology to reduce the profile combinations. The curving study presented key wheel-rail performance indicators related to the compatibility of the shapes of the profiles such as contact stress and $T\gamma$ as well as curving indicators such as rolling radius difference and angle of attack.

A wheel-rail interface summary sheet was developed for each of the simulated wheel and rail profile combinations, an example summary sheet is shown in Figure 9.1 on the following page.

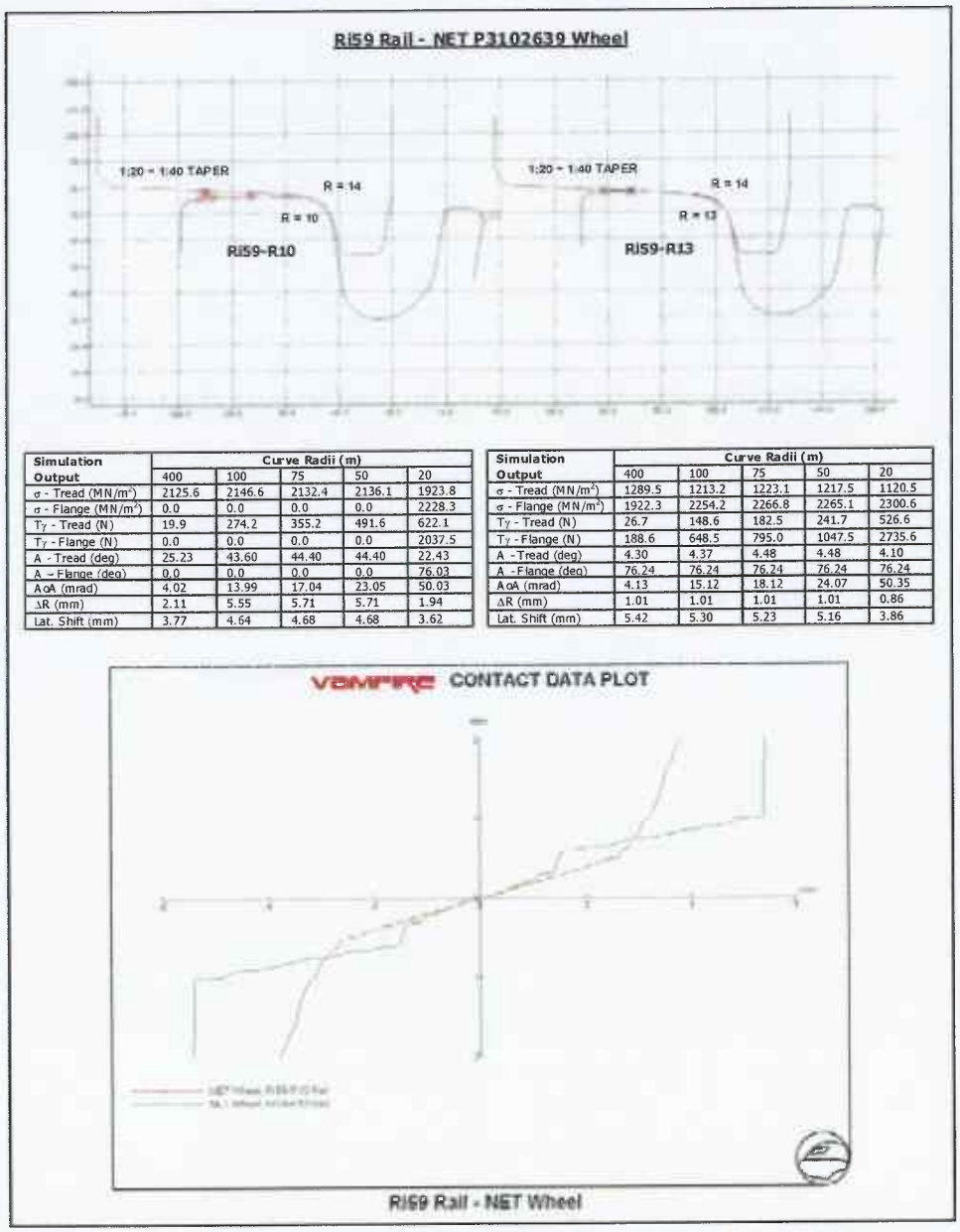

Simulation Output	Curve Radii (m)				
	400	100	75	50	20
σ - Tread (MN/m²)	2125.6	2146.6	2132.4	2136.1	1923.8
σ - Flange (MN/m²)	0.0	0.0	0.0	0.0	2228.3
Tγ - Tread (N)	19.9	274.2	355.2	491.6	622.1
Tγ - Flange (N)	0.0	0.0	0.0	0.0	2037.5
A - Tread (deg)	25.23	43.60	44.40	44.40	22.43
A - Flange (deg)	0.0	0.0	0.0	0.0	76.03
AoA (mrad)	4.02	13.99	17.04	23.05	50.03
ΔR (mm)	2.11	5.55	5.71	5.71	1.94
Lat. Shift (mm)	3.77	4.64	4.68	4.68	3.62

Simulation Output	Curve Radii (m)				
	400	100	75	50	20
σ - Tread (MN/m²)	1289.5	1213.2	1223.1	1217.5	1120.5
σ - Flange (MN/m²)	1922.3	2254.2	2266.8	2265.1	2300.6
Tγ - Tread (N)	26.7	148.6	182.5	241.7	526.6
Tγ - Flange (N)	188.6	648.5	795.0	1047.5	2735.6
A - Tread (deg)	4.30	4.37	4.48	4.48	4.10
A - Flange (deg)	76.24	76.24	76.24	76.24	76.24
AoA (mrad)	4.13	15.12	18.12	24.07	50.35
ΔR (mm)	1.01	1.01	1.01	1.01	0.86
Lat. Shift (mm)	5.42	5.30	5.23	5.16	3.86

Figure 9.1 – Wheel-rail interface summary sheet

With reference to the above figure, the wheel-rail interface summary sheets include interface information relevant to selecting compatible wheel and rail profiles, consisting of, Miniprof information to visually assess the contact conditions, the simulation output for key parameters at a range of curve radii and a rolling radius difference plot to indicate the equivalent conicity generated across the full range of lateral shift.

By comparison of the summary sheets and through consideration of other factors relevant to rail section selection, such as availability in terms of physical production levels of a section, the cross-sectional area from a stray current prospective, then the profile combinations could be reduced to a small number and grouped within the three profile sets described previously.

The wheel-rail interface summary sheets for each of the simulated wheel and rail profile combinations can be found in Appendix A2.

9.2 Definition of 'Profile Sets'

The requirement to form a group of compatible wheel and rail profile combinations based on commonly adopted wheel and rail profiles led to the development of three profile sets. These are described in further detail in the flowing section. A matrix will then be presented and explained, which shows the cross-compatibility of the selected wheel and rail profiles.

9.2.1 Profile Set 1 (New System)

From the analysis work carried out, it became apparent that there was a combination of wheel and rail profile which produced both good derailment protection and the most compatible wheel-rail interface conditions. This was found to be a CT3 based wheel profile, as shown in Figure 9.2 below.

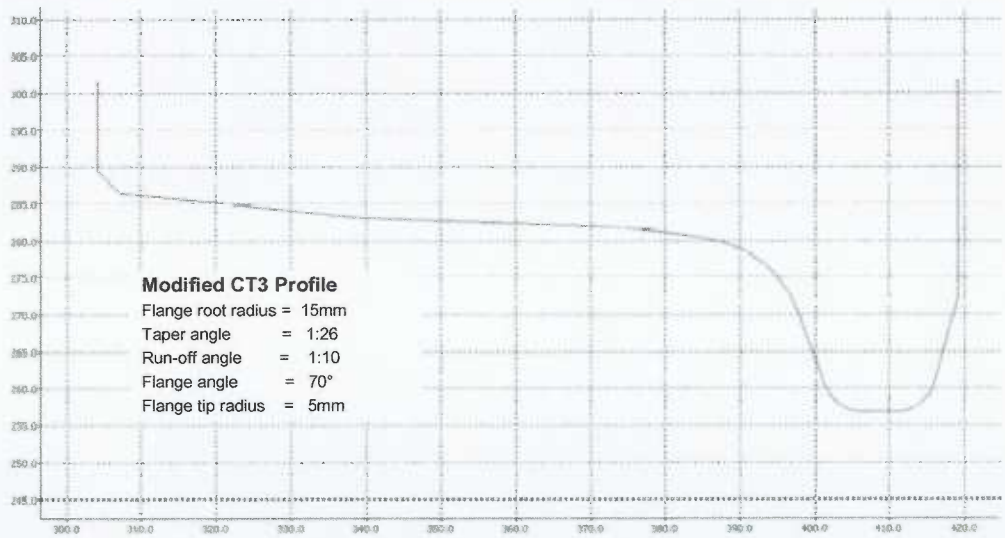

Figure 9.2 – 'Set 1' wheel profile

The modified CT3 profile, as shown above with the flat flange tip option, was selected as the optimal profile for new systems when combined with S49 and UIC54 non-grooved rail inclined

at 1:40 and Ri 59/60-R13 grooved rail with a 1:40 head inclination. The key features of the profile are summarised below:

- 15mm flange root radius reduces flange contact stress
- 1:26 taper angle assists conicity and lower tread contact stress
- 1:10 tread run-off assists in preventing contact between the outer section of the wheel and the road surface, particularly when embedded rail becomes head-worn or suffers from drop within the trackform
- 70° flange angle offers good derailment protection without being unnecessarily steep, which can promote higher contact stress through increased normal force and also reduces effective flangeway clearance at high angles of attack
- 5mm flange tip radius offers a good compromise between effective derailment protection and reducing the tendency for high contact stress, which can be caused by very small tip radii contacting a switch blade (small contact area). A very small radius can result in high initial wear, as evidenced with small radius flange tips at S&C in the UK
- Good derailment protection on all rail profiles studied
- Relatively low wear and contact stress when combined with selected rail profiles

9.2.2 Profile Set 2 (Existing Systems)

As opposed to producing a single profile set to address only the requirements for newly built systems or those happening to use the suggested rail profiles, it was considered essential to provide an alternative profile set which could be considered for use by some of the existing systems, already operating in the UK.

Through the analysis of the Phase 1 work, presented in Section 2, it is evident that a significant number of systems utilise grooved and non-grooved rail sections with a 10mm gauge corner radius. The simulation work demonstrated that the 15mm gauge corner radius of the 'Set 1' profile is not particularly well matched to these rail profiles and therefore a second, 'Set 2' profile set was generated.

A wheel profile based on a modified version of the SST profile was selected from the analysis work as being the most compatible profile for rail sections with a 10mm gauge corner radius, and worked well with the head profiles of these profiles. The SST profile was modified in that the gauge corner radius was reduced to 12mm, to reduce contact stress in flange contact and the flange geometry was modified to be the same as that of the 'Set 1' wheel, 70° flange angle and 5mm flange tip radius. This provides benefits in consistent flange geometry across the profile sets and could lead to the development of a standard switch blade design.

The 'Set 2' wheel profile is shown in Figure 9.3 on the following page.

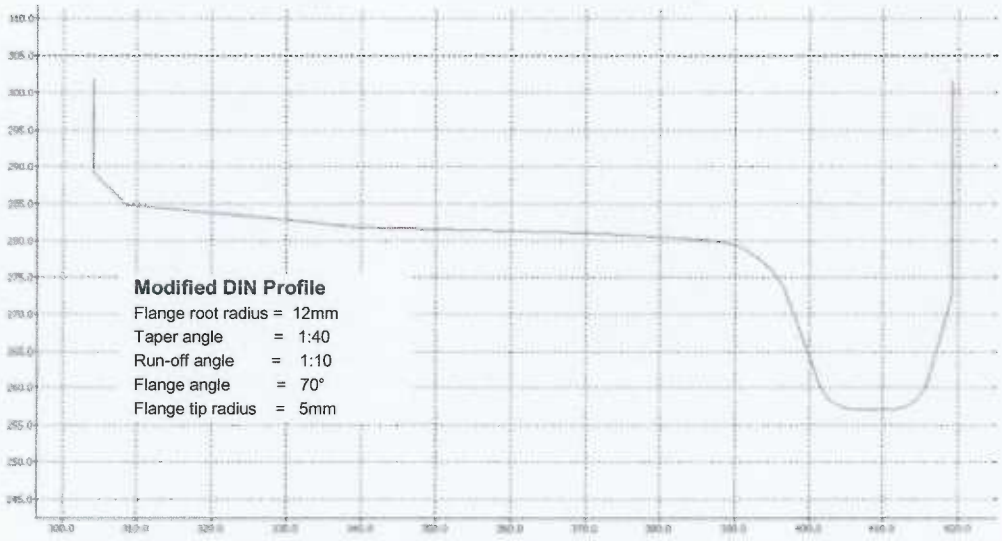

Figure 9.3 – 'Set 2' wheel profile

The modified SST 'Set 2' wheel profile was found to be the most compatible option of the profiles studied when running on BS 80A non-grooved rail profile, inclined at 1:40 and Ri 59/60-R10, SEI 35/41 grooved rail sections.

The key features of the profile are summarised below:

- 12mm flange root radius reduces flange contact stress on 10mm gauge corner radius
- Tread profile provides a good compromise when running on BS 80A and grooved rail sections
- 1:10 tread run-off assists in preventing contact between the outer section of the wheel and the road surface, particularly when embedded rail becomes head-worn or suffers from drop within the trackform
- 70° flange angle offers good derailment protection without being unnecessarily steep, which can promote higher contact stress through increased normal force and also reduces effective flangeway clearance at high angles of attack
- 5mm flange tip radius offers a good compromise between effective derailment protection and reducing the tendency for high contact stress, which can be caused by very small tip radii contacting a switch blade (small contact area). A very small radius can result in high initial wear, as evidenced with small radius flange tips at S&C in the UK
- Good derailment protection on all rail profiles studied
- Relatively low wear and contact stress when combined with selected rail profiles

9.2.3 Profile Set 3 (Tram-Train)

Profile Sets 1 and 2, provide a number of compatible wheel and rail profile options for tramway and light rail systems, however it is likely in the future that there will be an increased adoption of tram-train solutions.

Tram-train solutions allow dual mode compatibility between Network Rail (NR) heavy-rail infrastructure and light rail systems, including those which employ embedded (grooved) rail sections and associated crossings work.

There are a number of strategic high level decisions to be made, or perhaps derogations by Network Rail, before any proposed new tram-train profile could be widely adopted. However the work carried out within this report has highlighted profiles which may be suitable for tram-train applications.

The fundamental differences between heavy and light rail profiles are; a heavy rail profile will have a greater flange height, shallower flange angle and most significantly a smaller wheelset back to back (flangeback) dimension than a light rail wheelset. These points are discussed below:

- The difference in flange height can be addressed by running a light rail type wheel profile with an extended flange height to meet the NR standards, however, this would reduce the clearance to the bottom of the rail groove which may or may not be a problem depending on the grooved section used. (See Table 2.3 Section 2.2 pp.6). It may also cause issues at flange running crossings.

- Alternatively NR could consider allowing a derogation to run with a wheel profile with a reduced flange height, this would need consideration of issues at crossing such as switch blade overlap protection.

- The difference in flange angle, 68° typically for heavy rail and 70 to 75° for light rail systems, could be overcome in the flange design stage, with it being more beneficial to move towards the 70 to 75° range to increase derailment protection within the light rail system than moving towards the heavy rail angle.

- The difference in the wheelset flangeback dimension can be overcome by the simple adoption of a stepped or cut-out flangeback, as adopted at Manchester Metrolink (MML).

There are a number of other practical issues to consider in the development of a tram-train profile which are best addressed through light rail industry/NR committee, these aside the results of this study suggest that a modified version of the CT3 profile would be a good solution on the basis of performance and compatibility with both BS 113A and the proposed 'Set 1' rail profile groups.

At the time of writing it was known that industry discussions regarding tram-train wheel profiles have considered the MML and BR P8 wheel profiles as possible options, however the P8 would require significant flange modifications to allow grooved rail running and the MML profile has been shown to be less tolerant to flange climb when in the new condition, than other light rail profile designs.

The figures presented below compare the contact stresses on tread and flange between a new BR P8 profile, MML and the CT3, running on new BS 113A rail.

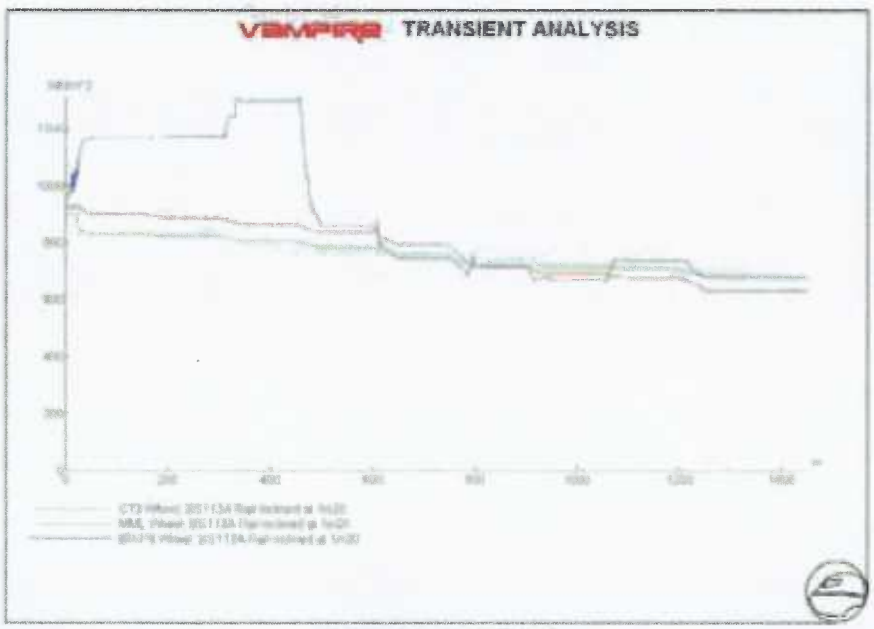

Figure 9.4 – Tread contact stress – tram-train

It can be seen from Figure 9.4 above that the MML and CT3 profiles are similar in terms of tread contact stress, with the P8 showing slightly higher values at radii of 600m and above, this is shown at between 0 and 450m simulation distance on the x-axis of the above plot.

In terms of flange contact stress the CT3 profile shows a clear advantage, as shown in Figure 9.5 below.

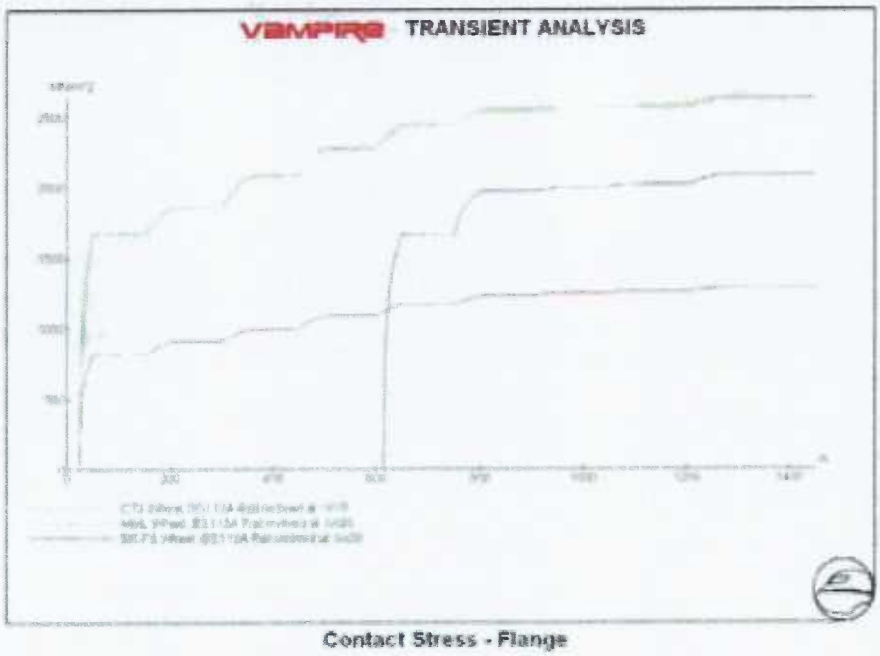

Figure 9.5 – Flange contact stress – tram-train

The flange geometry of the CT3 profile results in a significantly lower contact stress to the MML profile and the P8 profile, which can be seen to move into two-point contact at 600m on the x-axis, which relates to curves of 400m and below. The CT3 and MML profiles are in two-point contact throughout.

To conclude, it may be that practicalities and/or politics will dictate the shape of the tram-train ('Set 3') profile, however the work presented here would suggest that a suitable profile could be based on a modified CT3 type wheel which would provide cross compatibility with 'Set 1' systems.

As has been discussed, one of the issues relating to a tram-train profile is that it is not possible to develop a wheel profile which is entirely compatible with the standard BS 113A heavy rail profile and the complete set of rail profiles (grooved and non-grooved) used in the UK light rail sector. Therefore any tram-train profile will be a compromise or possibly designed to specifically suit the light rail system onto which the exchange will take place.

9.2.4 IRW Wheel Profiles

As part of this profile study work, the feasibility of adopting large flange root wheel profiles for use on IRW axles was investigated as means to reducing the tendency for IRW axles to run off-centre and thereby cause increased flange wear problems.

Analysis work presented in Section 8 demonstrated that even with a significantly increased flange root radius of 22mm, over that of a more conventional 13mm root radius wheel profile, there was insufficient lateral gravitational stiffness force produced to affect the guidance of an IRW wheelset.

Without designing a radical IRW wheel profile to produce increased gravitational self-centering, an approach to improving the performance of IRW axles, could be to accept the offset running issue and to reduce flange wear through improved contact conditions.

As the CT3 wheel profile has been shown to maintain single point contact at high lateral shifts, it is this profile which has been adopted to demonstrate the principle of reducing flange wear through lowering contact stress and $T\gamma$ wear values. Therefore profile combinations identified in 'Set 1' would be suitable for IRW equipped vehicles and would be expected to produce lower flange wear rates than conventional DIN type profiles, which promote two-point contact and hence higher $T\gamma$'s.

The benefit of reduced wear through single-point flange contact can be greatly increased through the adoption of effective bogie mounted wheel flange lubrication. Track based lubrication can be ineffective with IRW wheels due to their often unpredictable running behaviour.

9.2.5 Wheel-Rail Profile Selection Matrix

The recommended wheel and rail profiles described above can be represented by a matrix, as shown in Table 9.1 below.

		Rail Profile						
		S49	UIC 54	BS 113A	BS 80A	Ri 59/60-R13 (1:40)	Ri 59/60-R10 (Vert.)	SEI 35/41 (Vert.)
Profile Set	Set 1	✓ (1:40)	✓ (1:40)	×/✓ (1:40)	×	✓ (1:40)	×	×
	Set 2	×	×	×	✓ (1:40)	×	✓	✓
	Set 3	×/✓ (1:20)	×/✓ (1:20)	✓ (1:20)	×	✓ (1:40)	×	×

×/✓Indicates profiles will run acceptably but are not the optimal choice

Table 9.1 – Wheel-rail profile selection matrix

The above matrix summarises the profile sets described in the previous section and highlights the fact that it is not possible to produce a single wheel profile to suit all rails.

The 'Set 3', profile set is based on a CT3 type wheel profile, but it may be that an alternative may be used based on industry opinion. Additionally, the CT3 profile is not well suited to 10mm gauge corner rail, highlighting the conflict between these rail sections and the 13mm gauge corner radius of BS 113A.

Table 9.2 below shows how the current tramway systems would fit into the above selection matrix.

		Tramway Network				
		CTL	MML	NET	SST	MM
Profile Set	Set 1	✓	×	×	×	×
	Set 2	×	×/✓	✓	✓	✓
	Set 3	×/✓	×/✓	×	×	×

×/✓Indicates profiles will run acceptably but are not the optimal choice

Table 9.2 – Wheel-rail profile – current systems

It can be seen from Table 9.2 above that CTL is the only current system compatible with the 'Set 1' wheel profile due to its usage of Ri 59-R13 grooved rail and S49 non-grooved rail.

The 'Set 2' wheel is likely to be compatible with the rail profiles used at NET, SST and MM, all employing 10mm gauge corner radius rails and partly compatible with the MML system which has a wide variety of rails sections in use.

The 'Set 3' wheel is partly compatible with the CTL system due to the CT3 profile working well with BS 113A but being compromised on S49 at 1:20 inclination. Again, MML due to its relatively heavy usage of BS 113A rail can be considered to fit relatively well within 'Set 3'.

The profile sets recommended above represent fundamentally compatible wheel and rail profiles, however, the characteristic of any one particular system may dictate detail changes to the suggested profile forms. For example a system with a number of mid-range curve radii may benefit from an increased level of conicity.

10. Conclusions

A wide ranging study has been carried out to review current tramway systems and their wheel and rail profiles within the UK. This was reported under the Phase 1 ORR study, entitled 'A survey of UK tram and light railway systems relating to the wheel/rail interface' [1]. Phase 2 of the work, presented within this report, analyses this initial study and extends the work through the application of wheel-rail contact analysis techniques and railway vehicle dynamics modelling to determine optimised wheel and rail profile combinations which minimise derailment risk and wear.

The following sections summarise the conclusions which can be drawn from both the review and analysis sections of the Phase 2 work.

10.1 Phase 1 Report Review

- There are eight different designs of non-grooved rail and four different grooved rail profiles currently used in operation on UK tram and light railway systems
- The eight UK tramway systems each use a different wheel tread profile design
- Many of the UK systems use several different rail profile (with one particular system using seven different rail profiles)
- The modern 2nd generation systems use nine designs of vehicles from four manufacturers
- Up to 15 vehicle derailments have been cited by a single tramway operator
- 50% of all derailments, reported within the Phase 1 work, can be attributed to incidents at turnouts, the majority of these derailments were due to detection and closure failures rather than wheel-rail interface issue.
- 22% of cited derailments were caused by flange climb, these may be related to a combination of poor wheel rail interface conditions and contributory factors such as track twist, poor bogie set-up, high friction condition or poor wheel finish following turning.
- 7% of derailments were attributed to keeper wear. 4% and 2% respectively were caused by obstructed groove and un-specified causes at diamond crossings

- A wide variation in equivalent conicity was found across the systems operating in the UK, levels between 0.06 and 0.58

- Conicity should be considered when selecting wheel profiles for new and existing systems, especially where a significant number of mid range curves exist which can benefit from improved wheelset guidance

10.2 Profile Analysis and Selection

- Three profile 'Sets' have been identified; for new systems, for existing systems with 10mm gauge corner rails and for 'tram-train' schemes

- The recommended profile sets offer relatively low contact stresses and values of $T\gamma$ (wheel-rail wear index) when compared to many of the profile combinations in current UK operation.

- The recommended profile sets represent fundamentally compatible wheel and rail profiles, however, the characteristic of any one particular system may dictate detail changes to the suggested profile forms. For example a system with a number of mid-range curve radii may benefit from an increased level of conicity

- New wheel and rail profiles have been recommended which are geometrically compatible in the new condition, this prevents problems with high initial wear rates of wheels and rails and will generally provide profiles which are more stable in terms of shape change

- It has been shown that a conventional wheel profile with a significantly increased flange root radius will not provide sufficient gravitational stiffness force to improve IRW wheelset guidance

- The concept of adopting profiles which generate single point flange contact, particularly for IRW non-powered axles, has been shown to offer benefits in terms of decreased flange wear rates, these benefits also apply to conventional axles

- The Manchester Metrolink (MML) wheel profile in its new condition was shown to offer a lower level of protection against flange climb relative to the other profiles studied

- The MML wheel profile in the new condition is not considered as a derailment risk and relatively low levels of wheel flange wear has been shown to significantly improve the wheel's flange climb protection

- It was demonstrated that the flange design methods should include analysis of wheel-rail contact angle and wheel lift as an indicator to flange climb protection

- With the exception of the MML wheel profile, all other wheel profiles studied showed good derailment protection

- Wheelset fit analysis has demonstrated that consideration needs to be given to the groove width, especially in small radius curves, if premature keeper rail wear and subsequent replacement is to be avoided

- Vehicle configuration and highway/pedestrian safety should be a consideration in the selection of groove width, that is, a balance needs to be achieved between sufficient wear allowance and clearance for the wheelset in tight curves and maintaining acceptable levels of surface adhesion/entrapment hazard for other road/surface users

- A light rail and tramway wheel-rail 'Best Practice' guide has been developed which further expands on the practical issues related to the findings of the study and is presented in the best practice guide, titled 'A Good Practice Guide for Managing the Wheel-Rail Interface of Light Rail and Tramway Systems', RTU reference 90/3/B [9]

References

1. E.J Hollis, 'A survey of UK tram and light railway systems relating to the wheel-rail interface', Health and Safety Laboratory, FE/04/13, 2006, www.rail-reg.gov.uk/upload/pdf/Report_FE-04-14b.pdf.
2. BS EN 14811-1, Railway applications – Track – Special purpose rail – Grooved and associated construction.
3. BS EN 13674-1, 'Railway applications – Track – Rail – Part 1: Vignole railway rails 46kg/m and above'.
4. BS EN 13674-4. 'Railway applications – Track – Rail – Part 4: Vignole railway rails from 27kg/m to, but excluding 46kg/m'.
5. 'Local and regional railway tracks in Germany', (in German and English), VDV, Cologne, 2007, ISBN 978-3-87094-674-6
6. I. McEwen and R. Harvey, 'Interpretation of Wheel/Rail Wear Numbers', British Rail Research, Report Ref. TM VDY 004, July 1986.
7. R. Lewis et al, 'Integrating Dynamics and Wear Modelling to Predict Railway Wheel Profile Evolution', 6th International Conference on Contact Mechanics and Wear of
8. A.F Bower and K.L Johnson, 'Plastic flow and shakedown of the rail surface in repeated wheel-rail contact, Wear, vol. 144, pp.1-18, 1991.
9. J. Stow and P. Allen, 'A Good Practice Guide for Managing the Wheel-Rail Interface of Light Rail and Tramway Systems', Manchester Metropolitan University (RTU) document 90/3/B, February 2008

Appendix A1 Wheel-Rail Interface Plots

A1.1 Contact Position Plots

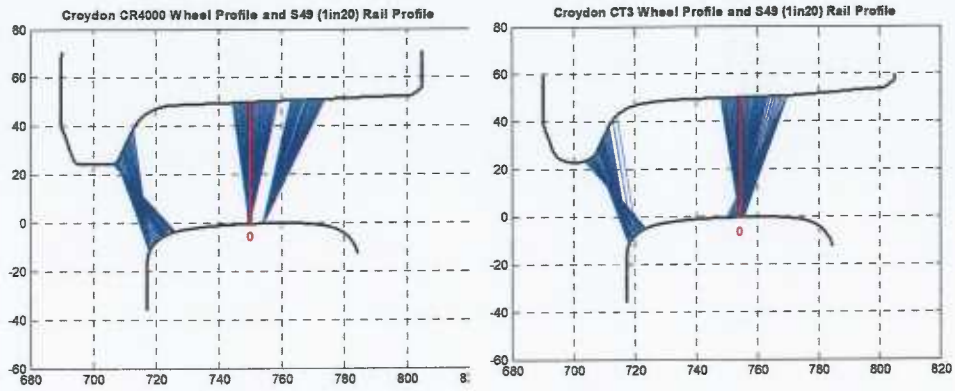

Figure A1.1 – Wheel-rail contact position, Croydon CR4000 (left) and CT3 (right) wheel on S49 (1:20) rail

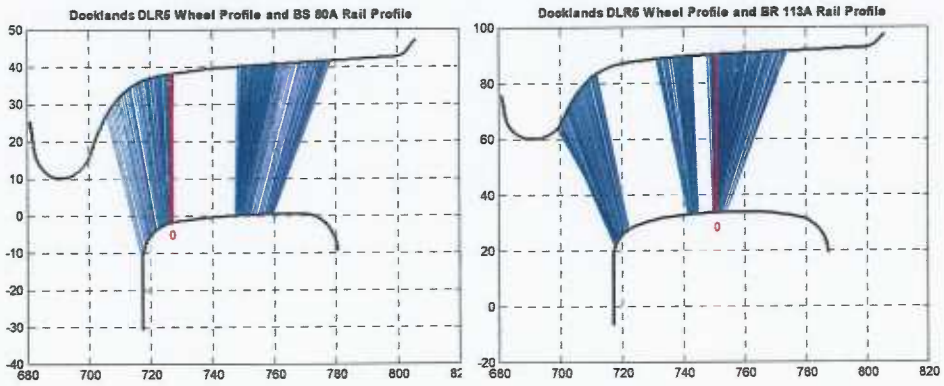

Figure A1.2 – Wheel-rail contact position, Docklands DLR5 wheel and BS 80A (left) and BR 113A (right) rail

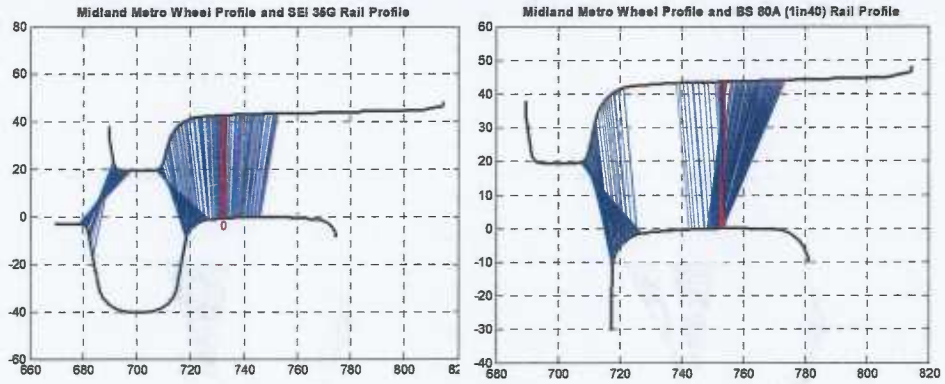

Figure A1.3 – Wheel-rail contact position, Midland T69 Rev. A wheel and SEI 35G (left) and BS 80A (right) rail

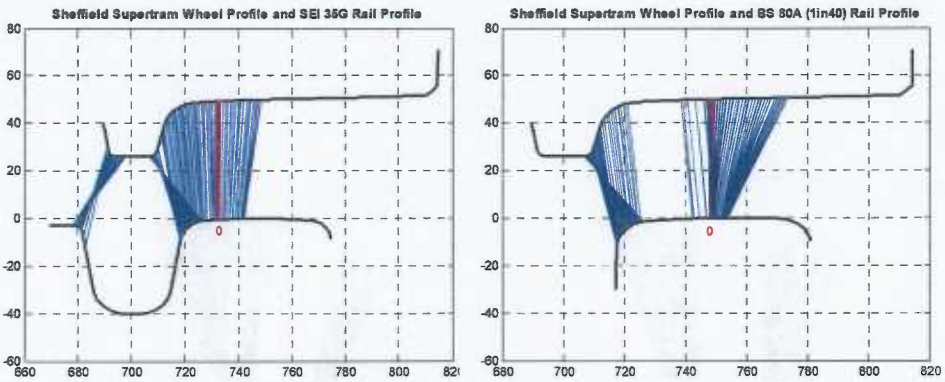

Figure A1.4 – Wheel-rail contact position, Sheffield Supertram wheel and SEI 35G (left) and BS 80A (right) rail

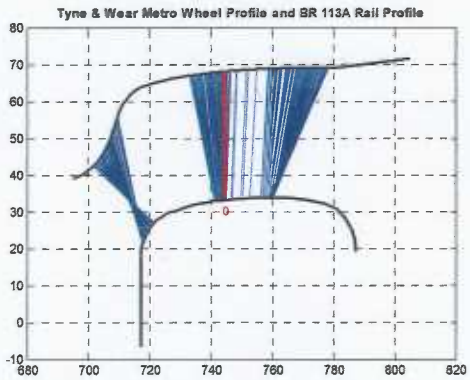

Figure A1.5 – Wheel-rail contact position, Tyne and Wear Metro wheel BR 113A rail

A1.2 Rolling Radius Difference Plots

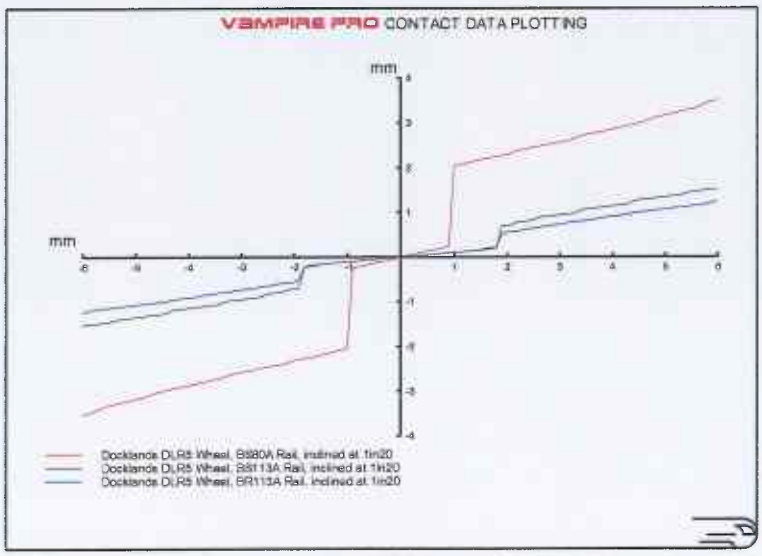

VAMPIRE Plot

Figure A1.6 – Rolling radius difference, Docklands Light Railway

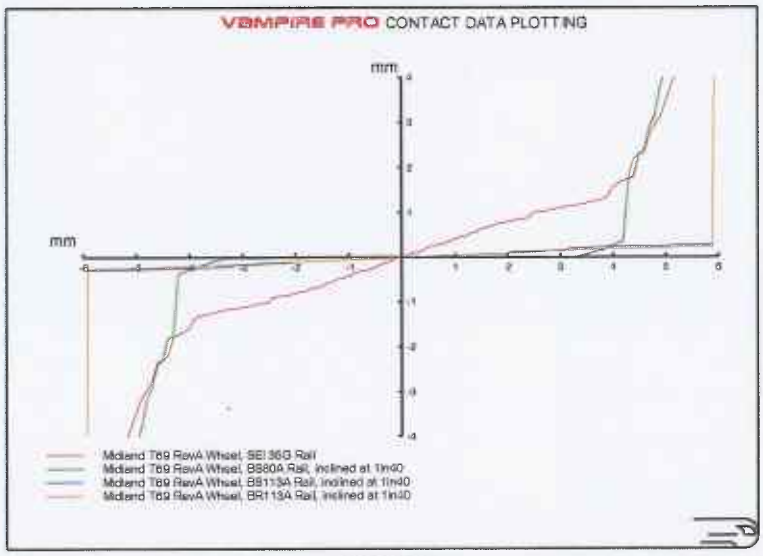

VAMPIRE Plot

Figure A1.7 – Rolling radius difference, Midland Metro

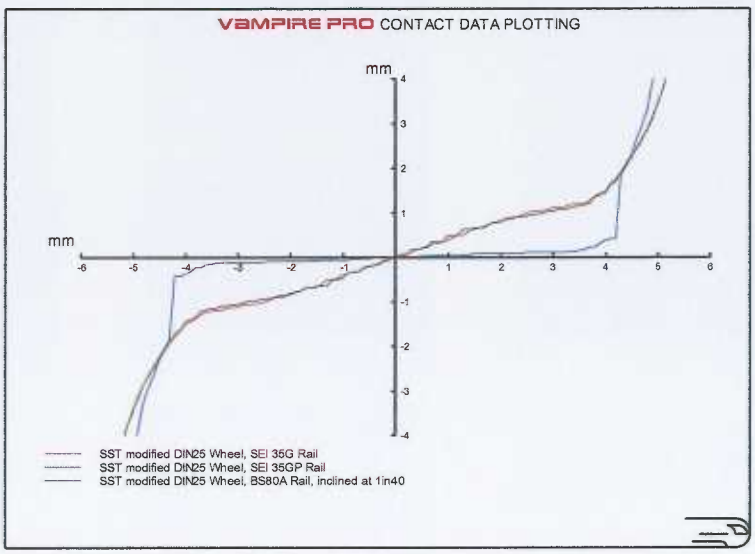

VAMPIRE Plot

Figure A1.8 – Rolling radius difference, Sheffield Supertram

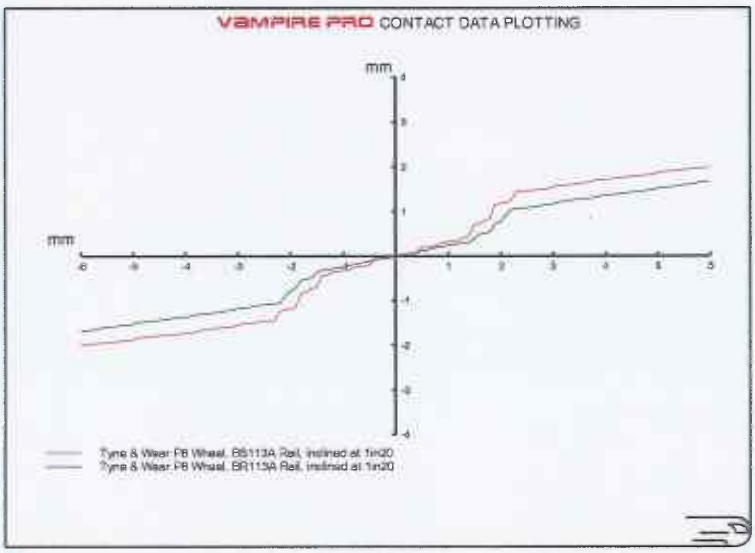

VAMPIRE Plot

Figure A1.9 – Rolling radius difference, Tyne and Wear Metro

A1.3 Contact Angle v Wheel Lift Plots

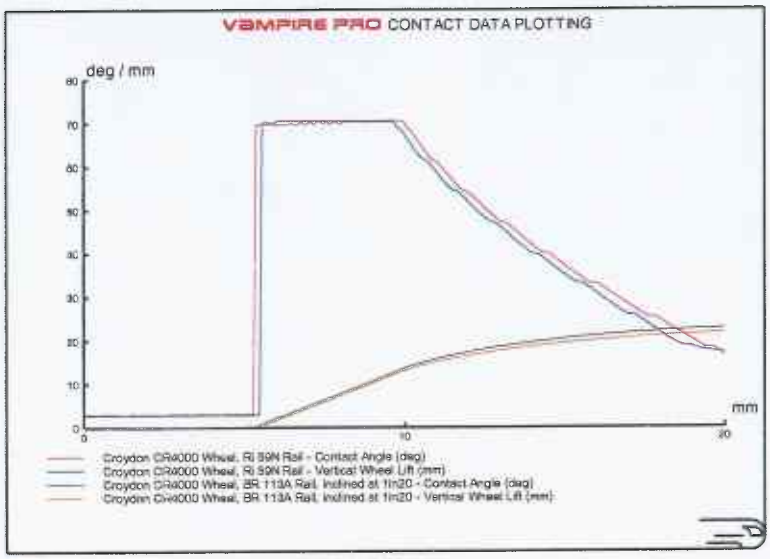

VAMPIRE Plot

Figure A1.10 – Contact angle v wheel lift, Croydon Tramlink CR4000

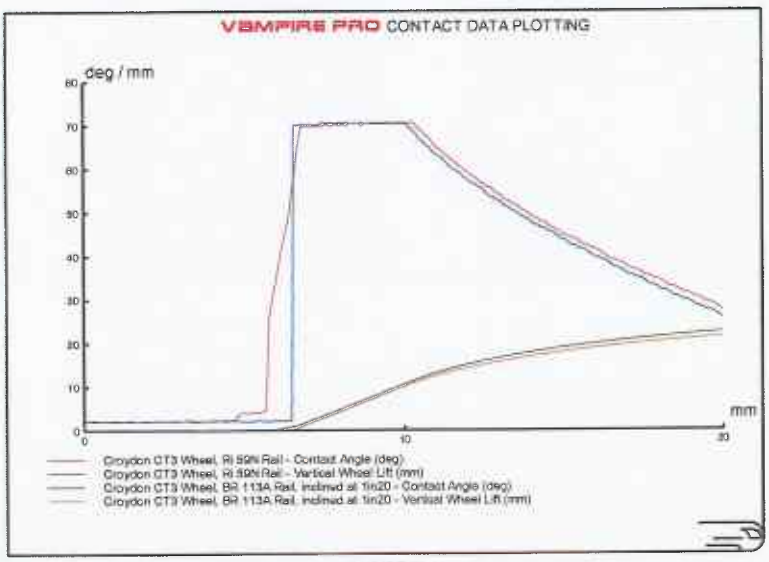

VAMPIRE Plot

Figure A1.11 – Contact angle v wheel lift, Croydon Tramlink CT3

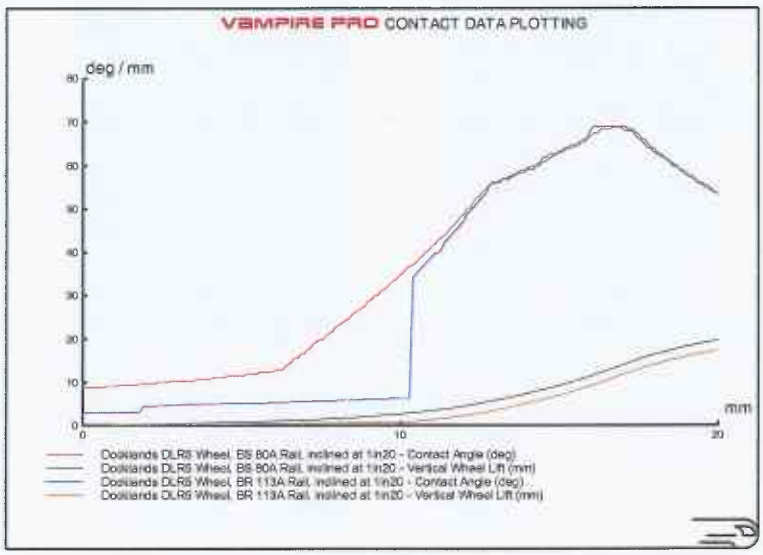

VAMPIRE Plot

Figure A1.12 – Contact angle v wheel lift, Docklands Light Railway

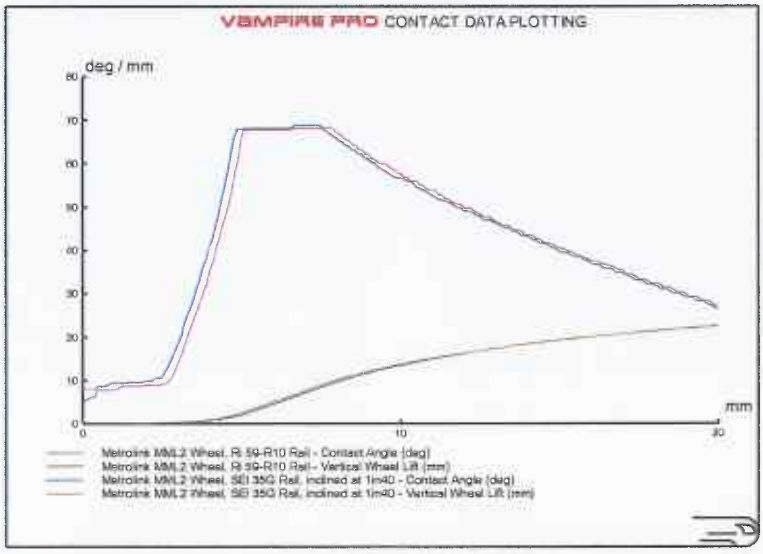

VAMPIRE Plot

Figure A1.13 – Contact angle v wheel lift, Manchester Metrolink grooved rail sections

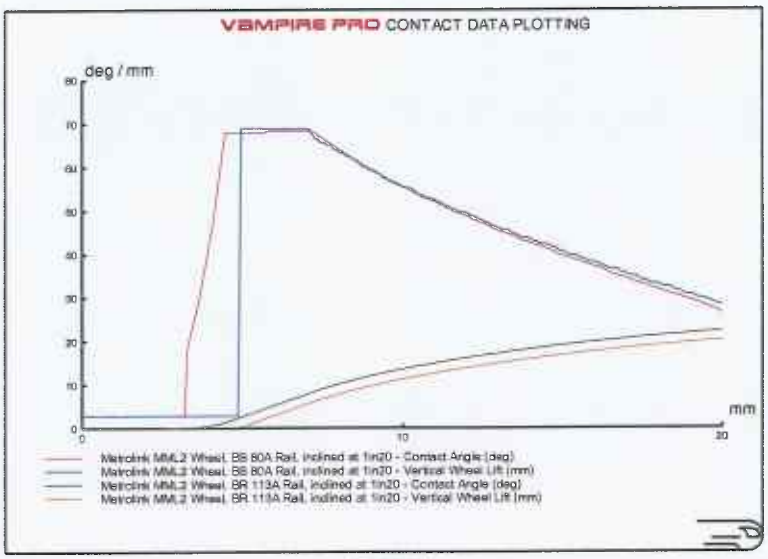

VAMPIRE Plot

Figure A1.14 – Contact angle v wheel lift, Manchester Metrolink non-grooved rail sections

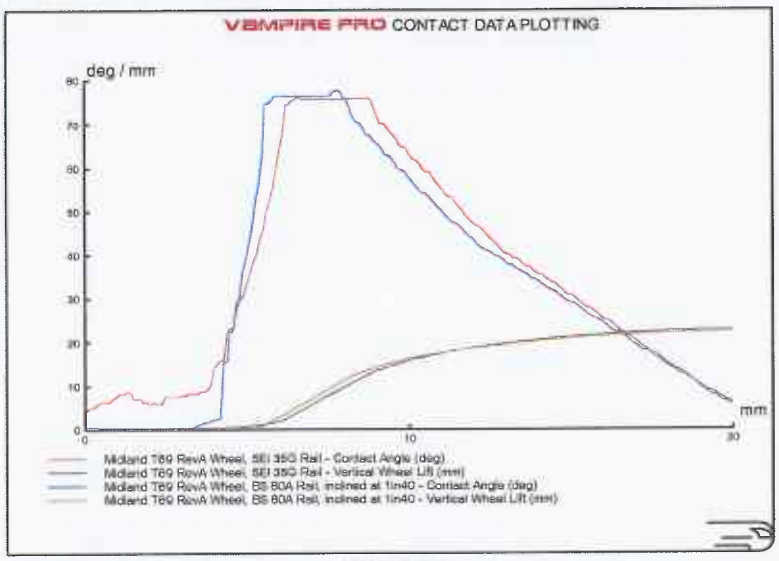

VAMPIRE Plot

Figure A1.15 – Contact angle v wheel lift, Midland Metro

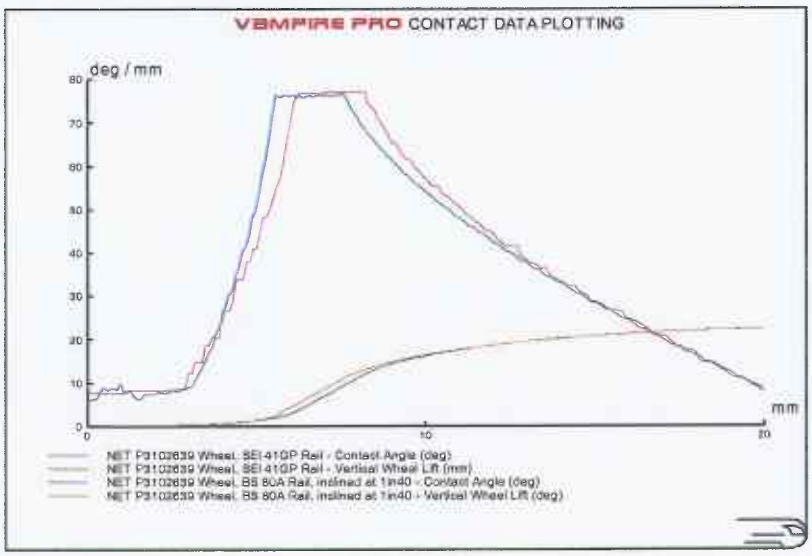

VAMPIRE Plot

Figure A1.16 – Contact angle v wheel lift, Nottingham Express Transit

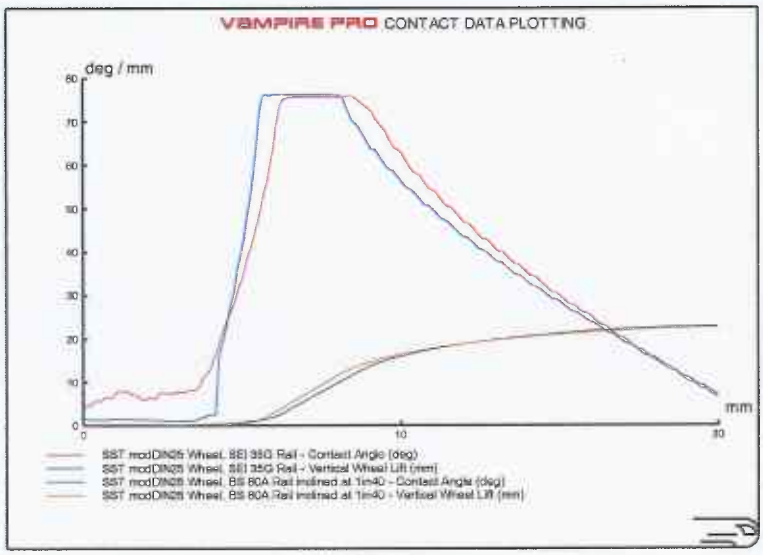

VAMPIRE Plot

Figure A1.17 – Contact angle v wheel lift, Sheffield Supertram

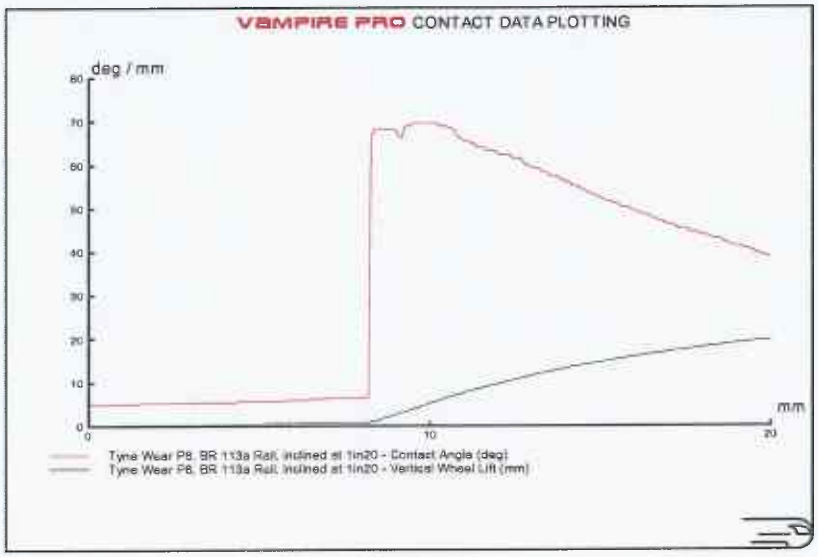

VAMPIRE Plot

Figure A1.18 – Contact angle v wheel lift, Tyne and Wear Metro

Appendix A2 Wheel-Rail Interface Summary Sheets

A2.1 BS 113A Rail Section

BS 113A Rail – CT3 Wheel

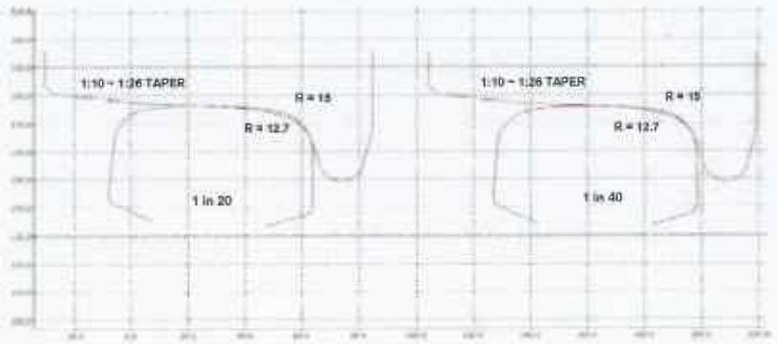

Simulation Output	Curve Radii (m)				
	400	100	75	50	20
σ - Tread (MN/m²)	835.7	711.1	690.6	675.8	630.1
σ - Flange (MN/m²)	1087.6	1231.9	1252.2	1258.9	1285.9
Ty - Tread (N)	25.8	98.0	112.9	140.3	259.9
Ty - Flange (N)	156.9	327.9	424.7	575.0	1499.4
A - Tread (deg)	2.21	2.21	2.21	2.21	2.21
A - Flange (deg)	58.79	58.79	58.79	58.79	58.79
AoA (mrad)	2.66	16.68	21.49	28.66	68.44
ΔR (mm)	0.60	0.67	0.67	0.65	0.53
Lat. Shift (mm)	6.23	6.26	6.25	6.18	5.60

Simulation Output	Curve Radii (m)				
	400	100	75	50	20
σ - Tread (MN/m²)	621.6	338.7	190.7	174.2	0.0
σ - Flange (MN/m²)	1188.0	1420.4	1450.3	1453.8	1445.6
Ty - Tread (N)	20.3	18.7	4.6	4.6	0.0
Ty - Flange (N)	100.9	275.9	384.2	514.9	1357.0
A - Tread (deg)	2.23	2.23	2.23	2.23	0.00
A - Flange (deg)	44.97	44.97	44.97	44.97	46.58
AoA (mrad)	2.28	16.44	21.11	28.46	68.22
ΔR (mm)	0.54	0.59	0.62	0.62	0.30
Lat. Shift (mm)	5.95	5.92	6.00	6.00	5.57

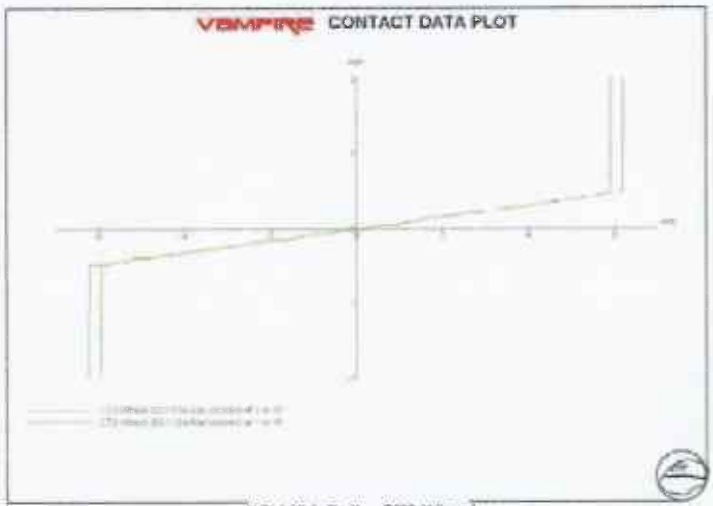

BS 113A Rail – CT3 Wheel

BS 113A Rail – NET P3102639 Wheel

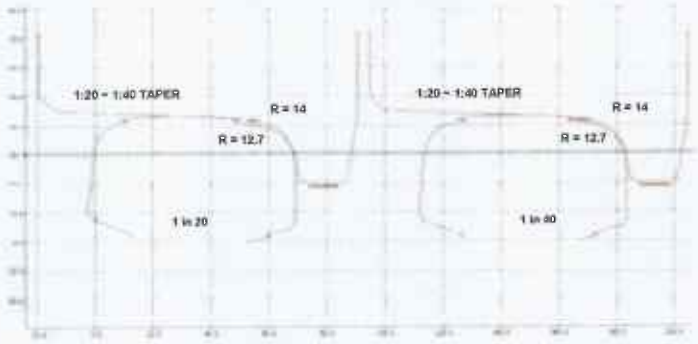

Simulation Output	Curve Radii (m)				
	400	100	75	50	20
σ - Tread (MN/m²)	1285.6	1204.5	1204.5	1243.7	1482.6
σ - Flange (MN/m²)	3192.9	3448.2	3477.6	3475.1	3552.6
T_γ - Tread (N)	37.2	164.1	196.6	259.5	545.5
T_γ - Flange (N)	359.3	721.5	836.0	1056.1	2765.7
A - Tread (deg)	1.07	1.10	1.12	1.09	1.10
A - Flange (deg)	75.68	75.68	75.68	75.68	75.68
AoA (mrad)	4.10	15.08	18.06	23.97	50.22
ΔR (mm)	0.38	0.38	0.37	0.35	0.01
Lat. Shift (mm)	5.42	5.30	5.23	5.09	3.88

Simulation Output	Curve Radii (m)				
	400	100	75	50	20
σ - Tread (MN/m²)	1244.9	1196.9	1217.3	1175.7	1113.4
σ - Flange (MN/m²)	2172.0	2479.8	2496.5	2495.1	2548.0
T_γ - Tread (N)	31.0	171.5	207.6	275.0	597.5
T_γ - Flange (N)	303.9	684.8	800.3	997.9	2579.0
A - Tread (deg)	4.15	4.16	4.12	4.10	3.99
A - Flange (deg)	75.52	75.52	75.52	75.52	75.52
AoA (mrad)	2.36	9.15	12.15	18.15	45.14
ΔR (mm)	0.89	0.88	0.88	0.86	0.76
Lat. Shift (mm)	5.36	5.30	5.22	5.09	3.84

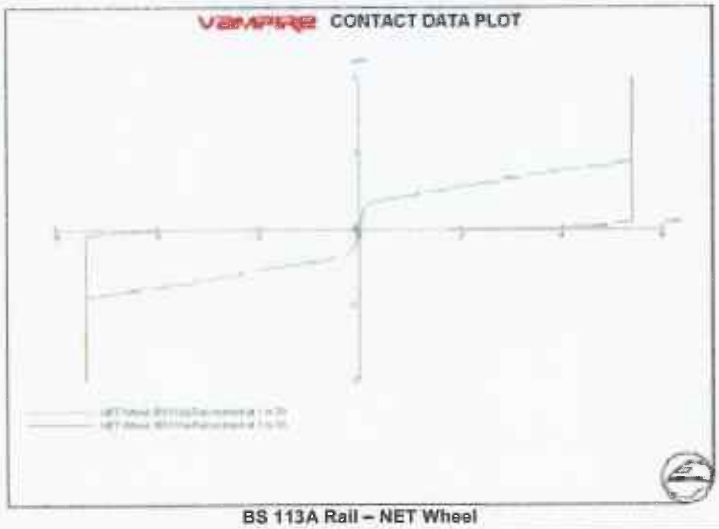

BS 113A Rail – NET Wheel

BS 113A Rail – SST Modified DIN25 Wheel

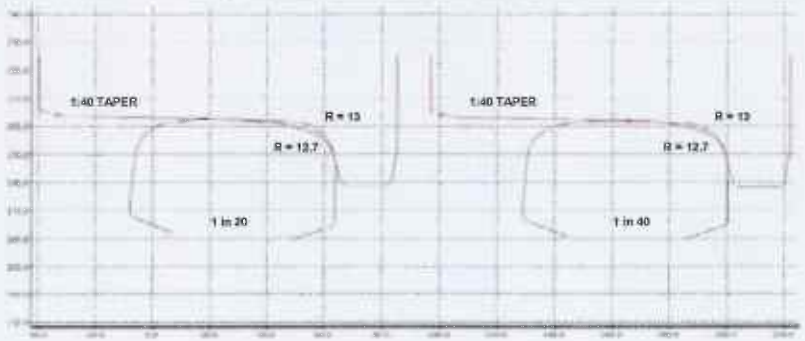

Simulation Output	Curve Radii (m)				
	400	100	75	50	20
σ - Tread (MN/m²)	1057.0	1005.3	998.1	980.6	945.5
σ - Flange (MN/m²)	5140.6	5556.5	5597.0	5600.08	5759.7
Tγ - Tread (N)	37.3	169.0	206.1	270.6	553.9
Tγ - Flange (N)	398.8	630.0	751.3	914.0	2301.5
A - Tread (deg)	1.07	1.06	1.04	1.05	1.11
A - Flange (deg)	73.06	73.06	73.06	73.06	73.06
AoA (mrad)	3.17	16.48	20.75	27.74	66.87
ΔR (mm)	0.42	0.41	0.41	0.40	0.23
Lat. Shift (mm)	5.76	5.60	5.53	5.46	4.14

Simulation Output	Curve Radii (m)				
	400	100	75	50	20
σ - Tread (MN/m²)	871.0	818.9	815.1	812.9	802.4
σ - Flange (MN/m²)	2082.4	2254.8	2275.6	2275.4	2315.7
Tγ - Tread (N)	36.9	158.9	192.7	253.8	534.1
Tγ - Flange (N)	300.0	675.7	809.1	1040.5	2695.7
A - Tread (deg)	1.21	1.24	1.24	1.26	1.48
A - Flange (deg)	75.52	75.52	75.52	75.52	75.52
AoA (mrad)	3.20	17.29	21.34	28.33	67.08
ΔR (mm)	0.43	0.42	0.42	0.42	0.24
Lat. Shift (mm)	5.72	5.54	5.52	5.45	4.06

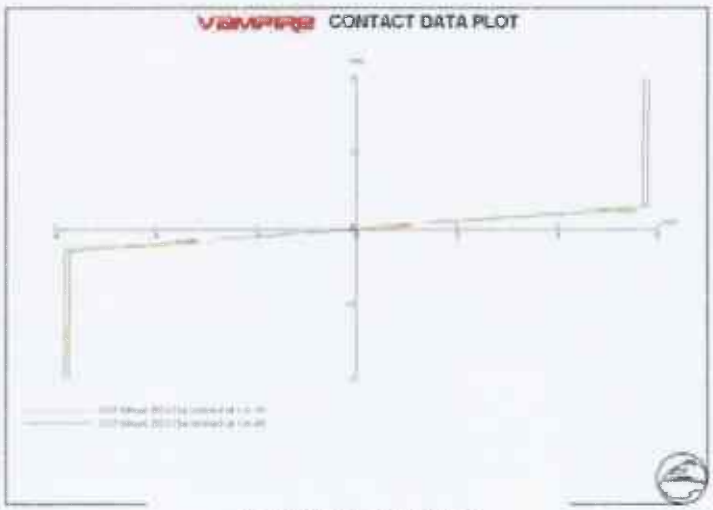

BS 113A Rail – SST Wheel

A2.2 BS 80A Rail Section

BS 80A Rail – CT3 Wheel

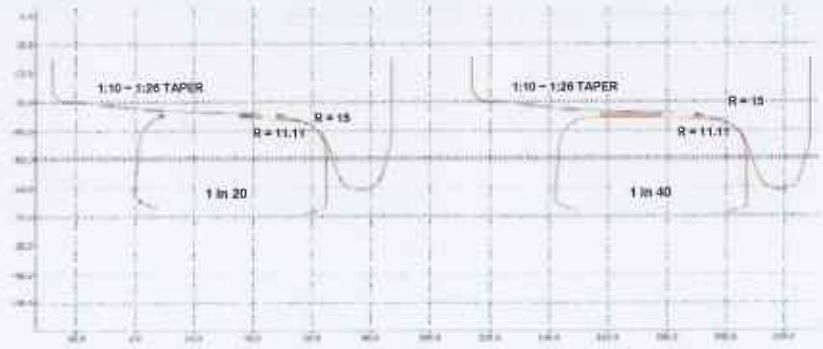

Simulation Output	Curve Radii (m)				
	400	100	75	50	20
σ - Tread (MN/m²)	3164.4	1936.4	1935.5	1939.4	1789.2
σ - Flange (MN/m²)	0.0	0.0	0.0	0.0	2046.10
Ty - Tread (N)	12.4	259.6	355.2	489.2	750.7
Ty - Flange (N)	0.0	0.0	0.0	0.0	1030.7
A - Tread (deg)	12.08	42.38	43.77	43.84	33.12
A - Flange (deg)	0.00	0.00	0.00	0.00	70.38
AoA (mrad)	0.60	15.22	19.74	27.4	67.44
ΔR (mm)	2.40	6.35	6.62	6.63	4.83
Lat. Shift (mm)	2.97	5.28	5.33	5.34	4.90

Simulation Output	Curve Radii (m)				
	400	100	75	50	20
σ - Tread (MN/m²)	3164.4	1936.44	1935.5	1939.4	1789.2
σ - Flange (MN/m²)	0.0	0.0	0.0	0.0	2046.1
Ty - Tread (N)	21.8	250.9	352.9	486.5	792.9
Ty - Flange (N)	0.0	0.0	0.0	0.0	919.1
A - Tread (deg)	16.02	42.25	43.38	43.44	34.48
A - Flange (deg)	0.00	0.00	0.00	0.00	70.03
AoA (mrad)	1.19	14.68	19.72	27.30	67.40
ΔR (mm)	2.58	6.08	6.28	6.29	4.75
Lat. Shift (mm)	3.84	5.20	5.24	5.24	4.87

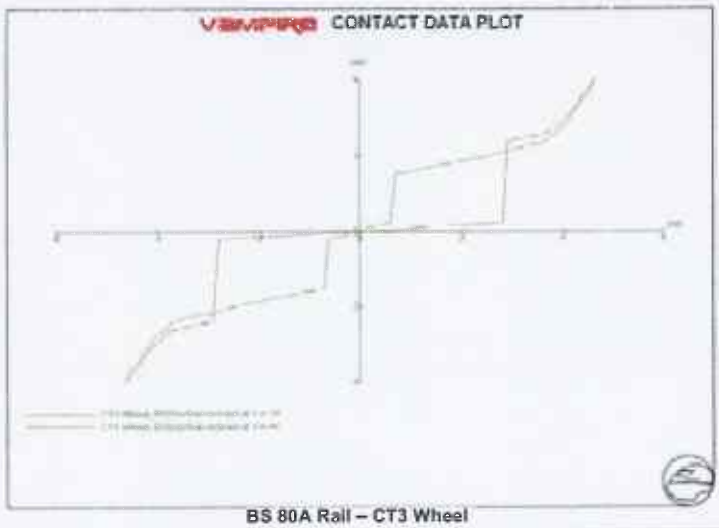

BS 80A Rail – CT3 Wheel

BS 80A Rail – NET P3102639 Wheel

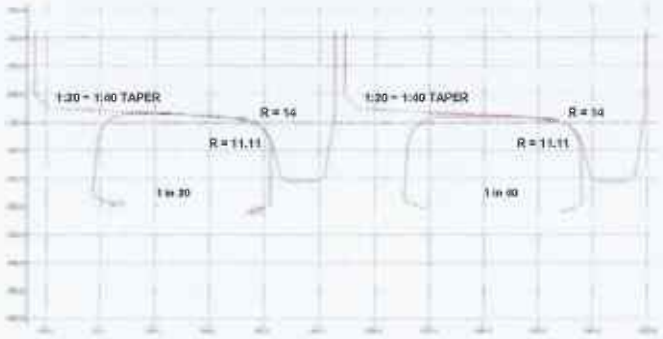

Simulation Output	Curve Radii (m)				
	400	100	75	50	20
σ - Tread (MN/m²)	611.3	0.0	0.0	0.0	0.0
σ - Flange (MN/m²)	1594.3	1752.1	1751.7	1753.2	1744.8
Tγ - Tread (N)	16.23	0.0	0.0	0.0	0.0
Tγ - Flange (N)	45.11	274.0	354.9	487.8	1335.3
A - Tread (deg)	1.47	0.0	0.0	0.0	0.0
A - Flange (deg)	29.94	43.42	44.59	44.63	46.49
AoA (mrad)	4.07	13.90	16.97	23.01	50.09
ΔR (mm)	0.10	0.24	0.24	0.24	0.05
Lat. Shift (mm)	4.07	4.57	4.60	4.67	3.99

Simulation Output	Curve Radii (m)				
	400	100	75	50	20
σ - Tread (MN/m²)	1773.3	1755.5	1754.7	1756.6	1402.8
σ - Flange (MN/m²)	0.0	0.0	0.0	0.0	2409.4
Tγ - Tread (N)	18.5	265.0	343.2	477.5	585.8
Tγ - Flange (N)	0.0	0.0	0.0	0.0	2262.5
A - Tread (deg)	17.58	43.04	43.78	43.86	12.73
A - Flange (deg)	0.0	0.0	0.0	0.0	76.02
AoA (mrad)	4.17	13.81	16.84	22.85	49.72
ΔR (mm)	2.38	5.57	5.70	5.71	2.06
Lat. Shift (mm)	3.53	4.46	4.49	4.49	3.30

BS 80A Rail – NET Wheel

BS 80A Rail – SST Modified DIN25 Wheel

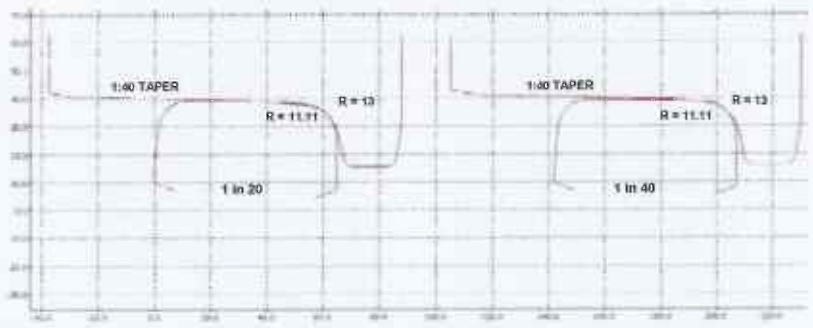

Simulation Output	Curve Radii (m)				
	400	100	75	50	20
σ - Tread (MN/m²)	814.1	627.8	604.1	594.2	521.9
σ - Flange (MN/m²)	1168.9	1341.0	1356.4	1358.9	1383.1
Ty - Tread (N)	25.4	64.2	69.5	88.0	149.59
Ty - Flange (N)	108.8	295.7	378.3	519.9	1368.0
A - Tread (deg)	1.46	1.47	1.46	1.48	1.38
A - Flange (deg)	53.05	53.05	53.05	53.05	53.05
AoA (mrad)	2.67	16.79	20.50	27.61	66.80
ΔR (mm)	0.44	0.44	0.46	0.44	0.21
Lat. Shift (mm)	5.14	5.11	5.17	5.10	3.71

Simulation Output	Curve Radii (m)				
	400	100	75	50	20
σ - Tread (MN/m²)	1523.8	1435.8	1470.3	1438.0	579.4
σ - Flange (MN/m²)	0.0	826.7	714.3	720.7	1235.7
Ty - Tread (N)	12.7	203.0	291.1	397.7	322.4
Ty - Flange (N)	0.0	110.1	86.0	123.0	1541.7
A - Tread (deg)	19.58	37.52	40.69	40.69	1.29
A - Flange (deg)	0.0	62.34	62.34	62.34	62.34
AoA (mrad)	0.67	16.33	20.17	27.47	66.36
ΔR (mm)	2.17	4.29	4.76	4.76	0.19
Lat. Shift (mm)	4.38	4.84	4.91	4.91	3.61

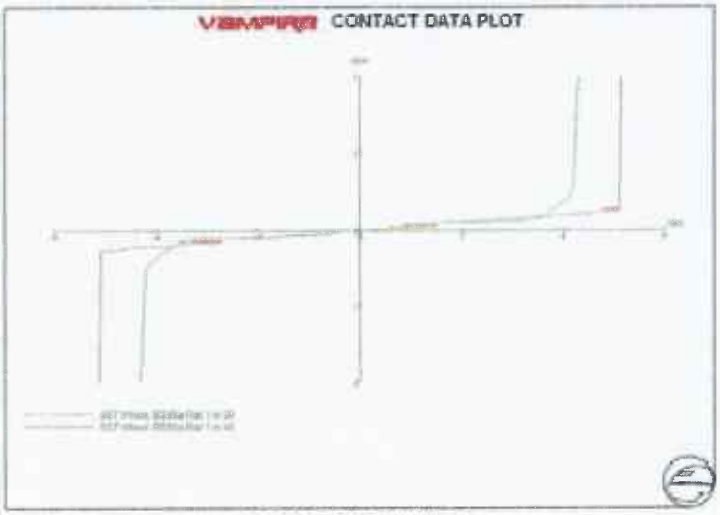

BS 80A Rail – SST Wheel

A2.3 S49 Rail Section

S49 Rail – CT3 Wheel

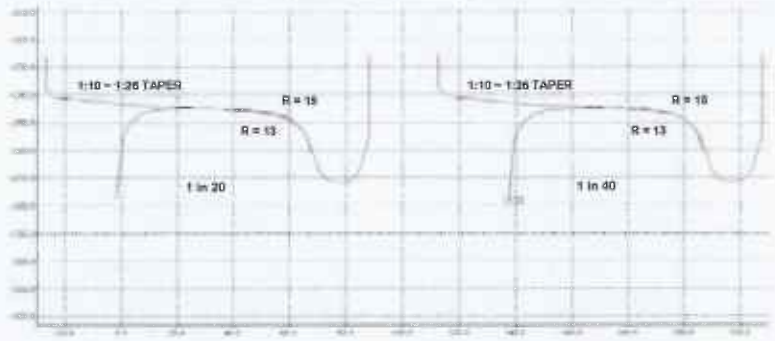

Simulation Output	Curve Radii (m)				
	400	100	75	50	20
σ - Tread (MN/m²)	832.2	1450.8	1487.1	573.8	347.0
σ - Flange (MN/m²)	1244.5	0.0	0.0	1483.1	1527.5
T_Y - Tread (N)	21.9	272.8	383.7	51.7	38.5
T_Y - Flange (N)	115.7	0.0	0.0	500.4	1355.5
A - Tread (deg)	2.01	42.23	44.27	15.57	2.01
A - Flange (deg)	47.93	0.00	0.00	47.93	47.93
AoA (mrad)	2.40	16.25	21.27	28.52	68.46
ΔR (mm)	0.54	6.69	7.01	2.65	0.53
Lat. Shift (mm)	6.14	6.19	6.19	6.22	5.81

Simulation Output	Curve Radii (m)				
	400	100	75	50	20
σ - Tread (MN/m²)	1457.8	1386.1	1292.8	1344.8	1014.5
σ - Flange (MN/m²)	0.0	0.0	1693.0	1023.0	2096.1
T_Y - Tread (N)	12.9	279.1	197.2	454.2	260.4
T_Y - Flange (N)	0.0	0.0	191.8	58.9	1240.1
A - Tread (deg)	15.86	42.85	36.26	43.29	19.61
A - Flange (deg)	0.00	0.00	54.28	54.28	54.28
AoA (mrad)	0.56	16.24	20.83	28.29	68.06
ΔR (mm)	2.37	6.04	5.01	6.12	2.81
Lat. Shift (mm)	5.24	5.98	5.94	5.99	5.49

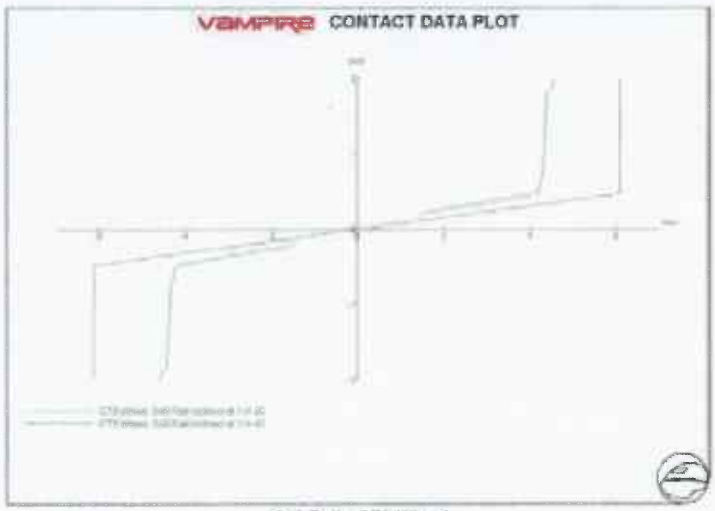

S49 Rail - CT3 Wheel

centro
transforming public transport

Metro Delivery Programme
Tram Bid Review Meeting

16 November 2011 Large Break-out room 2nd Floor Rear 1300 - 1600

A G E N D A

1. Summary of Financial Evaluation	GM
2. Summary of Technical Evaluation	?
3. Summary of Contractual Evaluation	UG
4. Overview of assessment	PN
5. Outstanding Issues/Concerns	PG
6. Best and Final Offer Process	PA
7. Documentation Required	PA
8. Timescales	PA
9. Announcements/Bidder Management	PA

S49 Rail - NET P3102639 Wheel

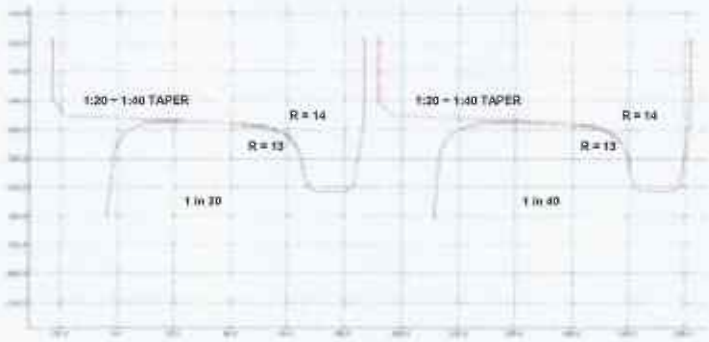

Simulation Output	Curve Radii (m)				
	400	100	75	50	20
σ - Tread (MN/m²)	577.3	538.5	534.3	812.9	1230.3
σ - Flange (MN/m²)	2845.5	3135.8	3163.1	3178.3	3248.9
T_Y - Tread (N)	29.9	151.5	182.9	241.0	504.2
T_Y - Flange (N)	267.2	636.6	756.5	993.1	2631.1
A - Tread (deg)	2.86	2.86	2.86	1.72	1.12
A - Flange (deg)	74.70	74.70	74.70	74.70	74.70
AoA (mrad)	4.09	15.15	18.18	24.13	50.38
ΔR (mm)	0.76	0.77	0.77	0.57	0.03
Lat. Shift (mm)	5.42	5.34	5.32	5.18	3.90

Simulation Output	Curve Radii (m)				
	400	100	75	50	20
σ - Tread (MN/m²)	1328.2	1243.6	1240.1	1238.1	1208.0
σ - Flange (MN/m²)	1926.6	2292.2	2312.7	2317.9	2352.5
T_Y - Tread (N)	21.3	151.0	184.3	245.7	535.9
T_Y - Flange (N)	170.4	725.0	888.6	1187.4	3098.2
A - Tread (deg)	4.89	4.89	4.70	4.13	4.13
A - Flange (deg)	77.85	77.85	77.85	77.85	77.85
AoA (mrad)	4.10	15.02	18.04	23.96	50.30
ΔR (mm)	1.18	1.18	1.16	1.08	0.71
Lat. Shift (mm)	5.31	5.23	5.21	5.07	3.76

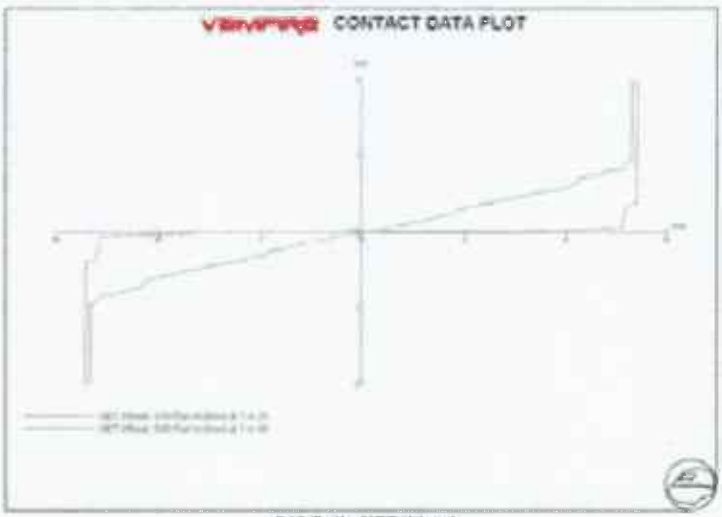

S49 Rail - NET Wheel

S49 Rail - SST Modified DIN25Wheel

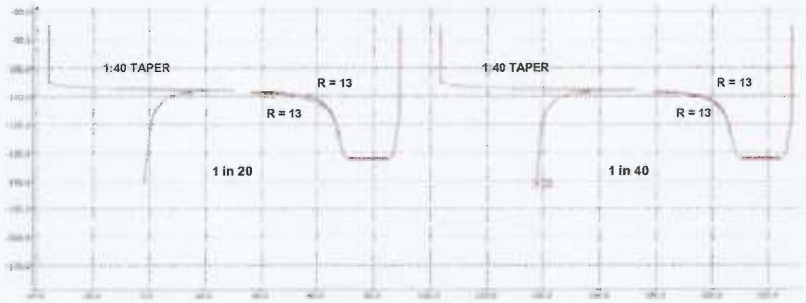

Simulation Output	Curve Radii (m)				
	400	100	75	50	20
σ - Tread (MN/m²)	1083.0	1029.0	1032.5	1176.6	1074.8
σ - Flange (MN/m²)	6547.2	7091.5	7150.3	7162.7	7376.3
Tγ - Tread (N)	37.1	167.9	205.0	268.8	546.1
Tγ - Flange (N)	390.8	603.83	717.4	875.5	2202.4
A - Tread (deg)	0.96	1.00	0.98	0.74	0.85
A - Flange (deg)	72.24	72.24	72.24	72.24	72.24
AoA (mrad)	3.18	16.38	20.70	27.68	66.86
ΔR (mm)	0.41	0.41	0.40	0.38	0.24
Lat. Shift (mm)	5.76	5.61	5.53	5.46	4.17

Simulation Output	Curve Radii (m)				
	400	100	75	50	20
σ - Tread (MN/m²)	1297.9	1215.5	1201.8	1194.0	1158.8
σ - Flange (MN/m²)	3373.0	3555.1	3557.9	3548.0	3544.9
Tγ - Tread (N)	28.0	151.3	184.3	242.5	525.1
Tγ - Flange (N)	197.1	708.2	873.8	1154.9	2967.9
A - Tread (deg)	3.41	3.41	3.41	3.41	3.41
A - Flange (deg)	77.20	77.20	77.20	77.20	77.20
AoA (mrad)	2.76	17.56	21.44	28.37	67.18
ΔR (mm)	0.75	0.75	0.74	0.73	0.48
Lat. Shift (mm)	5.62	5.53	5.42	5.35	3.98

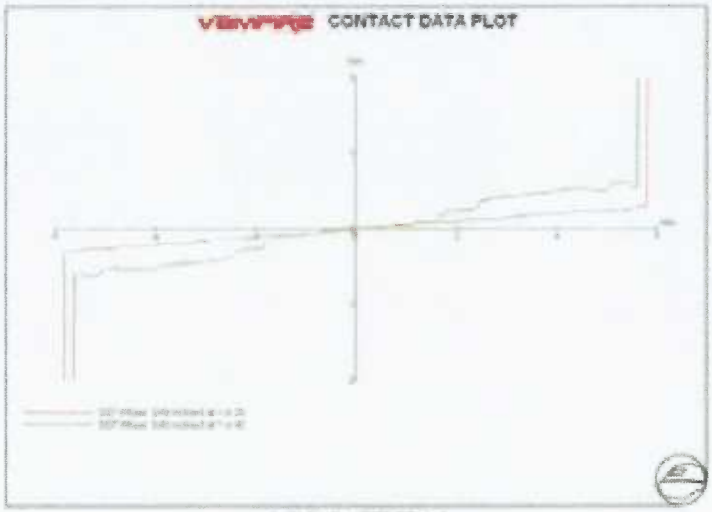

S49 Rail - SST Wheel

A2.1 Ri 59 Grooved Rail Sections

RI59 Rail – CT3 Wheel

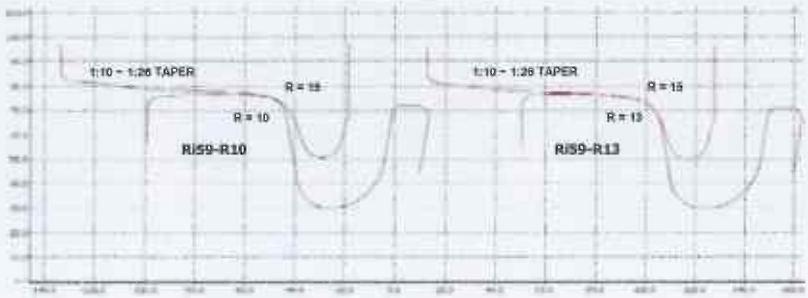

Simulation Output	Curve Radii (m)				
	400	100	75	50	20
σ - Tread (MN/m²)	2396.7	2271.3	2258.2	2262.6	2155.0
σ - Flange (MN/m²)	0.0	0.0	0.0	0.0	1724.4
Tγ - Tread (N)	16.2	268.1	352.9	487.5	905.4
Tγ - Flange (N)	0.0	0.0	0.0	0.0	703.8
A - Tread (deg)	15.69	42.10	43.13	43.13	37.71
A - Flange (deg)	0.0	0.0	0.0	0.0	70.42
AoA (mrad)	1.06	15.56	19.77	27.39	67.53
ΔR (mm)	2.26	6.25	6.56	6.59	0.81
Lat. Shift (mm)	3.62	5.33	5.41	5.41	5.09

Simulation Output	Curve Radii (m)				
	400	100	75	50	20
σ - Tread (MN/m²)	956.5	1360.0	1354.7	1355.8	583.2
σ - Flange (MN/m²)	0.0	0.0	0.0	0.0	1869.4
Tγ - Tread (N)	11.8	281.0	381.1	511.9	447.3
Tγ - Flange (N)	0.0	0.0	0.0	0.0	1986.9
A - Tread (deg)	15.66	42.67	44.36	44.53	4.21
A - Flange (deg)	0.0	0.0	0.0	0.0	69.88
AoA (mrad)	0.45	16.46	21.06	28.45	68.17
ΔR (mm)	2.29	4.73	5.95	5.95	4.95
Lat. Shift (mm)	5.65	6.06	6.08	6.09	5.59

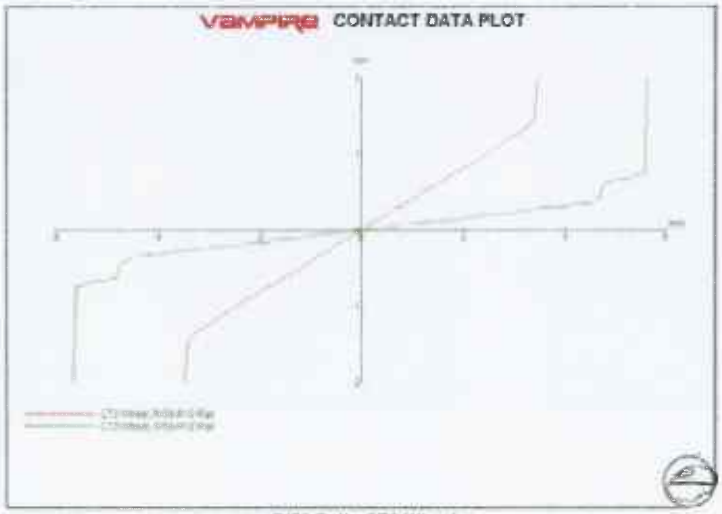

RI59 Rail - CT3 Wheel

Ri59 Rail - NET P3102639 Wheel

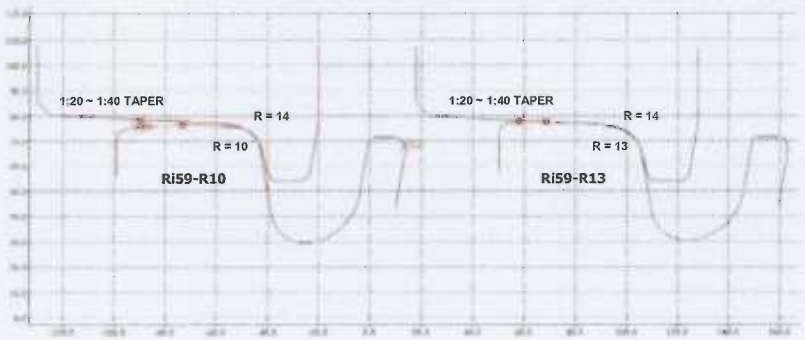

Simulation Output	Curve Radii (m)				
	400	100	75	50	20
σ - Tread (MN/m²)	2125.6	2146.6	2132.4	2136.1	1923.8
σ - Flange (MN/m²)	0.0	0.0	0.0	0.0	2228.3
Tγ - Tread (N)	19.9	274.2	355.2	491.6	622.1
Tγ - Flange (N)	0.0	0.0	0.0	0.0	2037.5
A - Tread (deg)	25.23	43.60	44.40	44.40	22.43
A – Flange (deg)	0.0	0.0	0.0	0.0	76.03
AoA (mrad)	4.02	13.99	17.04	23.05	50.03
ΔR (mm)	2.11	5.55	5.71	5.71	1.94
Lat. Shift (mm)	3.77	4.64	4.68	4.68	3.62

Simulation Output	Curve Radii (m)				
	400	100	75	50	20
σ - Tread (MN/m²)	1289.5	1213.2	1223.1	1217.5	1120.5
σ - Flange (MN/m²)	1922.3	2254.2	2266.8	2265.1	2300.6
Tγ - Tread (N)	26.7	148.6	182.5	241.7	526.6
Tγ - Flange (N)	188.6	648.5	795.0	1047.5	2735.6
A - Tread (deg)	4.30	4.37	4.48	4.48	4.10
A - Flange (deg)	76.24	76.24	76.24	76.24	76.24
AoA (mrad)	4.13	15.12	18.12	24.07	50.35
ΔR (mm)	1.01	1.01	1.01	1.01	0.86
Lat. Shift (mm)	5.42	5.30	5.23	5.16	3.86

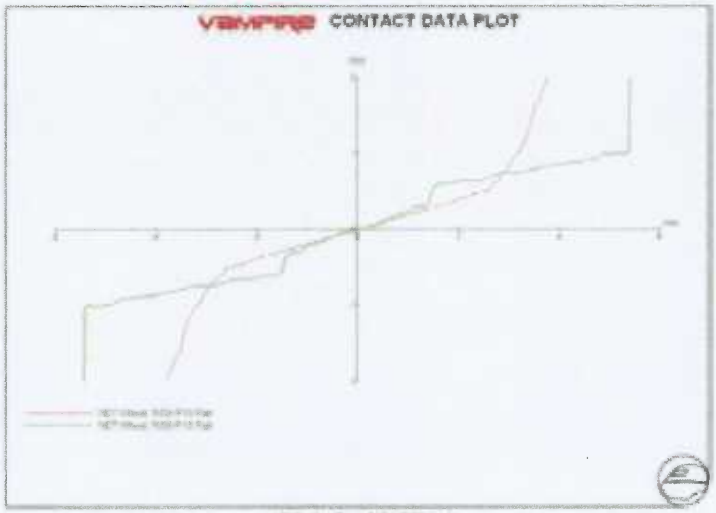

Ri59 Rail - NET Wheel

RI59 Rail - SST Modified DIN25Wheel

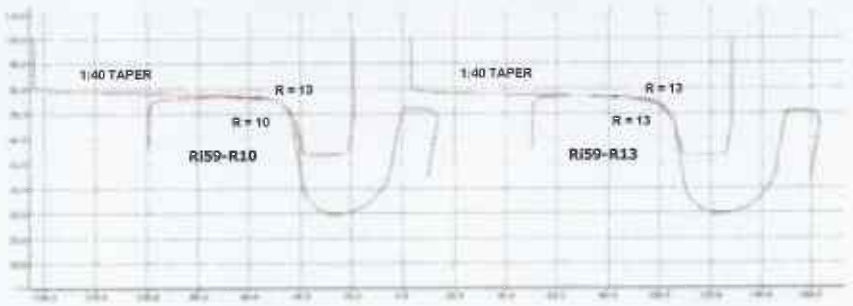

Simulation Output	Curve Radii (m)				
	400	100	75	50	20
σ - Tread (MN/m²)	1940.5	1929.1	1933.4	1934.9	1617.1
σ - Flange (MN/m²)	0.0	0.0	0.0	0.0	2311.0
T_γ - Tread (N)	22.8	283.4	356.2	489.7	560.3
T_γ - Flange (N)	0.0	0.0	0.0	0.0	2248.7
A - Tread (deg)	23.06	43.33	43.65	43.65	12.66
A - Flange (deg)	0.0	0.0	0.0	0.0	75.63
AoA (mrad)	1.66	16.05	20.15	27.55	66.54
ΔR (mm)	2.26	4.92	4.97	4.97	1.54
Lat. Shift (mm)	4.32	5.07	5.08	5.08	3.87

Simulation Output	Curve Radii (m)				
	400	100	75	50	20
σ - Tread (MN/m²)	858.4	644.9	622.7	578.1	774.7
σ - Flange (MN/m²)	1985.4	2219.3	2237.0	2241.9	2289.4
T_γ - Tread (N)	28.8	150.3	181.7	237.2	502.5
T_γ - Flange (N)	200.6	646.2	791.3	1050.7	2751.4
A - Tread (deg)	3.32	2.81	2.72	2.17	1.22
A - Flange (deg)	75.70	75.70	75.70	75.70	75.70
AoA (mrad)	2.77	17.65	21.48	28.41	67.39
ΔR (mm)	0.78	0.67	0.65	0.55	0.22
Lat. Shift (mm)	5.72	5.58	5.51	5.37	4.15

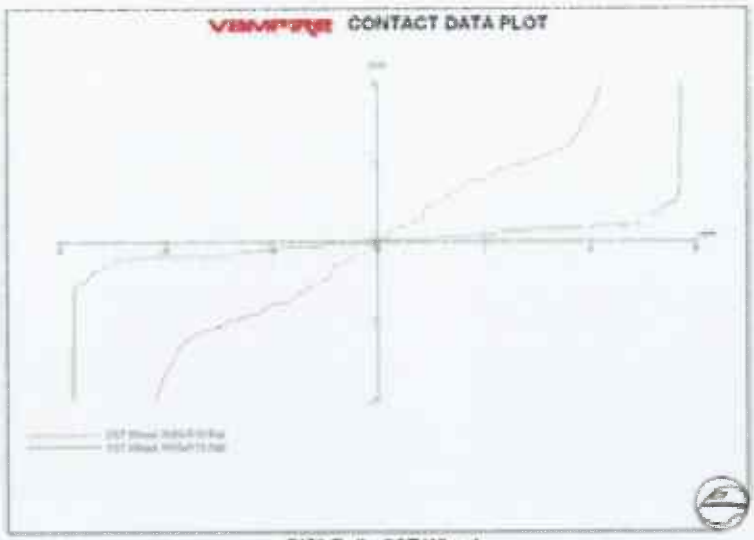

RI59 Rail - SST Wheel